UNICA

UNIVERSITÀ
DEGLI STUDI
DI CAGLIARI

Ph.D. DEGREE IN

International PhD in Innovation Science and Technology
Cycle XXXIV

TITLE OF THE Ph.D. THESIS

On the role of biomass on coastal morphodynamics in natural and urban Mediterranean beaches

Scientific Disciplinary Sectors
GEO/04 GEO/12

PhD Student: Daniele Trogu

Coordinator of the PhD Programme Prof. Roberto Orrù

Supervisor Prof. Sandro De Muro

Co-Supervisor Prof. Giovanni Coco

Final exam. Academic Year 2020/2021
Thesis defence: October 2022 Session

To my parents, friends, and Caterina, who always encouraged me to carry on, from the beginning to the end of these years.

I have the world's largest collection of seashells. I keep it on all the beaches of the world... perhaps you've seen it.

Steven Wright

ABSTRACT

The continuous sea level rise and the increase in the intensity of wave storms, amplified by global climate change, implies an adequate response from coastal management and environmental protection. To counter these phenomena, urgent measures should be taken to mitigate anthropogenic impacts and restore natural coastal resilience. This thesis deals with the role that biomasses (mainly *Posidonia oceanica* and, in some cases, *Arundo donax* rests) have within three Mediterranean beaches differentiated from each other by more or less marked human impacts. On a beach with almost irrelevant anthropic impacts, the deposition of the banquettes at the end of the most significant wave storms is analysed through a video monitoring system. It has been shown how this phenomenon generates a rapid accretion of the emerged beach, which restores its original extension, reduced during the storm, in two or three days. The spatio-temporal shift of the shoreline was investigated along two others urban beaches in Cagliari Gulf (Southern Sardinia, Italy), through orthorectified photographs, across a time frame of 62 years, in order to quantify and distinguish the factors controlling the shoreline evolution (erosion and/or accretion rates) in relation to a number of anthropic and natural forcings. The evolution of the geomorphological setting of the urban coastal belt of Cagliari was also carried out through a sea-land approach and a multidisciplinary and multi-temporal investigation summarized in a geomorphological map. Furthermore, the results of the water infiltration tests, carried out in different areas of the dry beach, showed that the presence of biomasses, above and inside the sand, considerably increases its permeability. This allows the beach to drain the overwashed water and its return to the sea during the most energetic storm events, limiting runup and flooding extension.

Finally, another original contribution of this work is related to the analysis of the banquette deposition and dismantling dynamics, through a four years video monitoring system database in one of the most urbanized portion of the Cagliari beaches. This study looked for a correlation between the wave and wind climate and the dynamics of the banquettes, and the results showed that wave motion plays a more important role in the deposition of the banquettes than in their erosion. For this last process the offshore and inshore winds plays a more significant role than the waves.

ACKNOWLEDGEMENTS

I want to express my heartfelt thanks first of all to my tutor Prof. Sandro De Muro, Director of the Coastal and Marine Geomorphology Group (CMGG) of the University of Cagliari, for having given me the opportunity to carry out this thesis with his support, infrastructures and instrumentation. Thanks to his effort, availability and planning necessary for executing the field campaigns.

I express my sincere thanks to my co-tutor Prof. Giovanni Coco, from the distant University of Auckland where, due to the pandemic emergence, I was unable to go physically, but thanks to his constant suggestions and advice it was almost like being there.

I am very grateful to the International PhD in Innovation Sciences and Technologies of the University of Cagliari for giving me the opportunity and the financial support to carry out this thesis work ("Borse di studio di Ateneo"-Dottorati di Ricerca XXXIV ciclo, voce CO.AN.A.06.01.01.01.01.02).

I gratefully acknowledge the support and funding rendered by the Projects Life+ Providune and NEPTUNE2, (Natural Erosion Prevision Through Use of Numerical Environment L. R. 7.08.2007, N.7: Promozione della ricerca scientifica in Sardegna e dell'Innovazione tecnologica in Sardegna), which have been an essential support for the acquisition of all the data analysed in this work.

I am very grateful also to MEDCOASTLAB (Mediterranean Geomorphological Coastal and Marine Laboratory) for the availability of the laboratory where I was able to carry out my work. Through the MEDCOASTLAB I would also thank Sardegna Progetta company for their support with the video monitoring network infrastructures and Battellieri di Cagliari company for the assistance during bathymetric surveys. Sincere grateful also to Teravista company for the drone surveys and Servizi Geotecnici company for the water infiltration tests

With a sense of gratitude, I acknowledge the ASL 8 Cagliari, Sardinia Sea Port Authority, the "Deposito PolNato Marina Militare (Navy PolNato Depot Marina Militare)" of Cape S. Elia–Cagliari and Comando supporto logistico di Cagliari (MARICAGLIARI) for their availability in providing me with infrastructural support and the data shared. Sincere thanks go also to the Comune di Cagliari (Alessandro Guarracino) for having allowed the seasonal monitoring survey during the pandemic lockdown.

I will always be grateful to my colleagues of the Coastal and Marine Geomorphology Group (CMGG), for allowing me to collaborate with them, motivating me day after day and making the laboratory feel almost like a second home inhabited by a beautiful circle of friends. Thanks to Dr. Angelo Ibba for his complete and continuous support and availability; Dr. Andrea Ruju for his essential help, supervision, moral support and precious suggestions

during these years; Dr. Carla Buosi for her availability, courtesy and patience at any time; Dr. Marco Porta for his moral and technical support in any field… from cameras to fishing advice; Dr. Manuela Biondo for her advice, encouragements and coffees. Their daily availability, moral support and suggestions have been of great importance and support in several ways during my research work.

An infinite and sincere thanks to Marco Pinna, an authentic dear friend who is always present in any situation and without whom I probably would not have even started this PhD.

My deepest thanks to my parents and my family, because it is thanks to you that I now write these lines, supporting me and helping me in every way possible for the past 37 years.

Last but not least, I want to express my biggest thanks to Caterina, a wonderful partner who I am lucky enough to have with me over these years. Thank you for your continued encouragement, for the patience and understanding with which you have always endured and supported me.

My thoughts and my affection go to all of you. I will never tire of thanking you in the deepest and sincerest way.

Place: Cagliari

Date: submitted 15/12/2021 Daniele Trogu

(This page is intentionally left blank)

Contents

List of Figures

List of Tables

Chapter 1
INTRODUCTION

The studies carried out to realize this PhD thesis are part of the research activity on the coastal areas and on the continental shelves done by the Coastal and Marine Geomorphology Group (CMGG, Scientific Coordinator: Prof. Sandro De Muro), belonging to the Department of Chemical and Geological Sciences of the University of Cagliari and MEDCOASTLAB (Mediterranean Geomorphological Coastal and Marine Laboratory). Data collection was made possible by the Projects B.E.A.C.H. ("Beach Environment, management And Coastal Hazard"), PROVIDUNE (LIFE07NAT/IT/000519), NEPTUNE and NEPTUNE2 ("Natural Erosion Prevision Through Use of Numerical Environment"; Scientific Coordinator: Prof. Sandro De Muro).

Coastal areas are the most populated zones in the world (Small and Nicholls, 2003; Crossland et al., 2005). This means that many of the infrastructures and human activities are also located in these areas (such as ports and shipping, roads, tourism and leisure, fishing and aquaculture, etc.). These anthropogenic impacts, considering the global scenario of climate change and sea level rise, have considerably increased the risk of coastal erosion, also generating a serious socio-economic hazard (McKay et al., 2011). In this context, the correct management of the coasts represents the most important form of defense against floods and erosion, therefore the sustainable development of coastal areas requires effective management that must take into account the natural dynamics of the sandy coastal systems, as these defend the coast from floods and increasing impacts due to the global scenario.

This work aims to improve the knowledge on the morphodynamics of Mediterranean microtidal beaches, examining two different coastal belts of southern Sardinia: Piscinnì beach, which presents a highly natural system; and the urban coastal belt of Cagliari which has instead undergone numerous anthropogenic impacts over the years, both structural (such as the construction of ports, roads and buildings above the dunes, etc.) and due to bad practices (such as the periodic cleaning of beaches with heavy vehicles). In particular, we try to better understand how the deposition of biomass on the emerged beach, and their correct management, can influence the resilience to storm waves of these beaches. The Covid-19 pandemic crisis helped to understand this process even in urban environments: during the PhD period, in fact, a total lockdown of about two months was imposed in Italy. During this period, in the absence of bad practices, it was possible to observe how Nature was able to act undisturbed even on urban beaches. Finally, we wanted to fill the gap in the literature regarding the wind and wave parameters that lead to the natural deposition and removal of banquette.

To achieve these objectives, a multidisciplinary approach has been adopted which includes both remote and in-field measurements such as topographic and bathymetric surveys, drone surveys,

analysis of images coming from coastal videomonitoring system, aerial orthorectified photographs, and specific instrumental measurements like water infiltrometric tests.

This thesis is structured in 8 chapters. In chapter 2 a review of the literature inherent to the topics studied is provided.

Chapter 3 explains the multidisciplinary methodology adopted for performing this research.

In chapter 4, a database of coastal videomonitoring system was analyzed to measure and map the position of the shoreline, before during and after significant storms events, in relation to the deposition of the banquettes in a natural Mediterranean microtidal beach (Piscinnì beach).

Chapter 5 carries out a historical morphodynamic evolution of the coastal area of Cagliari to evaluate the effects of anthropic activities and evaluate multi-decadal shoreline changes also induced by anthropogenic impacts, such as removal of beach cast litters, buildings, etc.

Chapter 6 highlights how the presence of biomasses on the beach (both as a superficial deposit and as buried layers) significantly increases the beach drainage capacity, especially during overwash events in an urban beach (Poetto beach).

In chapter 7, through another database of a coastal videomonitoring system, we want to measure the natural depositions and removals of the banquettes by analysing the relationship with the wave and wind parameters in an urban beach (Poetto beach).

In chapter 8 general conclusions of this work are summarized.

Chapter 2
REVIEW OF LITTERATURE

2.1. Coastal classification and morphodynamics of beaches

There are numerous types of coastal classification in the literature (von Richthofen, 1886; Suess, 1888; Davis, 1898; Gulliver, 1899; Johnson, 1919; Shepard,1963, Inman and Nordstrom, 1971; Davies, 1980; etc.). These schemes can be useful from a conceptual point of view and help to assess the different forcing factors and controls (e.g. sea-level history, geology, climate, waves, tides) that give rise to coastal landforms (Masselink, 2011). One of the older is the one that distinguishes the high coasts (mainly consisting of cliffs) from the low ones (mainly consisting of sandy beaches). Johnson's scheme (1919) is based on the role of sea-level variations, and so distinguish between submerged coasts (drowned river and glacial valley, termed rias and fjords respectively) and emerged coasts (coastal plains where sea level has fallen). Shepard (1963) makes a distinction based on the genesis of the coast between primary and secondary coasts. The primary coasts have evolved forms in a non-coastal environment or, in any case, due to the prevalence of morphogenetic agents other than marine ones. In the secondary coasts, on the other hand, there is a dominance of marine morphogenetic agents and modelling operated by wave motion (Figure 2.1).

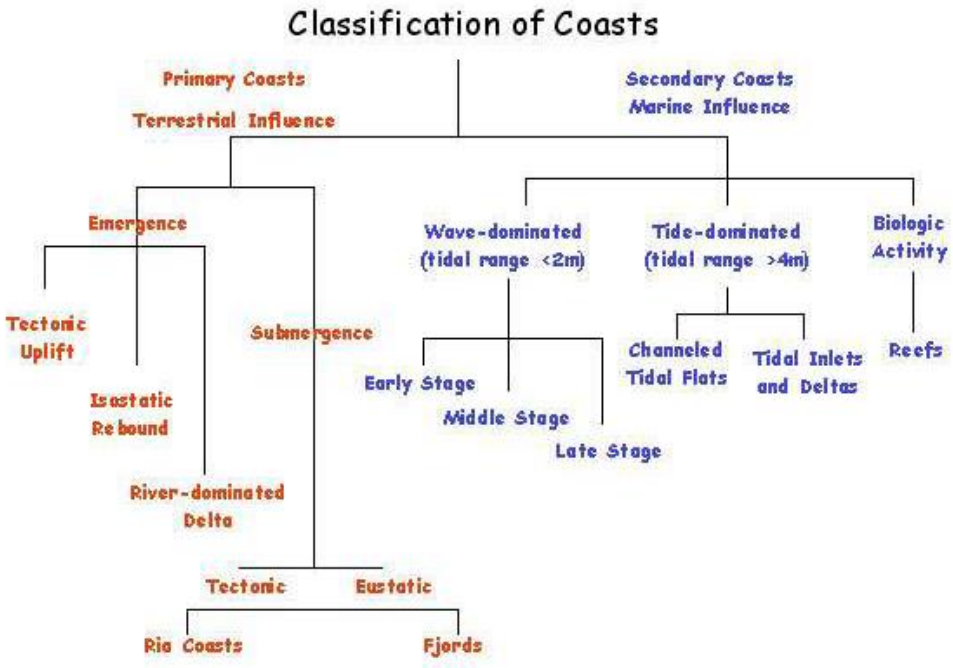

Figure 2.1 - Schematic classification of coasts proposed by Shepard (1963).

A classification based on the tectonic position has been proposed by Inman and Nordstrom (1971) identifying "leading edge coasts" (located adjacent to subducting plate margins) and

"trailing edge coasts" (far away to subducting plate margins, in zones tectonically stable) (Masselink, 2011).

The main shortcoming of these classifications is that they emphasise geological inheritance rather than hydrodynamic processes that shape coastal landforms. Davies (1980) identified coastal types based solely on wave height and tidal range (Figure 2.2, Figure 2.3). Because waves are generated by wind, the distribution of wave environments varies by latitude, reflecting global climate zones (Figure 2.2), (Masselink, 2011).

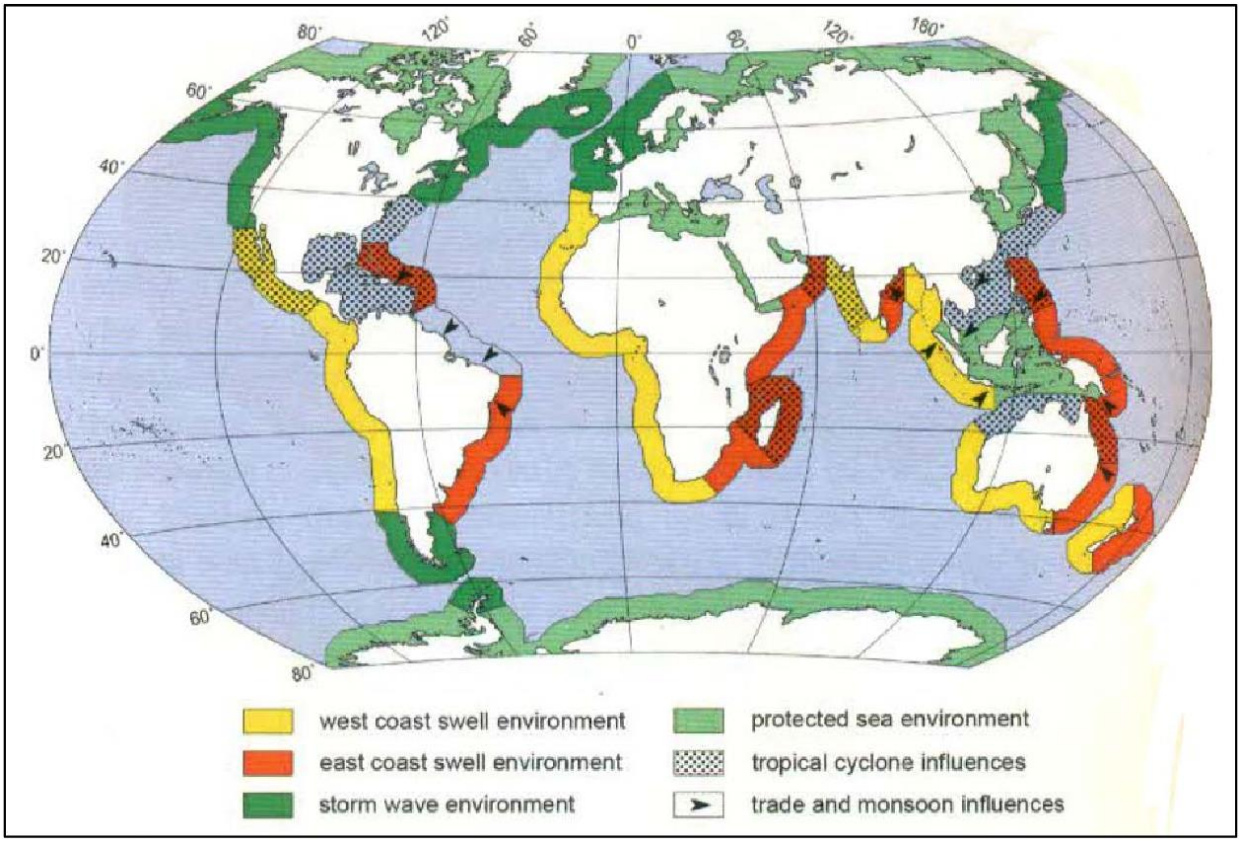

Figure 2.2 - Worldwide distribution of wave environments (Davies, 1980)

Macrotidal ranges exceeding 4 m are mostly observed in semi-enclosed seas and funnel-shaped entrances of estuaries, while microtidal ranges below 2 m occur along open ocean coasts and almost fully enclosed seas (Masselink, 2011). A typical example of an *almost fully enclosed sea* is Mediterranean Sea (Figure 2.3).

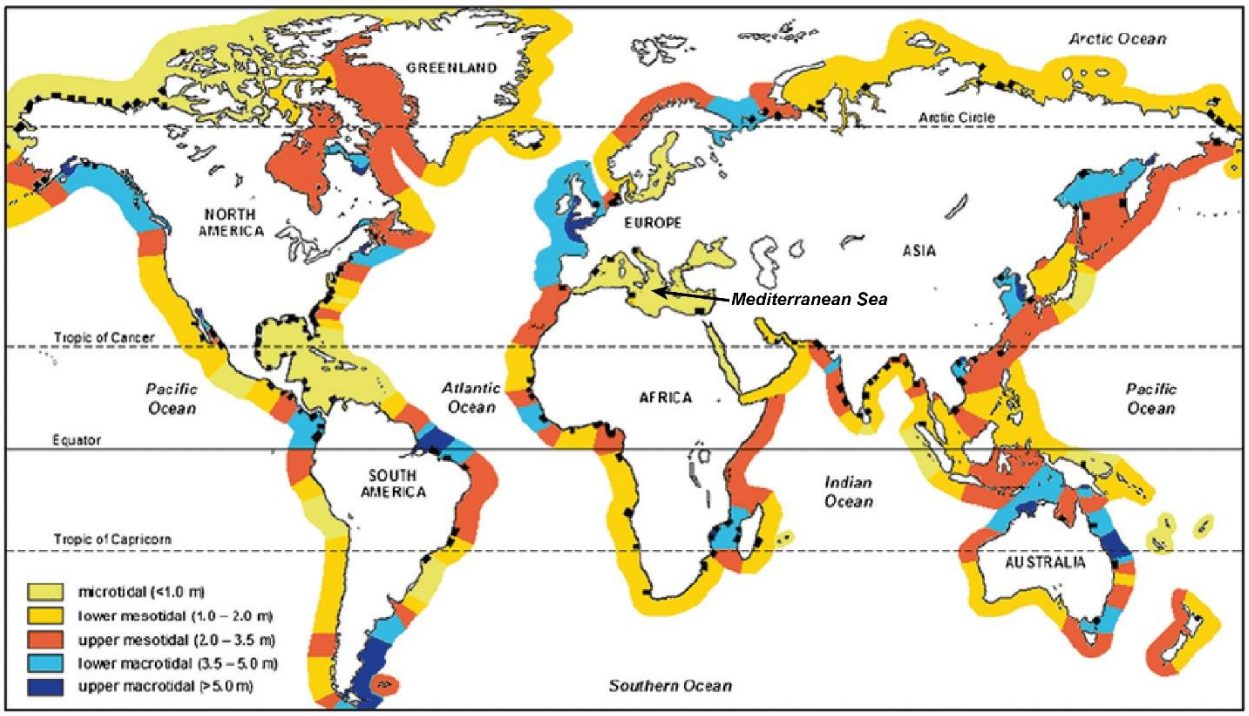

Figure 2.3 - World distribution of mean spring tidal range (modified from Pan J., et al., 2018)

The global distributions of wave height and tidale range (Davies, 1980) are often used to infer wave – and tide – dominance of coastal processes and morphology. However, the relative effects of wave and tides, rather than their absolute values, are more important in shaping the coasts. Thus, tide-dominated environments are not restricted to macrotidal coasts, but may also be found along microtidal coasts if the incident wave-energy is low. Davis and Hayes (1984) point out that there is a delicate balance between wave and tide processes for low values of wave height and tide range, and these low-energy regions converge in Figure 2.4. Therefore, tide-dominated, wave dominated or mixed-energy morphologiees may develop with very little difference in wave and tide parameters (Masselink, 2011).

The mean tidal range in Mediterranean Sea is about 40/45 centimeters – microtidal type – (with the exception of Gulf of Gabès, with maximum exursion of 2,5 meters and some towns in the Gulf of Trieste, with maximum exursion of 1,6 meters), and the tidal fluctuations are of a mixed semi-diurnal type, with two maximums and two minimums during the day. For this reason, following the classifications proposed by Davies (1980) and by Davis and Hayes (1984), we can identify the Mediterranean sandy beaches, or at least those studied in this thesis, in the category “microtidal, wave dominated” (Figure 2.4).

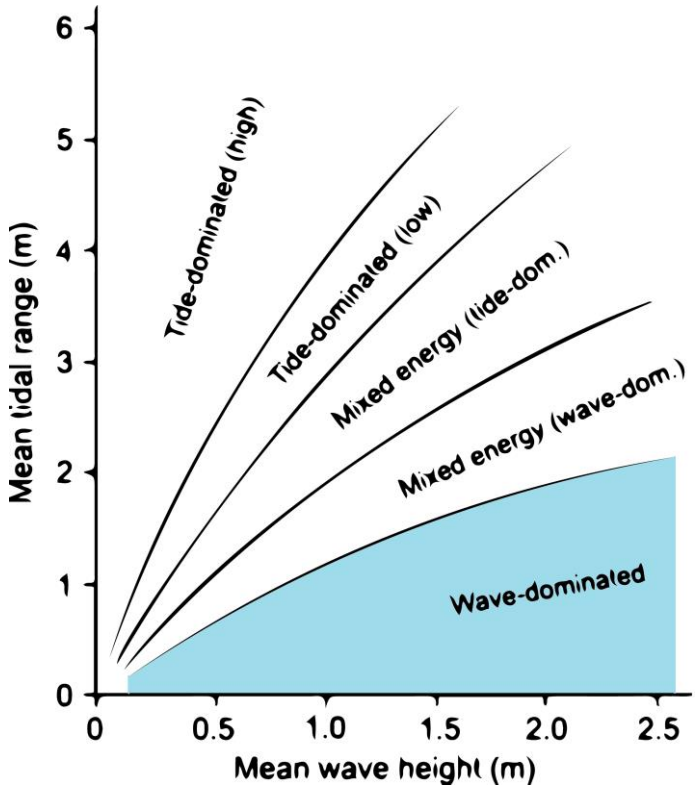

Figure 2.4 - Relationship between mean tidal range and wave height delineating different fields of wave/tide dominance (modified from Davis and Hayes, 1984)

Along the ideal profile of these beaches some areas can be distinguished: back beach, dunes, backshore, foreshore, shoreface and offshore (Figure 2.5).

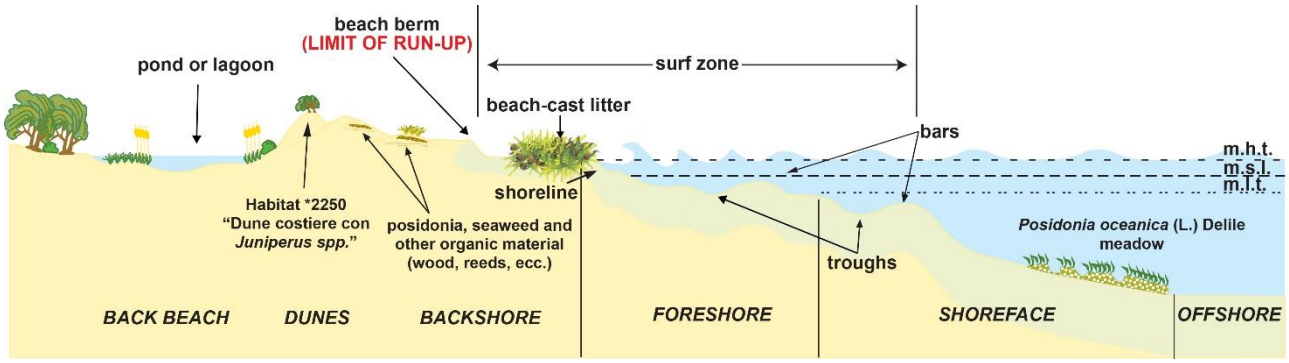

Figure 2.5 - Ideal profile of a Mediterranean microtidal sandy beach (modified from De Muro and De Falco, 2010)

Between the beach berm and the most external bar there is the surf zone, which rapresent the area where the wave motion is more energetic and where the waves break and this motion can modify the morphology of the beach.

Many authors (Gourlay, 1968; Wright and Short, 1984; Cowell and Thom, 1994; Masselink, 2011; etc.) examined these kind of beaches from a morphodynamic point of view, mainly analyzing the morphological changes from the foreshore to the beach closure depth (in the shoreface). The closure depth can be defined as $\lambda/2$ or half of the wavelength (Carobene and Brambati, 1975). It

is called closure because at this depth there is little or no sediment transport, except for extreme events. Furthermore, in the Mediterranean Sea the depth of closure almost always corresponds to the upper limit of the *Posidonia oceanica* meadow.

Wave dominated beaches can be classified using three parameters: breaker wave height (H_b), wave period (T) and grain size (as defined by sediment fall velocity, W_s). These parameters, for laboratory beaches, were first combined by Gourlay (1968) into the *dimensionless fall velocity*:

$$\Omega = \frac{H_b}{W_S\, T}$$

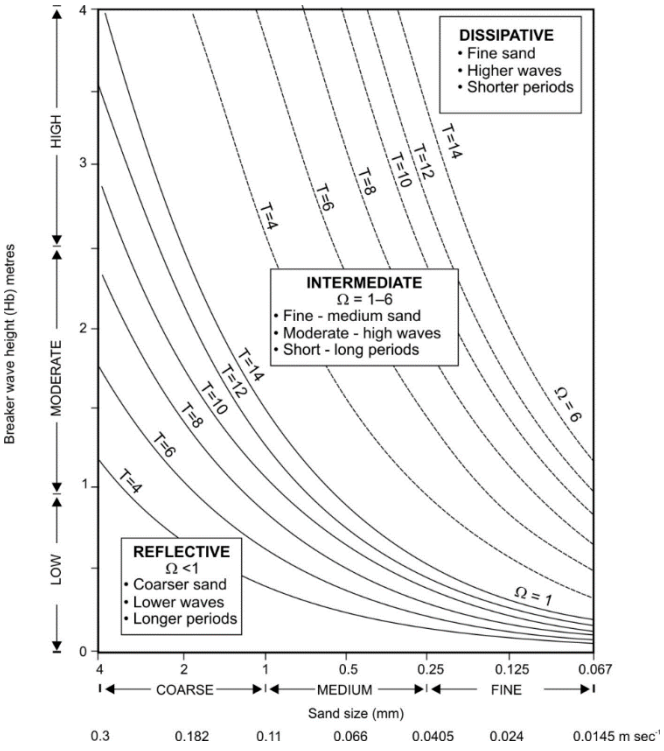

Figure 2.6 - Sensitivity plot of the contribution of breaker wave height, sediment size and wave period to Ω and beach type (Short, 1999).

Wright and Short (1984) adapted Ω for use on natural beaches and this model was subsequently used and implemented by numerous authors (Lippmann & Holman, 1990; Short & Aagaard, 1993; Short, 1999; Ranasinghe et al., 2004; Short, 2006; Masselink & Short, 2011). In particular Short (2006), has amply demonstrated the applicability of the classification, based on statistics of over 10,000 beach systems studied in various parts of the world including the Mediterranean, and has also shown that different values of Ω, as well as correspond to different morphotypes , also correspond different wave heights, different granulometry of sediments and different tidal range. Short (1999) formalized the morphological variability spectrum of the beach system (Figure 2.6) through 3 main morphodynamic states:

- **Dissipative beach** – DB (Ω > 6): represent the highest energy level of the beach spectrum. During the most energetic storm events the surf zone becomes very large, (> 200m) with a low gradient of slope. In this zone from 2 to 5 orders of longshore bars and troughs are generated. This means that the wave motion, through the friction of the orbital motions with the seabed, gradually dissipates its energy. The waves initially break in the outermost bar, then reform themselves in the next trough and refract in the next bar. This process causes the wave motion to lose a lot of energy and gives its name to this type of beach. Although many beaches tend to reach this morphodynamic state during the most energetic storm events, they rarely truly reach it completely and returning, at the end of the storm, to an intermediate morphodynamic state. True dissipative beaches have fine sand (<0.2mm) and are persistently subjected to high waves (> 2.5m) with a short period (T > 10s) and are most frequently found along ocean coasts. However, they are also common in storm-dominated seas and larger lakes and bays, where high, but short period (T = 2-5 s) storm waves act on fine sand beaches, such as a parts of the Arctic Ocean, Great Lakes, Mediterranean Sea, etc (Short, 1999). At the end of the storm, the outermost bar tends to remain inactive, and only the inner bars are active, with intermediate morphodynamics generated by lower waves or calms. The morphology of the coast in dissipative beaches tends to remain very stable and shows minimal changes in the shore line. The swash zone also has a very large area that can exceed 100m and is characterized by a low slope. It extends from the foot of the dune to the low tide limit.

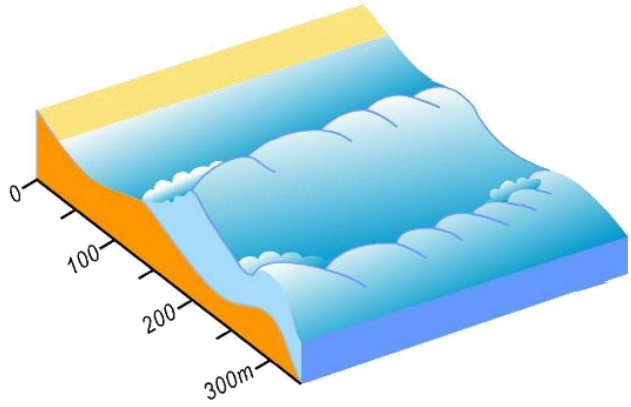

Figure 2.7 - Schematic example of dissipative beach. Courtesy of Short and Woodroffe (2009) in Short and Jackson (2013).

- **Reflective beach** – RB (Ω < 1): these kind of sandy beaches lie at the lower energy level of the beach spectrum, but not necessarily in areas with low waves. When the beach has medium-fine sand, the waves must not exceed one meter in height in order to have a reflective beach. In this case, the beach is generally located within bays or close to ports, islands or rocks. This type, however, is less frequent. When the beach is composed of coarse and/or pebbly sediment it can be of the reflective type

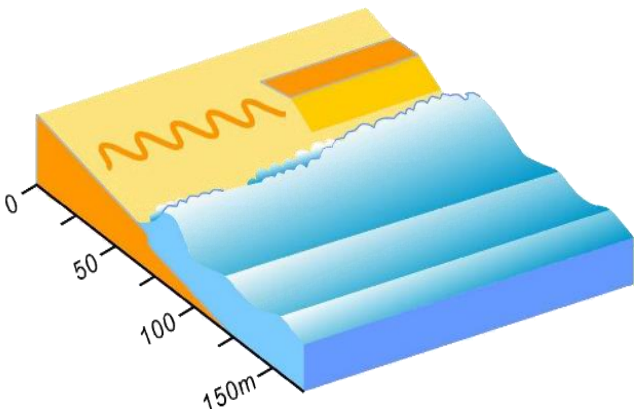

Figure 2.8 - Schematic example of reflective beach. Courtesy of Short and Woodroffe (2009) in Short and Jackson (2013).

even in the presence of high waves. In any case, beaches with coarse and / or pebbly sediment always tend to be reflective, regardless of the height of the wave. They have a steep bottom (regulated by the grain size) which reduces the swash zone to a very small area with frequent cusps in the emerged beach. If there is a granulometric range of sediment on the beach, the coarsest part will accumulate at the base of the swash zone as a step. Immediately after the step are the finer sands that do not generate defined shapes, except for the normal ripples formed by the waves. There are no bars or surf zone as the wave motion arrives undisturbed as far as the emerged beach and here they collapse, sometimes surmounting the emerged beach (Wright and Short, 1984).

- **Intermediate beach** – IB ($1 < \Omega < 6$)

The intermediate state refers to beaches that are intermediate between the high energy dissipative and the lower energy reflective beaches (Wright and Short, 1984). However, between these morphodynamic states, produced by waves between 0.5 and 2.5 m, there are substantial differences in the morphological characters of the beach. For this reason, intermediate beaches have been subdivided, into four morphodynamic states, ordered from highest to lowest energy level (Figure 2.9):

a) *Longshore bar and trough* (LBT) - $\Omega \sim 4{,}70$
b) *Rhythmic bar and beach* (RBB) - $\Omega \sim 3{,}50$
c) *Transverse bar and rip* (TBR), or *transverse bar and beach* (TBB) (Short, 1999b, 2006) - $\Omega \sim 3{,}15$
d) *Low tide terrace* (LTT), also known as *ridge and runnel* - $\Omega \sim 2{,}40$

It is important to remember that these are morphodynamic schemes and consequently, due to their dynamic character, they cannot always be found in nature so clearly developed. It often happens to be in intermediate situations between a morphodynamic state and another, or with some, but not all the characteristics of a morphodynamic state.

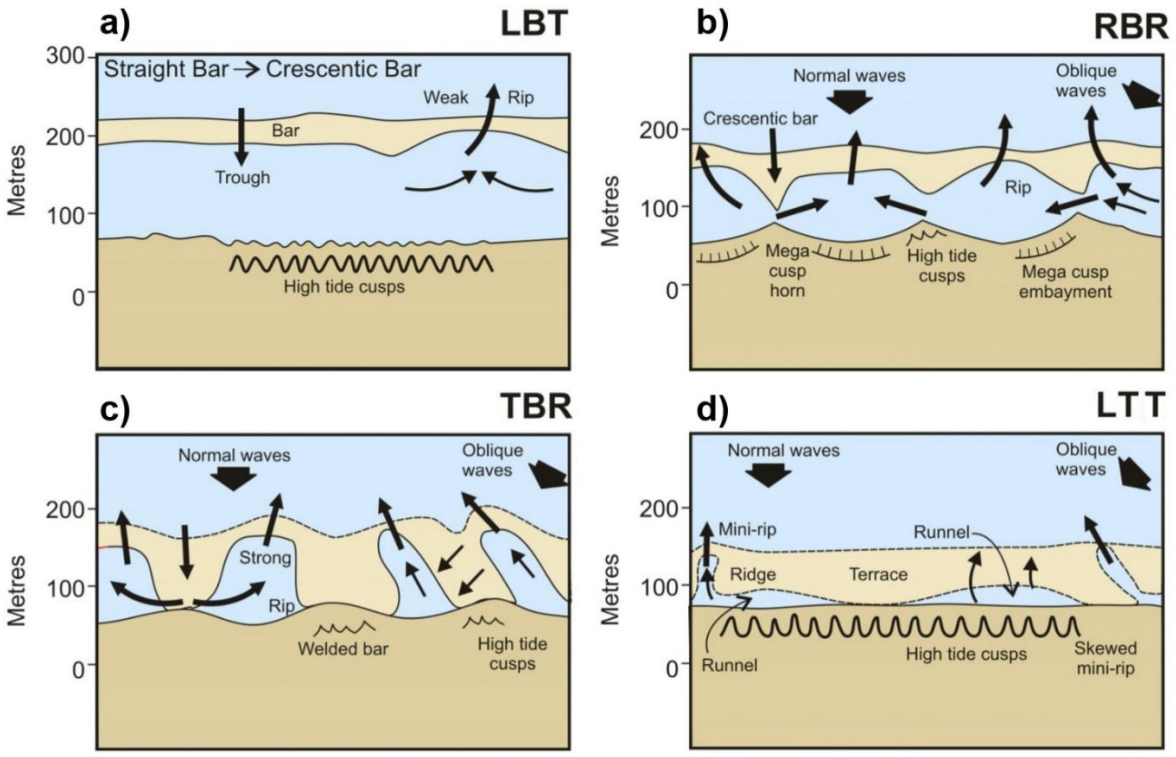

Figure 2.9 - Schematic illustration of the four morphodynamics states that an intermediate beach can assume, depending on the wave energy (modified from Short, 1999).

a) *Longshore bar and trough* (LBT) - Ω ~ 4,70 - are characterized by a longshore bar located between 100 and 150 meters from the shoreline and separated by a trough also parallel to the shoreline with an extension ranging from 50 to 100 m and a depth between 2 and 3 m. The longitudinal development of the beach, as in the dissipative ones, tends to be straight along the shoreline. The gradient depends on the size of the sediment and can range from low to moderate and can contain cusps or berms, with a step at the base. The shoreline and the trough are relatively straight, while the bars can vary from straight when they are made up of fine sands to slightly rhythmic in association with the cusps, when they are made up of medium sands, with loops that are generally crossed by rip currents every 250 - 500 meters during storm events (Short, 1999) – Figure 2.9a.

b) *Rhythmic bar and beach* (RBB) - Ω ~ 3,50 – consist of a longshore bar that proceeds with a rhythmic (crescentic) pattern, in phase with the cusps (or mega cusps) along the shoreline. Between the bar and the shoreline there is a trough which is also parallel to the shoreline. The waves that pass over the bar can follow two different paths: 1) passing on the crescentic bar, with a smaller depth, the waves break and reduce their speed; 2) the waves that pass on the area with the less developed bar, with a deeper section, they don't break while maintaining a high energy that generates a longshore gradient in wave breaking and direction in the surf. In correspondence with the embayments generated by

the crescentic bars they flow into rip current. The cusps are generated after the formation of the crescentic bars as the different paths of the waves, given by the refraction with the seabed, generate a longshore transport of sediment. This leads to the formation of circulation cells that give rise to the cusps accompanied by the micro bays. This system is repeated along the beach with a rhythmic trend (Short, 1999). This kind of beaches are generally composed of medium-fine sand – Figure 2.9b.

c) *Transverse bar and rip* (TBR) - $\Omega \sim 3{,}15$ - They get this name due to the fact that the bars are transverse or perpendicular to the shoreline. They are similar to the rhythmic bar and beach but with the difference that the bars are attached to the shoreline. This generates circulation cells that are more isolated from each other and each of them with its own rip current. Generally, the cross bars are spaced from each other by about 150-250 meters, but they can reach distances of 700 meters in the beaches with high energy wave motion. The resulting beach is characterized by an alternation of shallow areas, and others with deep channels where rip currents are set. The cusps attached to the bars often forming scarped embayments in lee of the rip channels. This type of beach is generated with medium to fine sediment and waves that can reach 1.5 meters in breaker height (Short, 1999) – Figure 2.9c.

d) *Low tide terrace* (LTT) - $\Omega \sim 2{,}40$ - It is the intermediate beach category subjected to less energy. They are also called *ridge and runnel*. The peculiarity of this typology is given by the presence of a step (whose size and slope depends on the granulometry of the sediment) which is joined, at the low tide point, to the bar or terrace, hence the name *low tide terrace*. The bar extends out to sea for about 20-50 meters (but it can also reach 100m in beaches with fine sand) and continues, joined to the shore, along the coast. In this type of beach state, the waves do not exceed one meter in height. The bar can be flat and without characteristic signs, except for a slight ridge from which the other name with which this type of beach is identified (*ridge and runnel*). The bar can be interrupted at intervals of a few tens of meters by small and shallow rip channels, called mini-rips (Short, 1999) – Figure 2.9d.

- **Multi-bar beaches**

Many microtidal beaches also have more than one bar. The occurrence of double and multiple bars along a beach has long been the subject of scientific investigations (Johnson, 1956; King, 1972; Short, 1999). Multiple bars are more prevalent in tideless seas and may be attributed to waves of different heights, and the inner bar is always the most mobile (King, 1972) (Figure 2.10). Two and occasionally three bars are common on swell coasts, while in seas three or five bars are more common. The importance of morphology is linked to the assumption that morphological variability more or less directly reflects the processes that control it (Wright & Short, 1984). For example, the number of bars seems to show an inverse relationship with the slope of the submerged beach, the decrease of which would correspond to an increase in the number of bars (Brambilla, 2014). Moreover, the spacing of standing waves is negatively related to wave period. In other words, the bars are more closely spaced where period is short and gradient low (Short, 1999). Longer periods and steeper gradients produce more widely spaced standing waves which puts the potential bar-forming dynamics into deeper water, where it is less likely to impact the deeper seabed. Consequently, for a given beach gradient, waves whit short period will produce more, more closely spaced bars, whereas in long swell environments fewer, more widely spaced bars can form (Short, 1999). In this scenario the outer bar will always receive more energy from the waves than inner bars due to the wave breaking and decreasing wave height across the bar system. For this reason, exist a *hierarchy of bar types*, where the outer bar will be at the most energetic type (LBT), and the subsequent bars, receiving less energy from the wave motion, will be arranged in types with a lower energy level (Figure 2.10).

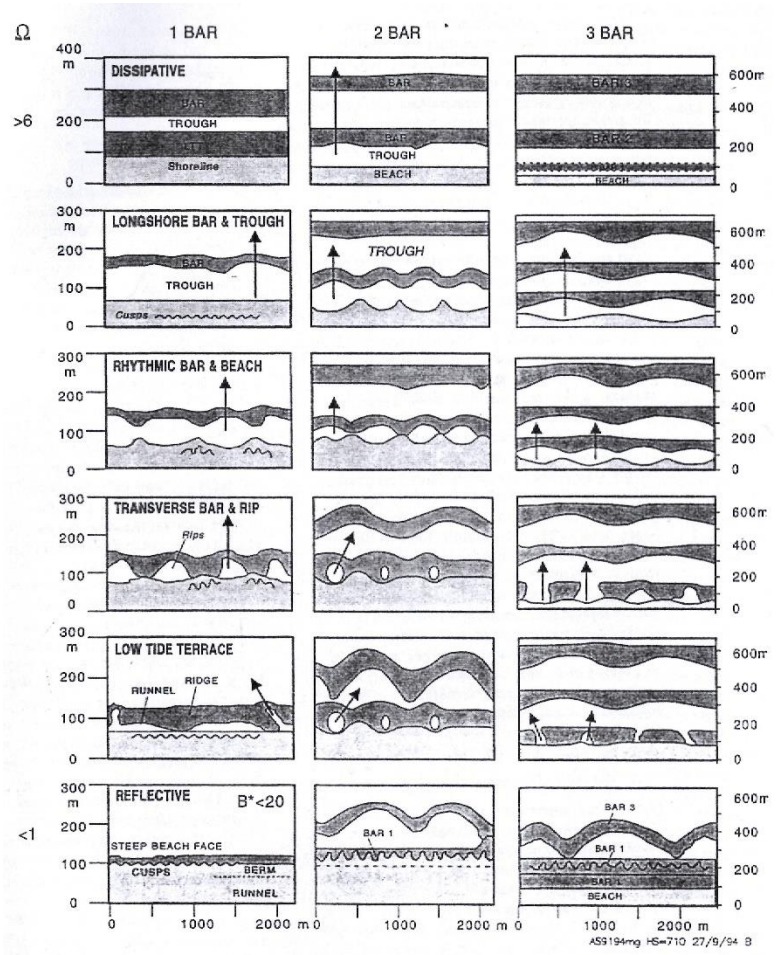

Figure 2.10 - Schematic example of multi-bar beaches. In Short (2009).

2.2. What about *Posidonia oceanica,* seagrass and beach-cast litter

Posidonia oceanica (L.) Delile, 1813, (also known as Neptune grass) is an endemic seagrass species (monocotyledonous angiosperms) in the Mediterranean Sea (Duarte, 1991; Procaccini et al., 2001) that grows all along the coast forming extensive and highly productive meadows from nearly the water surface to depths up to 40m, according to water clarity (Mateo et al., 2002; Telesca et al., 2015). As a matter of fact, *P. oceanica* needs transparent, oligotrophic and oxygenated waters to survive. The depth to which the meadows grow is often limited by light (Duarte 1991, Duarte et al. 2007). The minimum light requirements of this plant are 0.1 - 2.8 mol photons day^{-1} m^{-2} (Gattuso et al. 2006). *P. oceanica* also supports a narrow range of salinity, from 33‰ to 39‰ (Fernández-Torquemada and Sánchez-Lizaso 2005).

These meadows are identified as a priority habitat type (1120 - *Posidonion oceanicae*) for conservation under the Habitats Directive (Dir 92/43/CEE) and are safeguarded also by the Water Framework Directive (EPC, 2000) and the Marine Strategy Framework Directive, (EPC, 2008). Today this habitat (as well as all other seagrass habitats in the world) has largely been altered or totally disappeared due to increased coastal urbanization and human bad practices. In particular, for *Posidonion oceanicae*, the main threats are related to water and sediment enrichment (eutrophication), the disruption of the sedimentation/erosion balance along the coast and direct destruction by human modifications of the coastline, degradation by boat trawling and anchoring, salinity increase, the proliferation of invasive algal species, climate change effects and other human bad practices (Directive 92/43/CEE, Technical Report 2008 01/24). In 2008 it was estimated that 46% of the underwater meadows in the Mediterranean have experienced some reduction in range, density and/or coverage, and 20% have severely regressed since the 1970s (Directive 92/43/CEE, Technical Report 2008 01/24). The slow growth of *P. oceanica* meadows make difficult recovery, which can take centuries, once the cause of habitat perturbation is eliminated.

In daylight, *P. oceanica* meadows oxygenate coastal waters (Bay 1984), producing net oxygen releases to the atmosphere above the meadows. Due to the slow decomposition of lignified rhizomes and roots, the reef structure or “matte” acts as a long-term carbon sink (e.g. Gacia et al. 2002). The leaves and rhizomes increase the surface available to sessile species and offer shelter to mobile species, thereby sustaining a diverse community (Templado 1984). *Posidonion oceanicae* are especially valuable as nursery grounds for several commercial species (Francour 1997). The leaf canopy increases particle retention (e.g. Terrados and Duarte 2000), so enhancing water transparency. This function, combined with the active formation of calcareous and silica sand from shelled organisms (Canals and Ballesteros 1997) and cushions of seagrass litter, all contribute to reducing shoreline erosion. Moreover *P. oceanica* meadows are excellent indicators of environmental quality as they can only grow in clean unpolluted waters. Moreover, their

rhizomes concentrate radioactive, synthetic chemicals and heavy metals, recording the environmental levels of such persistent contaminants (Directive 92/43/CEE, Technical Report 2008 01/24).

Posidonia oceanica meadows are key ecosystems within the Mediterranean Sea. The high rate of plant production (0.25 ± 3 kg (dry weight) m^{-2} $year^{-1}$ (Ott 1980, Pergent-Martini et al. 1994), mainly due to annual leaf growth, and the abundance of epiphytes (which can reach up 20–30% of the biomass of leaves), support a high secondary production in situ and in detritivore compartments of other communities (around 80% of total production, Cebrián and Duarte 2001), thereby sustaining complex food webs from beaches to bathyal areas. A moderately wide (1 km) belt of *P. oceanica* meadow may produce litter in excess of 125 kg of dry seagrass material per meter of coastline each year (mostly during late summer and autumn, when the plant loses its leaves). This material accumulates on the beach, developing cushions up to 4 meters high (called banquette, seagrass litter, seagrass berm, beach-cast litter and/or beach wrack), which can in turn sustain a complex invertebrate food web, protect the shoreline from erosion, deliver sand in the form of carbonate and silica shells and, when transported further inland by the wind, act as seed material for dune formation (Borum et al. 2004). The formation of the banquette depends on the availability of seagrass litter (leaves and rhizomes) on the upper shoreface, and originates with the deposition and accumulation of this material, mixed with sediments, at the extreme landward point of wave influence (Simeone and De Falco, 2012; Gómez-Pujol et al., 2013; Vacchi et al., 2017) (Figure 2.11).

Figure 2.11 – Example of banquette on the Poetto beach – photo by Daniele Trogu

On sheltered beaches, the presence of leaf litter on submerged beaches is related to the proximity of *P. oceanica* meadows to the shoreline, as for other seagrasses and terrestrial plant species colonizing the foreshore (Jackson et al., 2002; Simeone and De Falco, 2012, Vacchi et al., 2017). On exposed beaches, leaf litter can be transported as floating material during storms and can be deposited, when the storm decreases in energy, far from the meadow from which the leaf litter originates (Simeone and De Falco, 2012, Vacchi et al., 2017). On embayed beaches, leaf litter deposited on the seafloor can remain enclosed by headlands for a long period of time (from days to seasons), and this can promote repeated cycles of deposition and erosion of seagrass berms on this beach typology (Simeone et al., 2013, Vacchi et al., 2017).

In the literature, the debate on the role that banquettes play during storm events against coastal erosion is still open (Gómez-Pujol et al., 2013; Simeone et al., 2013; Vacchi et al., 2017). Although banquettes are often suggested to play a role in beach protection from erosion (Boudouresque and Jeudy De Grissac, 1983; Mateo et al., 2003), very few studies have been published on this issue. On low energy and short fetch beaches, beach-cast leaf litter can resist waves and be effective in suppressing wave run-up and limiting beach change (Nordstrom and Jackson, 2012). In contrast, Gómez-Pujol et al. (2013) found that seagrass berms were eroded during swell conditions between two consecutive storms on a semi enclosed beach in the Balearic Islands. Under such conditions, the capacity of these features to protect beach from erosion during storms is thought to be negligible, because no interaction between waves and beach-cast leaf litter can occur. In other Mediterranean regions, the residence time of seagrass berms on beaches is higher than the time interval between storms (Simeone and De Falco, 2012; Simeone et al., 2013). In these cases, some proportion of storm energy may be dissipated by the destruction of the banquettes (Vacchi et al., 2017).

2.2.1 Legislation for the management of beached *Posidonia oceanica*

Posidonia oceanica meadows are protected by various international conventions and are classified by the European Community legislation as priority natural habitat types that are in danger of disappearing (Habitat Directive and the Water Framework Directive). Even when these plants die, their residues deposited on the beaches perform a crucial function of conservation of coasts and their ecosystems. Nevertheless, it is evident that these barriers of dead plants on Mediterranean beaches considerably limit the suitability for bathing. Therefore, in these cases, their removal must be considered, creating the problem of reconciling environmental protection and tourist use.

Due to its recognized services offered in terms of coastal protection, in Italy the regulation of *Posidonia oceanica* falls within the exclusive competence of the state legislator on protection of the environment and ecosystems (Resolution 8123/2006 "Management of beached *Posidonia*

oceanica" of the Ministry of the Environment). The regional legislative competence in the field of tourism can be exercised, only insofar as it is not in contrast with the state discipline. Moreover, the management of these deposits is subject to the regulation of waste, even though the ascription of *Posidonia oceanica* wracks to the notion of waste does not have that negative connotation associated with this term in everyday language. In the context of the European waste regulations, the Italian legislation provides for beached *P. oceanica* a specific rule, establishing that it can be buried on site without incurring in uncontrolled deposit or landfill waste crimes. In the same direction, only when the operations of collection, grouping, sorting of *P. oceanica* wracks are carried out in situ, the articulated rules on waste do not apply. The 2016 regional (Sardinian) resolution (40/13 of 6.7.2016) entitled "Operational guidelines for the management of *Posidonia oceanica* deposits on beaches" identifies the following management modalities:

- Keeping *Posidonia oceanica* wracks on site;
- Movement of the deposits and repositioning in the winter period;
- Permanent removal and disposal.

Other options introduced later may be:

- Burial;
- Repositioning on the dune.

The resolution suggests that the preferred strategy is to keep the wracks on site. In the event that, for technical reasons that objectively hinder the usability of the beach in the summer season, keeping the Posidonia deposits on site is extremely problematic, the option of moving and subsequent repositioning of the accumulations and the transfer to waste disposal or recovery plants can be pursued following some procedural and operating instructions. The most relevant instructions are:

• The removal operations of the wracks must be avoided in winter, as they would deprive the beaches of a natural protection system;

• The operations must be carried out with particular caution in order to avoid the removal of sand: the recovered sand must be redistributed along the beach;

• The selection phase of the plant material should preferably be carried out by manual means, but the use of mechanics of appropriate size is also allowed, which must in no case cause damage. The use of tracked vehicles is prohibited.

• The material collected and selected must be accumulated in a secluded area of the same beach, arranged so as not to negatively interfere with the morphodynamics and biocenosis of the beach;

• This movement must be seasonal, with the removal of *Posidonia oceanica* in spring or summer and possible repositioning in autumn.

Although the legislation is written specifically for the management of *Posidonia oceanica* banquettes, (in principle) its approach can be extended to any biomass deposited on beaches.

2.3. Global climate changes and 2030 Agenda

Coastal areas are one of the environments most exposed to the impacts caused by global climate change and sea level rise (Knutson et al., 2010; Kaarel et al., 2003). In this regard, climate change and the consequent ocean warming can modify the wave parameters (like significant wave height (Hs), mean wave period (Tm) and mean wave direction (degree) globally and locally (Young and Ribal, 2019; Reguero et al., 2019), causing flooding and damage to infrastructure built near the coast. Furthermore, given that coastal areas are the most populated zone worldwide (Small et al., 2003), it is essential to try to find actions that can mitigate the impacts caused by climate change. In recent decades, the management of these environments has received increasing attention both for reasons related to the exploitation of these areas for tourism / industrial purposes and for the management of extreme events and the rise of the average sea level, related to the climate change in progress. The coastal countries of the European Union are already experiencing the negative impacts of climate change and are required to react promptly to protect their territories, citizens and resources through the adoption of adaptation measures. Also for this reason, in September 2015, the United Nations General Assembly, through the governments of 193 UN member countries, established the 2030 Agenda for 'Sustainable Development', an action program for the people, the planet and the prosperity. It incorporates 17 Sustainable Development Goals, SDGs - into a large action program for a total of 169 'targets' or goals that are expected to be achieved by the year 2030.

In particular, goals 13 14 and 15 are closely linked to the topics analysed in this thesis:

- SDG 13: Take urgent action to combat climate change and its impacts
    - Target 13.1: Strengthen resilience and adaptive capacity to climate-related hazards and natural disasters in all countries
    - Target 13.3: Improve education, awareness-raising and human and institutional capacity on climate change mitigation, adaptation, impact reduction and early warning

- SDG 14: Conserve and sustainably use the oceans, seas and marine resources
    - Target 14.2: By 2020, sustainably manage and protect marine and coastal ecosystems to avoid significant adverse impacts, including by strengthening their

resilience, and take action for their restoration in order to achieve healthy and productive oceans.

- SDG 15: Sustainably manage forests, combat desertification, halt and reverse land degradation, halt biodiversity loss
    - Target 15.5: Take urgent and significant action to reduce the degradation of natural habitats, halt the loss of biodiversity and, by 2020, protect and prevent the extinction of threatened species

In this context of both climatic and socio / economic change, the key role of coastal monitoring programs, carried out by accredited research clusters (universities, etc.), which allow to collect the data necessary for the characterization of marine and coastal processes more significative, is evident. An extensive and structured database is an essential requirement for an adequate knowledge of the processes affecting a given coast, identifying the relative spatial / temporal scales of changes and separating seasonal fluctuations from possible long-term trends. Among the key parameters to be monitored are both seas forcing, such as the average sea level fluctuations, the height and period of the incident wave motion and the rise of the wave on the beach. In addition, the morphology and integrity of the coastal zone are to be considered as they determine its vulnerability and resilience. The role played by coastal ecosystems in coastal protection has been recognized by several studies (Boudouresque et al., 2009; De Falco et al., 2014, 2017; De Muro et al., 2017a, b, c; Trogu et al., 2020; Vacchi et al., 2017). Among the elements of coastal ecosystems that play a key role in reducing the negative impacts of erosion and flooding processes, we can identify the submerged *Posidonia oceanica* meadows, beached biomass and dune habitats (Buosi et al., 2017; Passarella, 2019; Passarella et al., 2018, 2020; Simeone et al., 2013). Monitoring the evolution of these elements is also necessary in the case of recovery and redevelopment of coastal strips (De Muro & De Falco, 2015).

2.4. The contribution of video monitoring for coastal morphodynamic studies

Studies carried out to understand the morphodynamics of a beach are based on the application of methodologies widely used to analyse the mechanisms that regulate the seasonal dynamics of a beach system (topographic, bathymetric and sedimentological measurements). In order to obtain the data, it is necessary to carry out seasonal land-sea field campaigns that require a considerable effort both in terms of money and of working hours. Furthermore, these do not allow a homogeneous control, in space and time, of the entire beach system and do not allow the collection of continuous data sets.

A first major change occurred in 1984 when the first Argus system was tested by the Coastal Imaging Lab (CIL) of the University of the State of Oregon. The novelty of this approach consisted in acquiring images at regular time intervals that allowed to study the wave run-up and the period of gravitational waves (long-term waves, 30 seconds), a common phenomenon in Oregon (Holman and Bowen, 1984). The data was played back one at a time and the swash zone was manually digitized. Argus' main product, however, appeared a few years later, when the potential of time-exposure images or images with long exposure times were discovered almost by chance during a study on a pocket beach. In 1987 a 35mm camera was installed with a 13 frame stop neutral density filter set at a 10-minute exposure. The result of the images was surprising, showing the morphologies of the surf zone quite clearly.

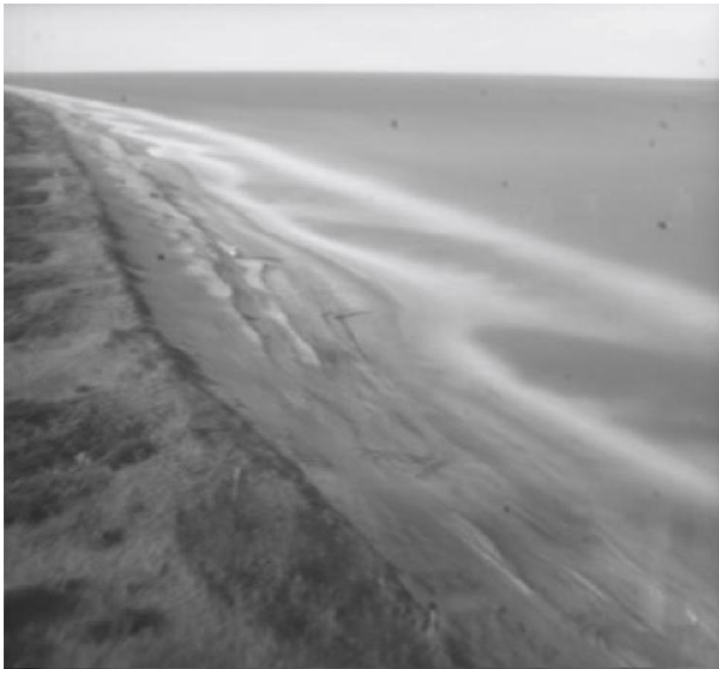

Figure 2.12 - A time-exposure image of the Argus project with clear morphologies of the surf zone. October 7, 1986, Duck, North Carolina (http://cil--www.coas.oregonstate.edu/argushistory.thml)

Numerous other projects were thus carried out, such as Argus-I, which aimed to improve the system adopted, obtaining an ever-greater automation of acquisition and possibility of data transfer. This made it possible to no longer have to manually carry out the processing and transfer

of data (at the time acquired on videotapes). The first automated station thus appeared in 1992 with the Argus-I project: this system was based on a "Dipix" processing card installed on a computer with a DOS operating system, installed in Yaquina Head, Oregon, and then sent to the University of State of Oregon via a modem. The images sent were always in black and white. Initially, the only processing that was carried out was the mediated image (time-exposure). Over the years this system has been further implemented, switching to the use of software on the Linux platform.

Numerous sites around the world are still videomonitored by systems evolved from the first Argus systems.

The main products obtainable from a video monitoring system can be catalogued in:

- **Snapshots:** this kind of images are the single images acquired at the frequency set by the video monitoring system and, consequently, represent an immediate snapshot of the beach system in that particular second but which are not able, on their own, to provide further quantitative data and about the dynamics of the beach.

Figure 2.13 - An example of a snapshot image from Poetto beach

- **Time-exposure (timex) images:** usually this kind of images are the first step for a subsequently morphodynamic study because allow us to understand the morphology of the shoreface (like the configuration of bars and troughs). Nowadays there are a large amount of scripts that are able to create timex images (like ArcGis, MatLab, etc.), through the arithmetic media of the luminous intensity RBG of each pixel of the image, for all the images acquired in the recording interval (for example, at Poetto beach, approximately 7200 images for interval). The bright zone of the timex images (red line, Figure 2.14) represents a shallow zone of the shoreface where the waves break above the breaker bars and near the shore. The dark band corresponds to slightly deeper zones where longshore and rip currents flow, creating trough and rip channels (blue arrow, Figure 2.14); here the waves do not break. The movement of bars and troughs during storms determines the morphodynamic state of the beach, that can be assessed using the classification proposed by Short (1999).

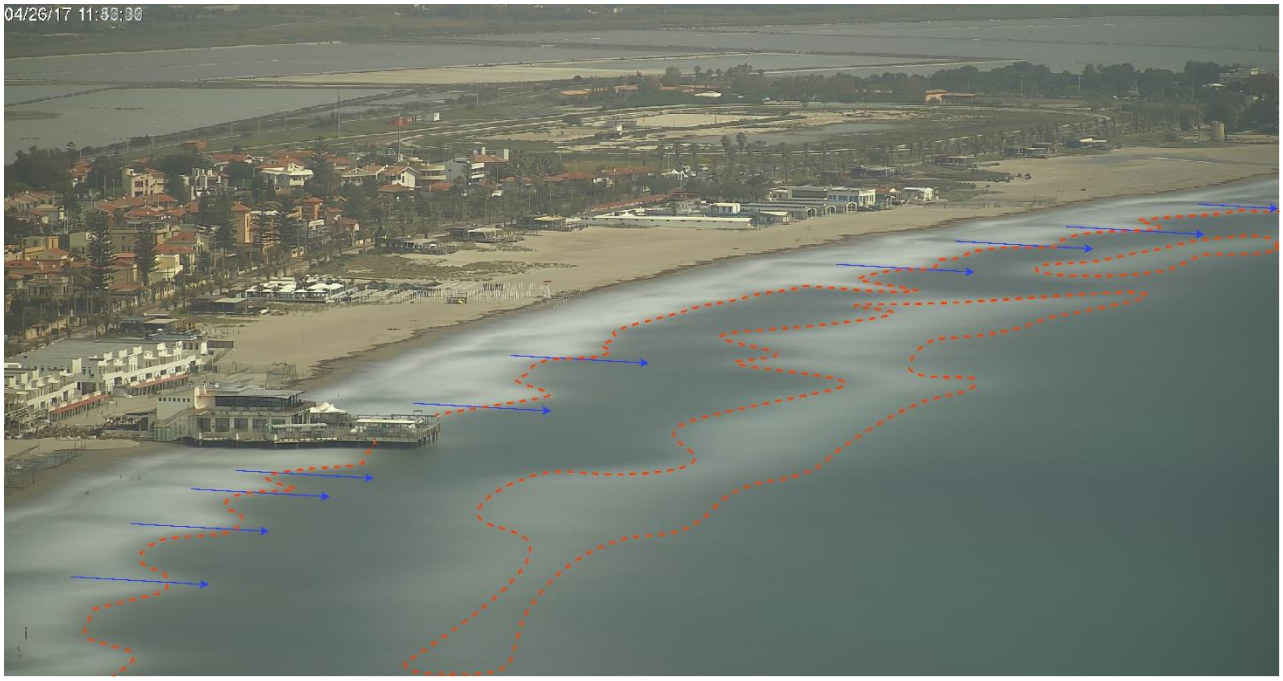

Figure 2.14 - An example of a time-exposure image from Poetto beach

- **Time variance images**: like timex images, they are obtained through statistical processing of the snapshot images. They differ from the timex in that the average intensity of each individual pixel is not calculated, but the statistical variance of the light intensity of the pixel that characterized it during the minutes of snapshot acquisition. In the equation below x_I represents each single snapshot, μ the average and N the total number of snapshots:

$$O_I^2 = \sum_{I=1}^{N} (x - \mu)^2 / N$$

Figure 2.15 - An example of a variance image from Poetto beach

This type of images, in addition to highlighting the morphodynamic states of the surf zone, can be used for runup and shoreline detection (Simarro et al., 2015).

- **Rectified images**: are images made perpendicular and georeferenced that allow to calculate volumes and thicknesses, trace the shore lines, trace the bars, banquettes and any other relevant factor using a GIS. For this work, the rectification is processed through the MatLab software, by entering fundamental parameters such as the coordinates of the shooting point, the height of the camera, the shooting angle, the coordinates of some fixed points of the image (called Ground Control Points, GCP) and other parameters required by the program. Once the rectified image has been obtained, it can be georeferenced in a GIS software.

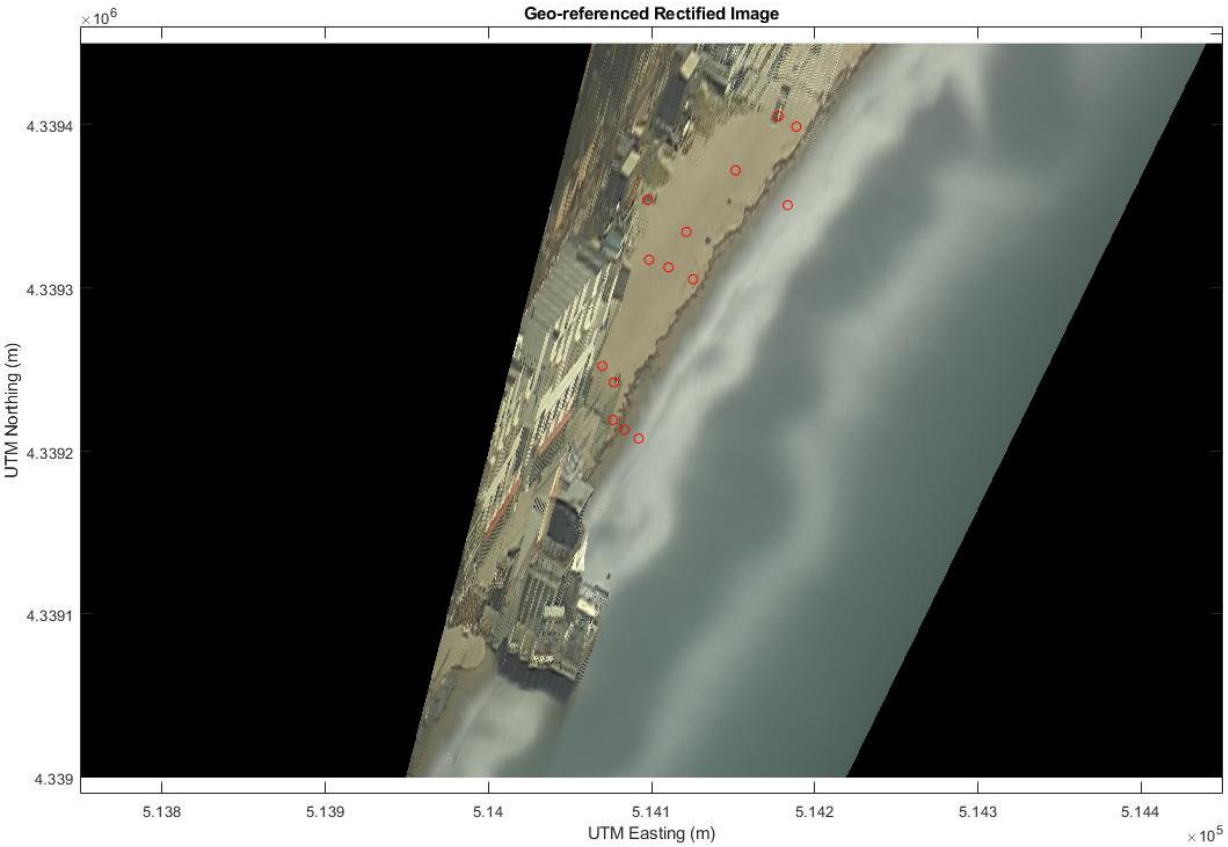

Figure 2.16 - An example of a rectified timex image from Poetto beach. Red circles represent the GCP.

- **Timestack images**: these images are used in analysis that concerns methods for evaluating and quantifying the hydrodynamic processes by tracing the characteristics of the wave field, the speed of the currents and the runup processes (swash and uprush). Fixed, on a base image, a vector of pixels, in the cross-shore direction or in the long-shore direction, the historical series of their luminous intensity can be extracted in rapid succession over time, called a time-stack. The concept behind this approach is that each pixel has been treated as if it were a monitoring tool positioned in situ at that point. So while traditional measurements require the in situ installation of tools with a high

maintenance cost, the use of pixels is much more practical and economical. This type of processing is used to measure wave speed and direction, wave run-up and swash excursion, to monitor shore line migration, and to calculate the bathymetry of the offshore area. (http://www.planetargus.com). In the time-stack images (Figure 2.16) time and space (cross-shore or long-shore) are the axes of the graph (the space can be set in the X axis and the time in the Y axis and vice versa). The white streaks indicate the trend of the breakers of the waves. The images can be used to quantify the celerity and angle of incidence of waves traveling towards the shore (Lippmann and Holman, 1991) and to calculate the statistic of the breaking waves and the wave breaking patterns along the surf zone (Lippmann and Holman, 1992). Thanks to visible signs that remain on the surface of the sea (traces of foam and turbulence at the passage of a wave), the time-stacks allow the monitoring of longshore currents (Chickadel and Holman, 2002a; Chickadel et al., 2003, Cohen et al., 2004) and cross-shore (Chickadel and Holman, 2002b), induced by the passage of the waves and the motion of the tidal wave, a process studied in particular for a coastal bay (Davidson and Morris, 2002). Time-stacks representing the shore area, perpendicular to the shore, (Holland and Holman, 1993), were used to evaluate the characteristics of the wave run-up in a natural beach (Holland et al., 1995) and the hydro- and morpho-dynamics of the swash region (Holland and Puleo, 2001, Passarella, 2018).

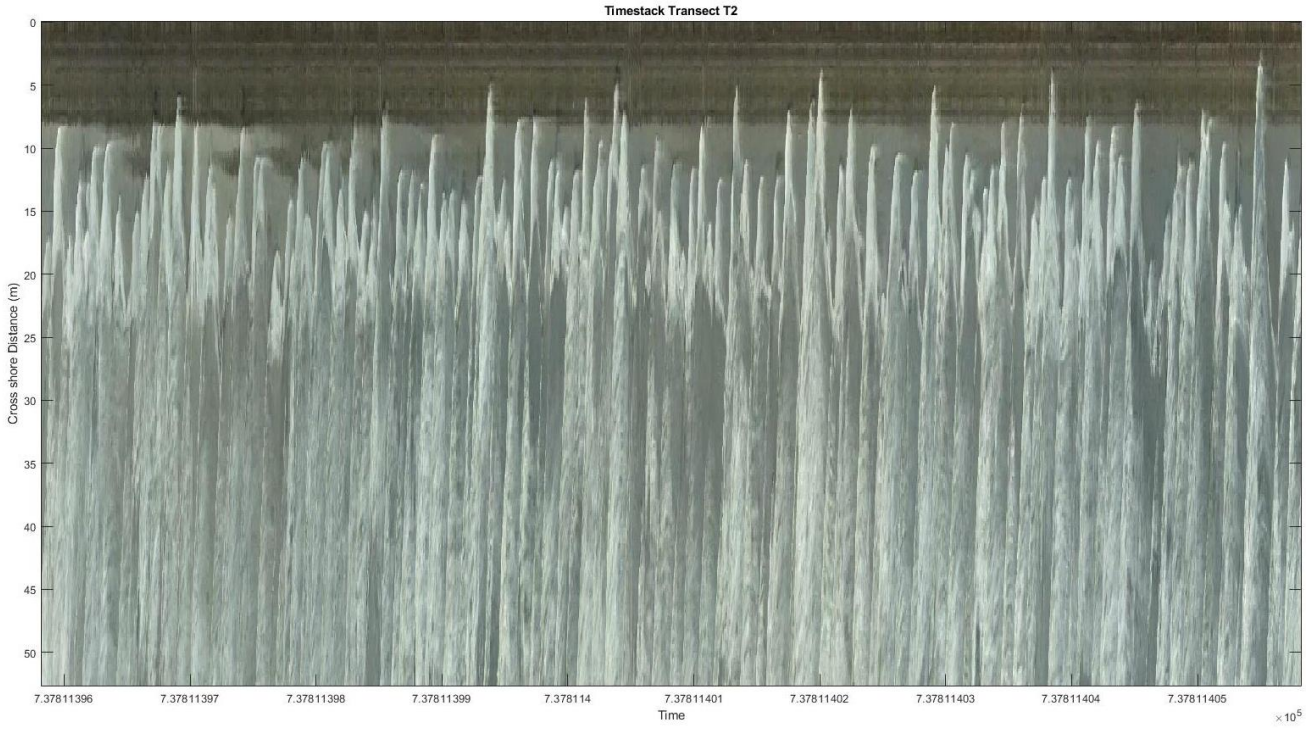

Figure 2.17 An example of a timestack image from Poetto beach.

Chapter 3
METHODOLOGY

In this thesis three beaches in southern Sardinia are studied and analysed through a multidisciplinary approach, which includes both remote and in-field measurements such as topographic and bathymetric surveys, drone surveys, analysis of images coming from coastal videomonitoring system, aerial orthorectified photographs, and specific instrumental measurements like water infiltrometric tests.

3.1. Topographic surveys in dry beach

The surveys in dry beach were carried out in Poetto and Giorgino beaches, along transects, perpendicular to the shoreline, that run over the dry beach from behind the dune system to the shallow shoreface at about one meter depth, where the topographic survey can connect to the bathymetric survey. The number and distance of transects varies according to the experiment and / or study conducted, even within the same beach. For example, in the Poetto beach a survey of the entire beach foresees 21 transects spaced about 300m apart, while for another study (reported in chapter 8) only 4 transects on dry beach (spaced about 150m apart) and 8 transects in submerged beach were used (spaced about 50m). A DGPS (Differential Global Positioning System) or GNSS (Global navigation satellite system) and / or StarFire (Navcom SF3040) systems connected in real time (Real Time Kinematic - RTK) to a correction network ashore (subscription to the NETGEO network) was used to acquire the *XYZ* coordinates of the points. The horizontal accuracy of the instrument is 1 cm + 0.5 ppm, while the vertical accuracy is 2 cm + 1 ppm.

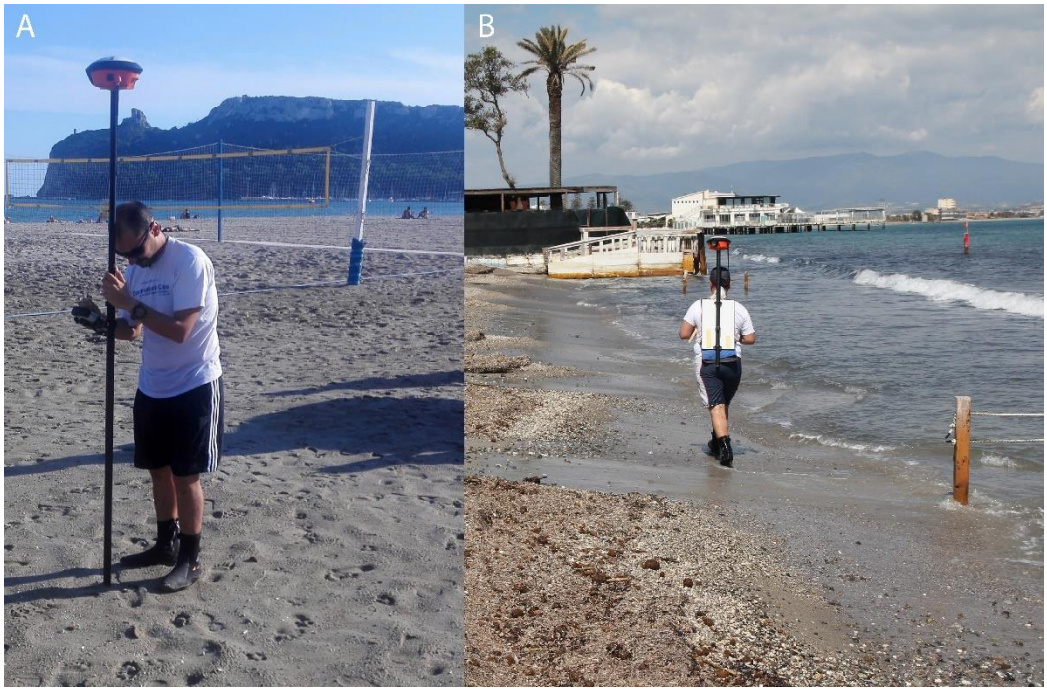

Figure 3.1 - Topographic survey at Poetto beach. A) data acquisition whit the rod; B) data acquisition with the backpack.

To limit operator errors to a minimum, especially as regards z values, for the transepts surveys the instrument was placed above a rod and the acquisition took place once the instrument was level. For each point, 10 xyz data were acquired on average, which in turn were averaged to obtain a value as accurate as possible (Figure 3.1 A). The acquisition frequency of the points used for the surveys was 1Hz. The position of the shoreline and the seaward limit of the dune vegetation (dune foot) were also acquired. To carry out these last surveys, where z's errors can be most neglected, the instrument was placed on a special backpack (Figure 3.1 B).

3.2. Bathymetric surveys in submerged beach

Also the bathymetric surveys were carried out in Poetto and Giorgino beaches using a Reson Navisound 215 dual-frequency single-beam ultrasound system (emission frequencies at 210 and 33KHz), connected to DGPS Omnistar 8300HP and interfaced through a personal computer using the dedicated Reson PDS2000 navigation and acquisition software. The accuracy declared by the instrument is 1 cm at 210 kHz (1 sigma), 7 cm at 33 kHz (1 sigma), assuming correct sound velocity, transducer draft. The bathymetric profiles of the Poetto and Giorgino submarine beaches were measured along transects perpendicular to the shoreline. The processing of the bathymetric data included corrections for tidal fluctuations and vertical draft of the instrument. All single-beam profiles were subsequently cleaned of spikes (outliers) and exported in ASCII format (x, y, z). Data interpolation and profile analysis were performed on GIS software. In order to compare two profiles relating to the same transect, "traces" were created with coincident start and spacing, so as to be able to compare the temporal variations between one survey and another.

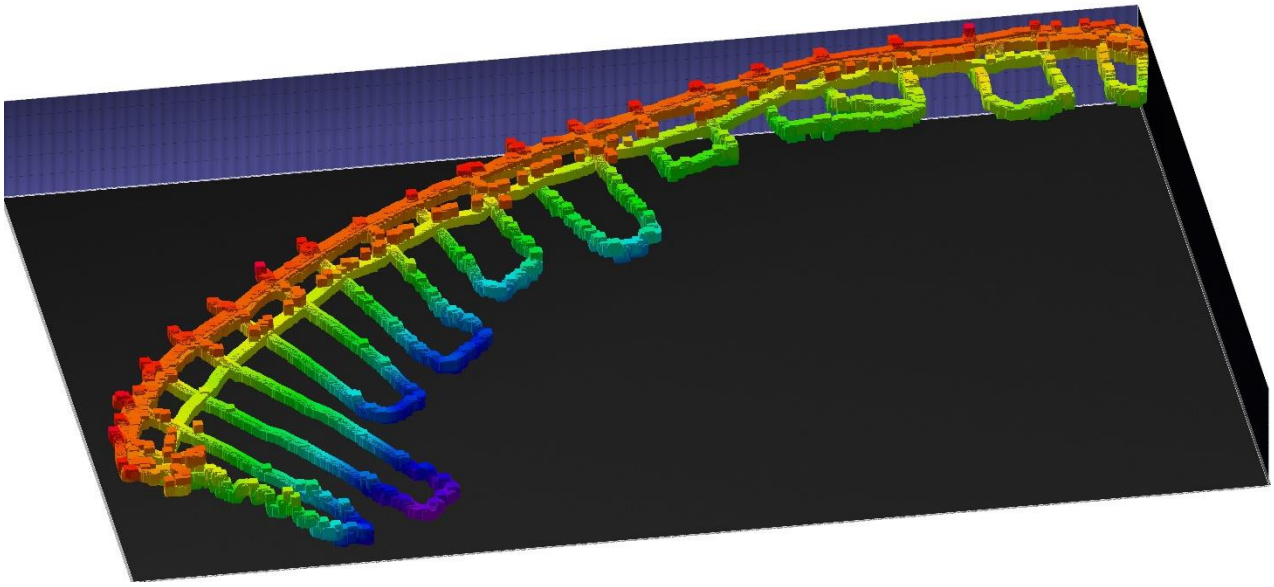

Figure 3.2 - Bathymetric survey of 21 May 2019 at Poetto beach.

3.3. Drone surveys

There were three drone surveys, in collaboration with *Teravista* Company: the first one in May 2019 which covered the entire Poetto beach, and two others (one in April and one in May 2020, before and after the removal of *Arundo donax* reeds, chapter 6) carried out only in the areas linked to the videomonitoring system. For georeferencing the drone images were mapped 271 ground control points in total with a DGPS (Differential Global Positioning System) and StarFire (Navcom SF3040) connected in real time (Real Time Kinematic - RTK) to a ground correction network (subscription to the NETGEO network). The elaboration of drone surveys provides a DTM (Digital Terrain Model) with possible contour lines every 2cm and orthophotos with a resolution of 20 Mpx.

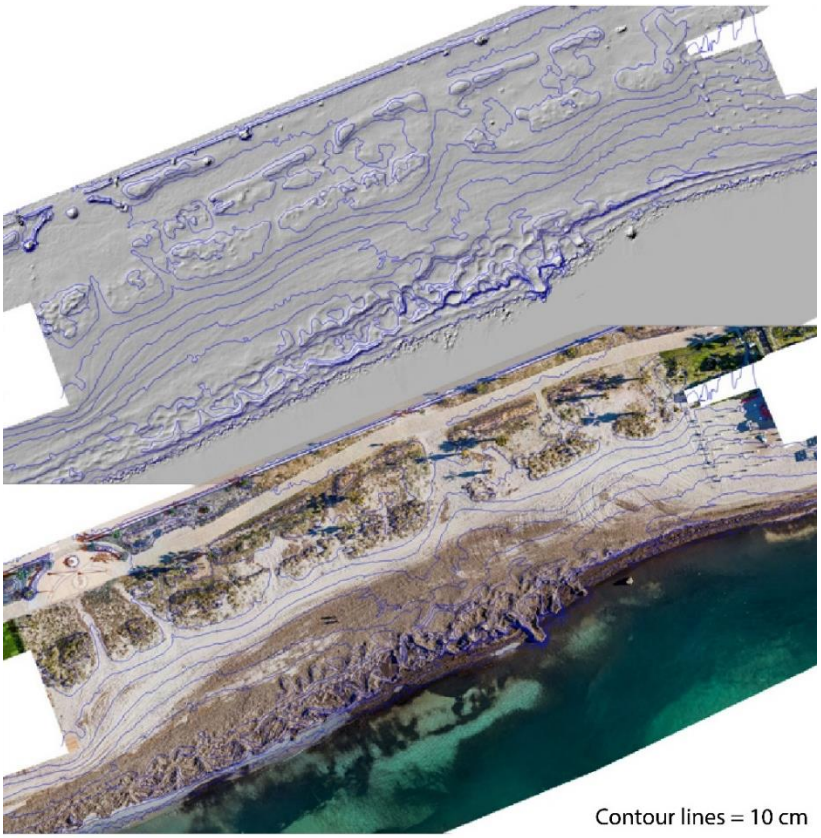

Figure 3.3 – DTM and orthophoto with contour lines at Poetto beach, from the survey of 21 May 2019.

3.4. Videomonitoring system data

For the realization of the chapters 4 and 8 of this thesis were analysed images that coming from two different videomonitoring system station installed in southern Sardinia, Italy. The first one is located at Piscinnì beach (red rectangle in Figure 3.4) and the other one at Poetto beach (yellow rectangle in Figure 3.4). Both of these beaches are microtidal and wave dominated Mediterranean beaches, but the difference is that Piscinnì (examined in chapter 4) is a natural beach, whereas Poetto (examined in chapter 5) is an urban beach.

The camera for Piscinnì beach, powered by a photovoltaic system, is a Samsung IP Megapixel SNC-1300P, equipped with megapixel optics *Fujinion Varifocal* protected by an IP600 outdoor housing, coupled with a meteo station Davis Vantage Pro2 wireless. This system was installed on a promontory at south-east of the beach (geographical coordinates 38.90900°N; 8.78575°E) at a high of 117m above SWL and acquired images at a frequency of 1Hz (resolution: 1280x720 pixels) for two daily interval of five minutes each.

The camera for Poetto beach, also this one powered by a photovoltaic system, is a Dahua 12 Megapixel Ultra HD Network Cameras (model DH-IPC-HF81200E) and was installed at Sella del Diavolo promontory (geographical coordinates 39.18992°N; 9.15824°E) at a high of 125m above SWL. This camera is set to record data four times per days, every 3 hours (from 8:00 to 17:00), for 30 minutes long intervals at a frequency of acquisition of 4Hz (resolution: 4096x2160 pixels). In order to correct the images from the distortions induced by the camera lens, the internal camera parameters were computed (e.g. focal length, principal point position, radial and tangential distortion coefficients) and the camera, in 2017, was calibrated (Passarella, 2019).

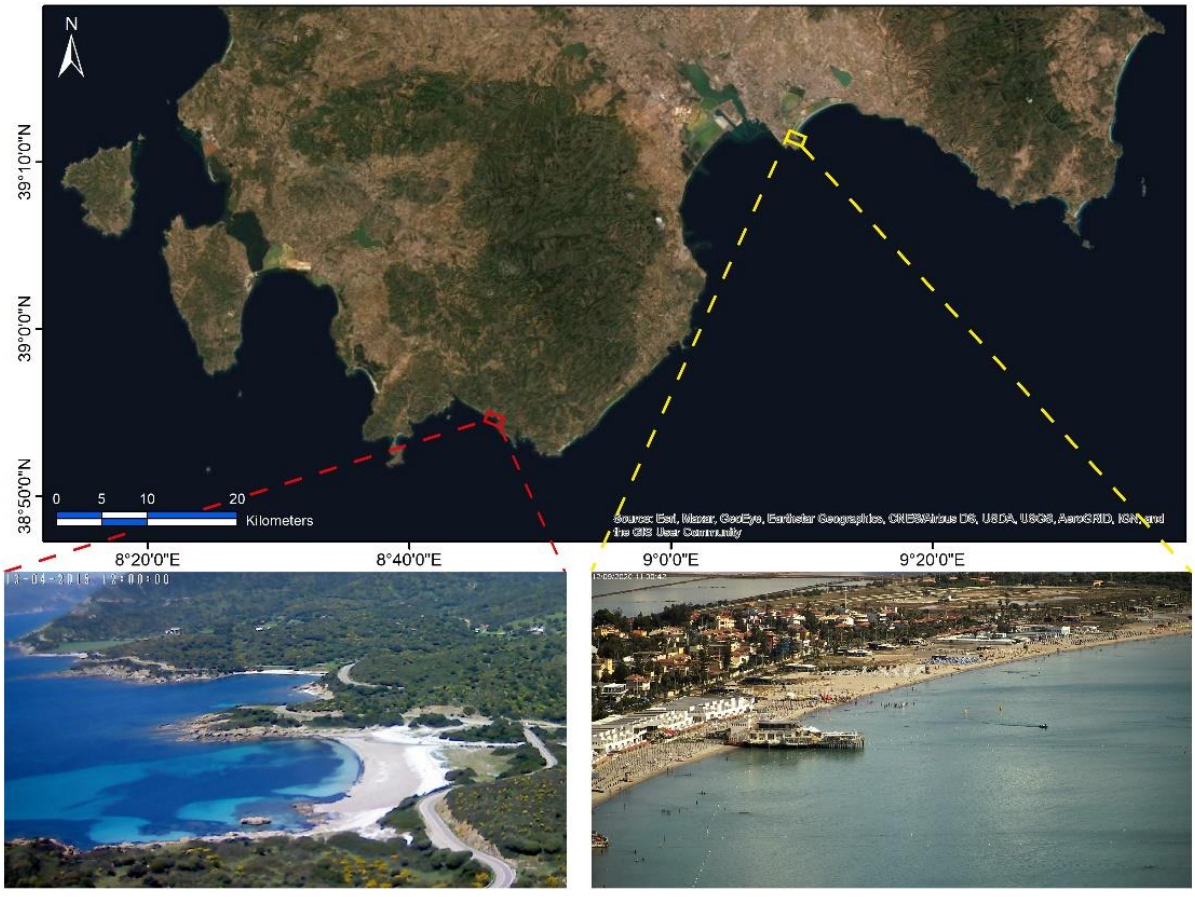

Figure 3.4 – Two of the videomonitoring station managed by the CMGG and used for this thesis.

3.5. Water infiltrometric tests

Chapter 6 analyses a field experiment, carried out in collaboration with '*Servizi Geotecnici*' company, aimed at measuring the water infiltration rate in the various sectors of the Poetto beach, from the beach berm to the foot of the dune system, whereas another one is on banquette (Figure 3.5B). The tests simulate the actual drainage conditions of the beach and are used to experimentally define the drainage coefficients of the sediment. The tests were performed through a double ring infiltrometer following the ASTM d3385 standard. The instrument consists of two concentric metal rings of 32 and 57 cm in diameter, 30 cm high and with a sharp edge at the bottom, which are introduced into the sediment for about 10 cm. During the test, clean water was poured over the bottom of the outer ring and then the inner ring to a height of about 10 cm, until the same level was reached in the two rings. After having filled the two rings to the same level, the variation in the level contained in a certain time interval t in the inner ring was measured. The test was considered completed when, after subsequent fillings, the infiltration capacity of the sediment became constant over time. During the experiment, the following were measured: the height of the water in the inner ring, the duration of the test and the lowering. In total were carried out 5 permeability tests: 4 along a transect, and another one on the banquette, see Figure 3.5B.

Figure 3.5 – Two drone images with location points of water infiltrometric tests, at Poetto beach.

3.6. Aerial orthorectified images and DSAS method

The use of satellite and aerial imagery is widespread for many studies. For most of the location maps of the chapters of this thesis, aerial orthorectified photographs were analysed. These images are available for consultation on the open access website "Sardegna Geoportale" (www.sardegnageoportale.it) which is part of the SITR ("Sistema Informativo Territoriale Regionale"). Through the WMS (Web Map Service), is possible to upload and analyse, on a GIS client, these orthorectified images (the total coverage of Sardinia is

available from 1954 to 2019, but for some coastal areas also from 1940, with pixel resolution up to 20 cm).

Figure 3.6 - An example of a 1940 aerial orthorectified image of the southern portion of Poetto beach

Moreover, in chapter 5, we also adopted the DSAS method (Digital Shoreline Analysis System, an extension of ArcGIS™ software), that enables a user to calculate rate-of-change statistics from multiple historical shoreline positions. It provides an automated method for establishing measurement locations, performs rate calculations, provides the statistical data necessary to assess the robustness of the rates. DSAS generates transects that are cast perpendicular to the reference baseline at a user-specified spacing alongshore. DSAS measures the distance between the baseline and each shoreline intersection along a transect, and combines date information, and positional uncertainty for each shoreline, to generate the following change metrics: end point rate (EPR), the linear regression rate (LRR), the shoreline change envelope (SCE) and the net shoreline movement (NSM). The first two parameters represent the speed of accretion and erosion in meters per year. The EPR is obtained by dividing the distance (m) between two shorelines by the time spanning between the earliest and the latest shoreline (Thieler et al., 2009; Genz et al., 2007), the LRR is determined by fitting a least squares regression line to all shoreline points and, therefore, represents a modelled forecast of the shoreline rates of change. The SCE is a measure of the total change in shoreline movement considering all available shoreline positions and reporting their distances, without reference to their specific dates. NSM reports the distance between the oldest and the youngest shorelines (Thieler et al., 2009; Temitope D. Timothy Oyedotun, 2014).

3.7. Side-scan sonar and modelling approach

As mentioned above, a multidisciplinary approach has been adopted for this PhD thesis, which includes both remote and in-field measurements but also, in some cases, a modelling approach. Another in-field survey that has been used marginally in chapter 5 is that relating to a side-scan sonar survey coming from *Mappatura delle praterie di Posidonia oceanica lungo le coste della Sardegna e delle piccole isole circostanti* (Ministero dell'Ambiente e della Tutela del Territorio – Servizio difesa del mare, 2000). The side-scan sonar sends and receives the acoustic pulses that help map and recognize the morphologies of the seafloor, through the different acoustic responses that the different types of seabed have (for example: rocks, sand, or *Posidonia oceanica* meadows).

Two different modelling approaches were also adopted in chapter 6, to simulate the interactions between waves and the organic berm. The first one, the SWAN model, is a spectral wave model based on the wave action equation and numerically propagates in the nearshore the incident wave conditions collected at the six nearshore grid nodes of the Copernicus Marine Environment Monitoring Service (CMEMS) system. The grid used in the SWAN simulation has a spatial resolution of 1/16 of nautical mile (about 115 m) and allows the achievement of the wave conditions in the proximity of the beach and the identification of the main wave transformation processes in coastal water. The spectra obtained as output of the SWAN simulations were used as a boundary conditions for the wave-resolving model XBeach (Roelvink et al., 2018) covering the shallow water area. We used the nonhydrostatic module of XBeach, based on the nonlinear shallow water equations. The numerical domain covered the nearshore area from 14 m of depth up to the toe of the dune system. Simulations were setup in 1D cross-shore mode along the two transects of Poetto beach (see chapter 6).

Chapter 4
SHORT TERM EFFECTS OF STORM EVENTS ON THE COASTLINE MORPHOLOGY OF A MEDITERRANEAN MICROTIDAL WAVE-DOMINATED BEACH (PISCINNÌ, SW SARDINIA)

The main findings of this chapter have been published in:

Trogu, D.; Buosi, C.; Ruju, A.; Porta, M.; Ibba, A.; De Muro, S. *What Happens to a Mediterranean Microtidal Wave-dominated Beach during Significant Storm Events? The Morphological Response of a Natural Sardinian Beach (Western Mediterranean)*. J. Coast. Res. 2020, 95, 695–700.

4.1 Introduction

Coastline dynamics of Mediterranean microtidal wave-dominated beaches with an inner shelf characterized by *Posidonia oceanica* meadow are still poorly documented especially during significant storm events. These beaches represent a common environment in natural and anthropized zones of the Mediterranean coasts, where storms can induce important morphodynamic responses and morphological changes such as beach and dune erosion, overwash and/or inundation in natural areas as well as infrastructure damage on developed coast (Mendoza and Jimenez, 2006, 2009). Nowadays, the understanding of the interaction between beach dynamics (e.g., classification and distribution of morpho-sedimentological features in relation to wind, waves and hydrodynamic processes), human impact (e.g., beach cleaning operations, bulldozing, dumping, dredging), benthic marine habitat (e.g., distribution of seagrass meadow) and climate forcing is crucial for scientist and coastal planners to evaluate coastal risks and to develop the best measures to mitigate them (De Muro et al., 2017a, 2018; Gervais et al., 2012). In particular, an integrated sea-land, beach management approach has to take into account the identification, the understanding and the description of static and dynamic processes in coastal area, including the connection with the sea-level rise and increasingly common extreme events linked to global warming (Buosi et al., 2017; Muro et al., 2017b). In this regard, climate change and the consequent ocean warming can be considered as factors affecting waves globally and locally (Young and Ribal, 2019; Reguero et al., 2019), that are able to generate variations in the wave parameters (like significant wave height (Hs), mean wave period (Tm) and mean wave direction (degree). Within this context, remote and in situ observations allow the monitoring of beach dynamics providing relevant data to understand their evolution under climate change scenarios.

In this work, the main shoreline changes, in terms of displacements of the shoreline position, are evaluated and quantified on Piscinnì, a Mediterranean beach located in southern Sardinia (Italy; western Mediterranean Sea). In addition, this research aims to: (i) correlate the shoreface

variability with the wave energy flux; (ii) understand the role of *Posidonia oceanica* beach-cast litter and (iii) investigate the morphodynamic states of a Mediterranean beach during the main significant storm events.

4.2 Study area

Piscinnì is a South-West oriented, microtidal, wave-dominated beach, about 270 m long, located in the south-western coast of Sardinia (Figure 4.1). This area is part of the rias coastal system, extending for about 25 km, between Cape Spartivento to the South, and the Cape Teulada Promontory to the West. A seasonal stream (Piscinnì river) flows into the beach generating a pond in the depression behind the dunes.

The main geographical fetch of Piscinnì beach is between 211° and 245°, with all possible direction for approaching storm ranging from 211° to 262° (Figure 4.1). The presence of promontory of Cape Teulada limits the geographical fetch width, that is long between 240 km and 530 km.

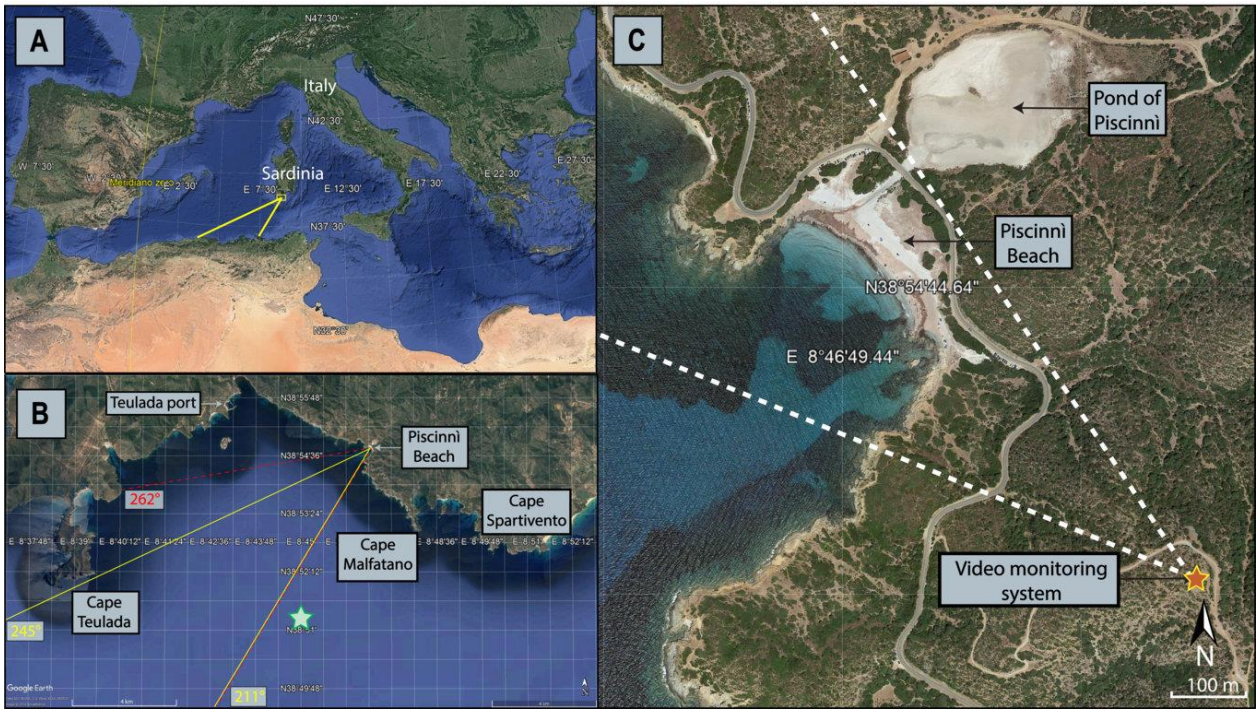

Figure 4.1 - Geographical setting of the study area. The geographical fetch and the effective fetch of 500 km in relation to Piscinnì beach (a, b), exposure field of wave motion. The green star in panel (b) shows the position of Copernicus hindcast, whereas the orange star in panel (c) indicates the location of video monitoring system.

We obtained the wave climate (Figure 4.2) offshore of Piscinnì beach from the Mediterranean Sea Waves Hindcast product (Ravdas et al., 2018), made available by the Copernicus Marine Environment Monitoring Service. This product is a 10-year wave hindcast covering the period February 2006-December 2016. It is based on the third-generation spectral wave model WAM Cycle 4.5.4 (Günther and Behrens, 2012). The model runs over a rectangular grid covering the

Mediterranean basin with a spatial resolution of 1/24°. Wave simulations include the refraction induced by both the bathymetry and the ambient currents obtained from CMEMS Med MFC Reanalysis. The wind forcing is represented by the ECMWF Integrated Forecasting System at 1/8° resolution.

We extracted the wave parameters (significant wave height, peak period and mean direction) computed at the grid node of coordinates 38.85°N, 8.75°E (green star in Figure 4.1b) as representative conditions of the incoming sea states at Piscinnì beach. The water depth, obtained from the EMODnet Digital Terrain Model (EMODnet Bathymetry Consortium, 2018), at this location is 105 m, thus yielding minimal effects on wave propagation.

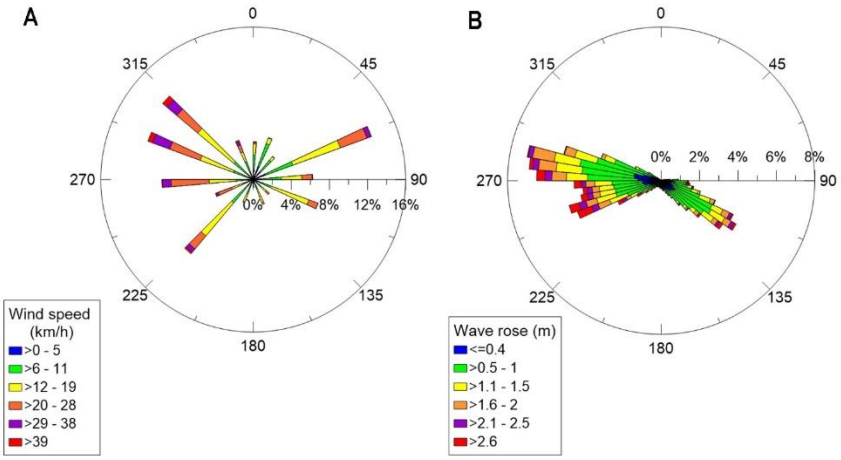

Figure 4.2 - Schematic illustration of (a) wind speed and direction at the Piscinnì weather station and significant wave height and direction at the Copernicus hindcast dataset point (b).

4.3 Methods

To estimate the shoreline position and the beach morphological variability, a video-camera system was installed in the promontory located SE of the beach, at about 117 m above msl (Figure 4.1c). This system was settled within the project LIFE07NAT/IT/000519 PROVIDUNE and consists of a video-camera Samsung IP Megapixel SNC-1300P with viewpoint megapixel Fujinion Varifocal and a weather control unit Davis Vantage Pro2. The study was conducted by analyzing video monitoring data for two years, from 01/08/2013 to 01/08/2015. The camera takes every day a sequence of snapshot for five minutes with a frequency of 1Hz, by 12:00 to 12:05. The 300 snapshot images of the pre-set daily interval were processed to obtain timex images, that allow us to understand the morphology of the shoreface (configuration of bars and troughs). The bright zone of the timex images (red arrow, Figure 4.3) represents a shallow zone of the shoreface where the waves break above the breaker bars and near the shore. The dark band (blue arrow, Figure 4.3) corresponds to slightly deeper zones (troughs) where the waves do not break. The movement of bars and troughs during storms determines the morphodynamic state of the beach, that can be assessed using the classification proposed by Short (1999).

The georectification of the timex images was achieved using the package "g_rect" for Matlab (Pawlowicz, 2003), that solves the geometric equation for each pixel of the image: the external orientation parameters define the position of the camera in real space, their calculation allows to establish the geometric relationship between the image coordinates (u, v) and the spatial coordinates (x, y, z). The parameters that define the external geometry of a camera system are defined by three angular values: azimuth (υ), tilt (τ) and roll (σ). The relation between image coordinates (u, v) and spatial coordinates (x, y, z) is formalized by a series of linear coefficients (1, 2):

$$u = \frac{L1xL2yL3zL4}{L9xL10yL11z1} \quad (1) \quad \text{and} \quad v = \frac{L5xL6yL7zL8}{L9xL10yL11z1} \quad (2)$$

L1 – L11 are linear functions of seven variables that represent the position of the videomonitoring system and f (effective focal):

$$\begin{aligned}
L &= -(x_c m_{31} + y_c m_{32} + z_c m_{33}) \\
L_1 &= \frac{(u_0 m_{31} + f m_{11})}{(\lambda_u L)} \\
L_2 &= \frac{(u_0 m_{32} + f m_{12})}{(\lambda_u L)} \\
L_3 &= \frac{(u_0 m_{33} + f m_{13})}{(\lambda_u L)} \\
L_4 &= (L_1 x_c + L_2 y_c + L_3 z_c) \\
L_5 &= \frac{(v_0 m_{31} + f m_{21})}{\lambda_v L} \\
L_6 &= \frac{(v_0 m_{32} + f m_{22})}{\lambda_v L} \\
L_7 &= \frac{(v_0 m_{33} + f m_{23})}{\lambda_v L} \\
L_8 &= -(L_8 x_c + L_9 v_c + L_{10} z_c) \\
L_9 &= \frac{m_{31}}{L} \\
L_{10} &= \frac{m_{32}}{L} \\
L_{11} &= \frac{m_{33}}{L}
\end{aligned} \quad (3)$$

The m-coefficient describe the rotations: azimuth (υ), tilt (τ) and roll (σ) (4):

$$\begin{aligned}
m_{11} &= cos\phi cos\sigma + sin\phi cos\tau sin\sigma \\
m_{12} &= -sin\phi cos\sigma + cos\phi cos\tau sin\sigma \\
m_{13} &= sin\tau\, sin\sigma \\
m_{21} &= -cos\phi sin\sigma + sin\phi cos\tau cos\sigma \\
m_{22} &= sin\phi sin\sigma + cos\phi cos\tau cos\sigma \\
m_{23} &= sin\tau\, cos\sigma \\
m_{31} &= sin\phi\, sin\tau \\
m_{32} &= cos\phi\, sin\tau \\
m_{33} &= -cos\tau
\end{aligned} \quad (4)$$

With the spatial coordinates (x, y, z) of at least three Ground Control Points whose image coordinate (u, v) are known, is possible to solve the variables (parameters of external geometry).

With those variables is possible to georeferencing the images with the equations (5):

$$\begin{bmatrix} L_1 - L_9 u & L_2 - L_{10} u & L_3 - L_{11} u \\ L_5 - L_9 \upsilon & L_6 - L_{10} \upsilon & L_7 - L_{11} \upsilon \end{bmatrix} \begin{bmatrix} x \\ y \\ z \end{bmatrix} = \begin{bmatrix} \upsilon - L \\ \upsilon - L_8 \end{bmatrix} \quad (5)$$

Figure 4.3 - Timex exposure of Piscinnì beach showing the morphology of the shoreface during a wave event. Red arrow shows the bar, blue arrow shows the trough and orange line represents the hypothetical transect.

A MatLab script (Pawlowicz R., 2003) solves the equation for each pixel of the image. The resulting images were analyzed with a GIS software for mapping shoreline positions (before, during and two days after the storm event), measure overwash, accretion rate and morphodynamic state (Table 4.1). The maximum overwash and the shore accretion were measured in a hypothetical transect located in the middle of the beach (orange line in Figure 4.3), two days after the end of the storm. Table 4.1 includes the day with maximum overwash, the wind direction, the mean wind speed during the storm event, the wave direction and period (from Copernicus hindcast), significant wave height and energy flux.

During the two-year camera recordings, nine storm events of various intensity (Table 4.1) were identified through the analysis of the videomonitoring system data. Moreover, some other storms that occurred during the night, when the camera was turned-off, were not documented.

To calculate the energy flux, in deep water, we used the following formula (6):

$$Ep = {H_s}^2 T_p \frac{\rho g^2}{64\pi} \qquad (6)$$

where Hs is the significative wave height, Tp is the wave period, ρ is the water density and g is the gravitational force.

4.4 Results

The results of our investigation are shown in Table 4.1. During the monitored period, the study area was affected by severe storm events mainly related to south-westerly winds (up to 50 km h^{-1}, 30 km h^{-1} on average). These storms drove wave conditions that reached Piscinnì beach with

mean wave directions comprised between 235° and 273°. During the major storm events (Table 4.1), characterized by wave height (Hs) ranging from 2.1 and 4.9 m and wave period (Tp) between 8.4 and 12.2 s, the flux energy ranged from 18944.1 (30/09/2013) to 122299.3 KW/m (26/12/2013), we measured an accretion of the backshore ranging from 12 (06/11/2013) to 31 m (25/03/2015) associated with significant changes in the shoreline positions (Figure 4.5). The recorded overwash varied from 11 (06/11/2013) to 35 m (25/03/2015) with an average value of 20 m. Piscinnì beach had mainly morphologies classifiable as LBT (Longshore Bar and Trough), TBR (Transverse Bar and Rip) and RBB (Rhythmic Bar and Beach), see Figure 4.4.

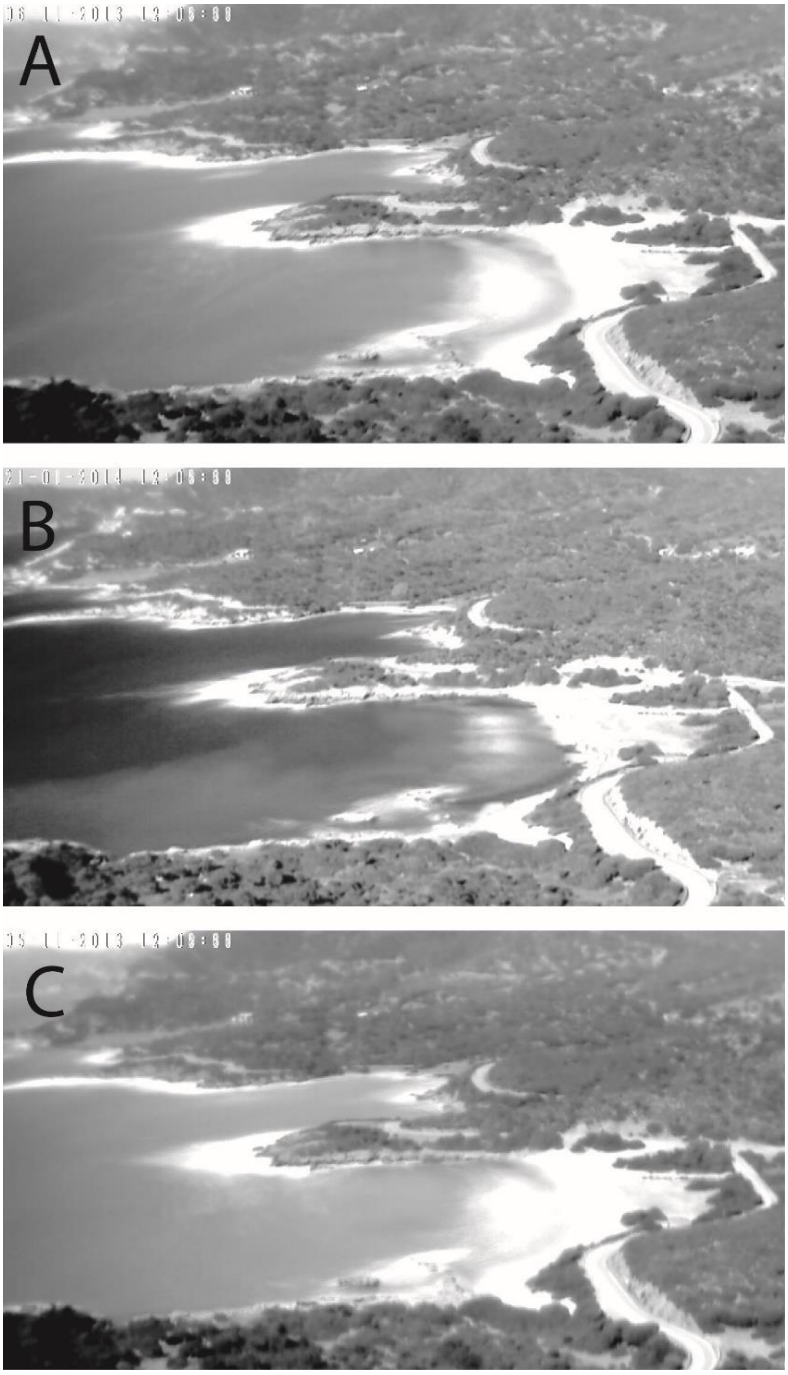

Figure 4.4 – Morphodynamic states in Piscinnì beach: A) LBT; B) RBB; C) TBR

Snapshot images showed that the shore accretion was linked to the deposition of seagrass beach-cast litter (the so-called 'banquette'; Figure 4.6).

Table 4-1 Mean wind (direction and speed), incoming wave (direction, height Hs, period Tp, energy flux Ep), overwash and morphodynamic state recorded during significant storm events at Piscinnì beach. The accretion rate values refer to two days after the storm end.

Date of the storm	Wind direction (°)	Mean wind speed (km h^{-1})	Wave direction (°)	Hs (m)	Tp (s)	Ep (KW/m)	Overwash (m)	Morpho-dynamic state	Accretion (m)
30/09/2013	225	19.5	248	2.1	8.4	18944.1	18	LBT	17
06/11/2013	315	34.9	273	2.7	9.2	34062	11	LBT	12
26/12/2013	225	48	254	4.9	10.2	122299.3	20	LBT	20
20/01/2014	225	26	242	3.5	9.2	55535.3	24	TBR	24
04/04/2014	225	26	235	3.4	10.2	57852.8	20	LBT	20
05/11/2014	225	20	245	2.7	9.2	32468.7	19	LBT	18
02/12/2014	225	41	238	4.5	10.2	98706.8	18	LBT	13
05/02/2015	225	30	250	3.5	9.2	55291.3	19	LBT	20
25/03/2015	225	53	271	3.6	12.2	79464.7	35	LBT	31

4.5 Discussion

The results of our investigations have shown that storm events mainly related to south-westerly winds (about 50 km h^{-1} on average) can induce important morphological variations in a natural Mediterranean wave-dominated beach. These changes include shoreline accretion/progradation and reconfiguration of nearshore bars. From the image processing acquired with the video monitoring system, large and voluminous deposits of seagrass beach-cast litters, mainly *Posidonia oceanica*, accumulated in the shoreline causing beach accretion (up to 30 m) two days after the storm event. After a storm event, the seagrass deposit can persist on the shoreline or can be dismantled in few hours. The permanence of these accumulations is quite variable and complicated to predict.

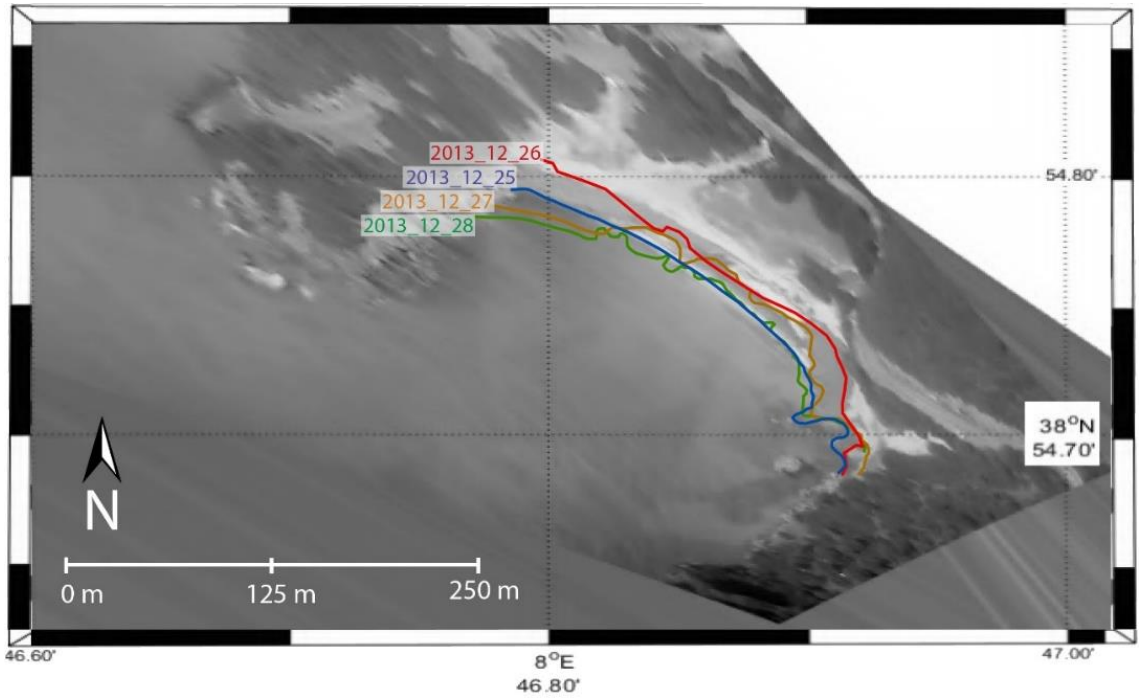

Figure 4.5 - Rectified image of 25/12/2013 showing shoreline positions before (blue line), during (red line), one and two days after (orange and green lines) the storm event.

Several studies, also based on video monitoring system, have tried to characterize the permanence of seagrass berm on beach face (Gómez-Pujol et al., 2013, Oldham et al., 2014; Simeone et al., 2012) but this process has not been fully understood yet. In several cases, we observed that the seagrass berm can be covered by sand transported by winds blowing from the backbeach and the dune zones. This process contributes to stabilize the seagrass deposit and can lead to a progradation of the shore. Moreover, beach rotation was observed during several events, relating to the incident wave direction.

Figure 4.6 - Snapshot of 28/12/2013, two days after the storm event, showing depositions of seagrass berm.

Piscinnì beach has undergone a low human impact over the years (no beach cleaning operations, no bulldozing, etc.), this has allowed the preservation of its natural condition. The comparison of the different shoreline positions, that we mapped before and after the storm events, showed a high resilience for this beach. This is also the consequence of the large accumulation of *Posidonia oceanica* beach-cast litter on the beachface. In fact, it is well known that the *Posidonia oceanica* meadow has a fundamental role in protecting the coastline from erosion because it decreases wave energy, increases the sediment retention and reduces sediment resuspension (De Falco et al., 2017; De Muro et al., 2010, 2017b; Simeone et al., 2008; 2013). These factors contribute to beach stability, further enhanced by biogenic sediment supply from the meadow (Tecchiato et al., 2016). In addition, the presence of seagrass beach-cast litter can influence wave runup shifting the process offshore and modifying the swash energy (Passarella, 2019).

4.6 Conclusions

Piscinnì beach had mainly morphologies classifiable as LBT (Longshore Bar and Trough, 74% of the events, Figure 4.4 A) and subordinately as TBR (Transverse Bar and Rip, 21% of the events, Figure 4.4 C) and RBB (Rhythmic Bar and Beach, 5% of the events Figure 4.4 B). The analysis of weather data showed, for the stretch of coast analyzed, that 56% of the total winds come from the third and fourth quadrant, while 44% from the first and second quadrant. By crossing the weather data with the camera recordings, it emerged that the winds from the third quadrant are the only ones to generate significant storm waves for the purposes of structuring the surf zone. The winds of the first and fourth quadrant, on the other hand, are more significant for the aeolian transport and the processes that control the forms and deposits of emerged beaches and dunes.

The comparison of the shoreline positions, mapped in the days before and after the storm events, shows how the Piscinnì beach has a high resilience, an index of the naturalness of the system.

A significant outcome of this study is the implications for coastal management. By providing an overview of the complex interaction between hydrodynamic and ecogeomorphological processes, this study is crucial for coastal managers to plan beach management (e.g., beach cleaning practice) and to understand the importance of seagrass berm deposition in the formation and maintenance of natural Mediterranean beaches.

Chapter 5
HISTORICAL EVOLUTION OF THE URBAN COASTAL BELT OF CAGLIARI

This chapter reports a summary of two papers both concerning the historical evolution of the urban coastal belt of the Gulf of Cagliari, analyzed with two different approaches.

The first paper (Porta, M.; Buosi, C.; Trogu, D.; Ibba, A.; De Muro, S. *An integrated sea-land approach for analyzing forms, processes, deposits and the evolution of the urban coastal belt of Cagliari*. J. Maps 2020.) consists of a geomorphological map where the main geomorphological evolutions of the area are represented, from 1885 to 2019.

The second paper (Biondo, M.; Buosi, C.; Trogu, D.; Mansfield, H.; Vacchi, M.; Ibba, A.; Porta, M.; Ruju, A.; De Muro, S. *Natural vs. Anthropic Influence on the Multidecadal Shoreline Changes of Mediterranean Urban Beaches: Lessons from the Gulf of Cagliari (Sardinia).* Water 2020, 12.) is based on the application of the Digital Shoreline Analysis System (DSAS) (Thieler et al., 2009), an extension of the ArcGIS software, to observe changes in the area's shoreline, from 1956 to 2016.

5.1 Introduction

Urban coastal belts are complex, narrow transition areas that connect terrestrial and marine environments. They are characterized by dynamic interactions between bio-physical, human and socio-economic forces, and are among the world's most productive and valued ecosystems (Blumberg & Bruno, 2018; Crossland, Kremer, Lindeboom, Crossland, & Le Tissier, 2005). These environments are consequently exposed to pressures and hazards from both land and sea (Cummins et al., 2014). Properly managing these complex zones requires an understanding of the interactions between physical processes, eco-geomorphological settings and urbanization, and can be crucial when it comes to reducing vulnerability and planning appropriate interventions.

Nowadays, most sandy beaches worldwide show a tendency of progressive shoreline retreats or advances for years or even decades (Jaramillo et al., 2020). Rivers, coastal currents and waves move sediments inside, outside and within the nearshore zones, causing loss or gain of material from or to the system (Mentaschi et al., 2018). Changes resulting in a negative sediment budget can be caused by natural factors, however, in the majority of cases, these are triggered or affected by anthropogenic stressors, such as: (1) the construction of dams on rivers and changes in land use; (2) the building of man-made coastal structures interfering with sediment transport; (3) harbor siltation and maintenance dredging; and 4) recreational use of littoral zones and beach cleaning operations (De Muro et al., 2018; Loureiro et al., 2012). Morphological evolution tends to accelerate under extreme events, such as severe storms that drive intense erosion and lead to irreversible changes (Ciavola et Coco, 2017). The magnitude of these changes depends on a variety of local hydrodynamic factors (e.g., number and intensity of storms, wave and tidal conditions) and on other controlling factors, such as the beach morphology type (Haerens et al., 2012; Qi et al., 2010), the mean sediment size and the geological setting (Loureiro et al., 2012;

Prodger et al., 2016; Gallop et al., 2020). In natural pristine beaches, the impact of storms is less severe than in highly urbanized beaches because they are less impacted by human-induced degradation and, therefore, present a greater recovery ability and resilience (Trogu et al., 2020; Buosi et al., 2019). In urban beaches, morphological alterations and modifications are exacerbated by anthropogenic activities that intensify and accelerate the deterioration of the coastal environment (Syvitski et al., 2005). In addition, relative sea level rise due to climate changes further aggravates these impacts, contributing to more frequent flooding and increased coastal erosion (Nicholls et Cazenave, 2010; Pilkey et Cooper, 2004).

In the nearshore zone, a wide range of ecological roles are played by seagrasses (Campagne et al., 2015; Nordlund et al., 2018). In the Mediterranean, the endemic *Posidonia oceanica* meadows play a fundamental role in beach stability through the supplying of biogenic sediments (Tecchiato et al., 2015; De Falco et al., 2017), in protecting the coastline from erosion by acting as a buffer to wave energy and in increasing sediment retention and reducing sediment resuspension (De Muro et al., 2010; De Falco et al., 2014). The presence of seagrass necromass (leaves and rhizomes mixed with sand, also called banquette or beach-cast litter) contributes to the protection of the shore from the erosion exerted by swell and waves during winter storms (Simeone et al., 2008; Vacchi et al., 2017) and can also influence wave run-up by shifting these processes offshore and modifying the swash energy (Passarella, 2019; Passarella et al., 2020). The removal of these deposits through mechanical cleaning can have a negative impact on shore stability, as it causes a considerable loss of sediments from the beach, ultimately resulting in changes in beach morphology, flattening of the beach profile and obliteration of sedimentary features (e.g., sediment berms, cusps, embayments, beach-face steps) (De Muro et De Falco, 2015; Simeone et al., 2013; Porta et al., 2020). Thereby, the removal of beach-cast litter deposits, extensively practiced as part of beach management (Vacchi et al., 2017; De Falco et al., 2008) in Mediterranean coastal areas, might make these systems more vulnerable to erosional processes (De Falco et al., 2008b).

As a consequence of beach erosion, the risk of rising water levels and related flooding hazard arises (Pollard et al., 2018) along with the negative socio-economic implications derived from the threats posed to coastal infrastructures and residential areas. Because of the future climate change scenarios, and the expected rise in rates of urbanization, costal erosion is also expected to increase (Idier et al., 2017). Quantitative knowledge of long-term shoreline changes can provide important information on trends and rates of coastal evolution and give the coastal planner an essential tool for designing adequate future coastal management and adaptation strategies. Shoreline position and geometry are generally extracted from remote sensing and aerial images, while rates of shoreline changes are calculated and described through different statistical methods (Dolan et al., 1991).

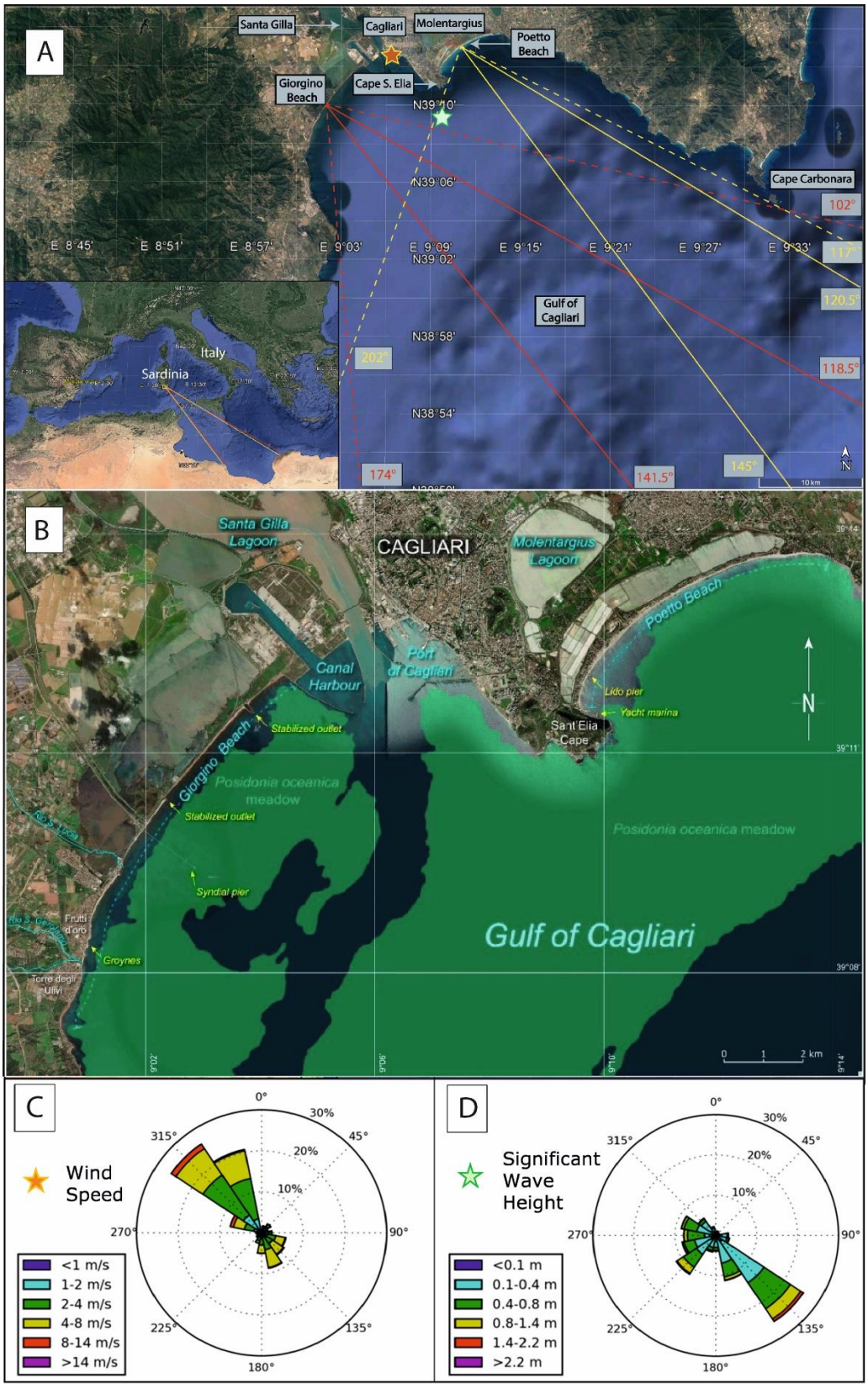

Figure 5.1 - Geographical setting of the study area, located in the Western Mediterranean Sea, Gulf of Cagliari (A), including the wave exposure angles (referred to the N = 0°) and fetch of Poetto (yellow lines) and Giorgino (red lines) beaches. Wind speed and direction (C) from Cagliari station of the national tidal monitoring network (location: orange star in panel A); significant wave height and direction (D) at the NOAA hindcast dataset point (location: green star in panel A).

With such premises, these studies aim at providing an improved understanding of the past and present patterns of shoreline changes to support best management practices in a context of future of climate change scenarios. The specific objectives were to: (i) quantify net movement and rates of retreat and accretion along the beach systems of the Gulf of Cagliari, (ii) assess the main anthropogenic and natural factors driving retreat/accretion patterns, (iii) evaluate the role played by *P. oceanica* meadows in coastal sediment dynamics.

5.2 Geographical settings, wave climate and hydrodynamics

From a geological point of view, the Cagliari Gulf, which is located between two Paleozoic tectonic blocks (Figure 5.2), contains both the extreme eastern edge of Cenozoic structures related to the Oligo-Miocene graben-system (Casula, Cherchi, Montadert, Murru, & Sarria, 2001; Cherchi & Montadert, 1982) and the NW-SE Plio-Quaternary Campidano graben. The calcareous Cape S. Elia (horst) promontory divides two Pleistocene-Holocene beach systems (Giorgino – La Maddalena to the west and Poetto to the east), Figure 5.2.

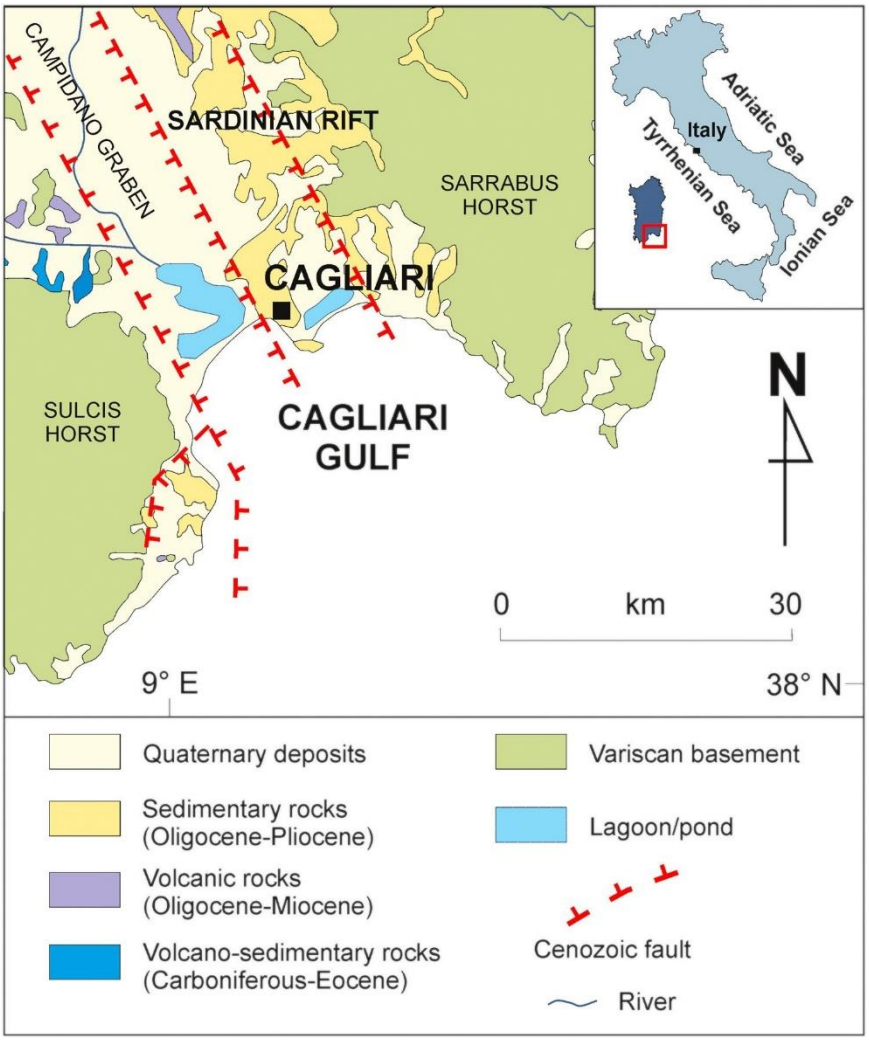

Figure 5.2 - Geological map of southern Sardinia (from Carmignani, Oggiano, Funedda, Conti, & Pasci, 2016)

Currently, the city of Cagliari (southern Sardinian, Italy, western Mediterranean; Figure 5.1), which faces the Gulf of Cagliari, stretches over several hills about 80–100 m in height and is surrounded to the east, north and west by wet environments, namely marshes, ponds and lagoons. In particular, on the western side, the Lagoon of Santa Gilla covers an area of about 15 km^2. This is an elongated, NW-SE-orientated depression, which is roughly deltoid in shape and is connected to the Mediterranean Sea through a narrow channel located in the south, with a long sandy bar (Giorgino beach) separating it from the sea. On the northern shore, the lagoon has two major freshwater inflows from the Fluminimannu and Cixerri rivers. A second wet, saline environment, called the Molentargius pond, and a wide system of saltworks extend east of Cagliari (Figure 5.1).

The study area includes two urban beaches, Poetto and Giorgino. These are, respectively, located to the east and west of Cape S. Elia, a calcareous promontory of Miocene age (Figure 5.1) and are classified as microtidal, wave-dominated systems. These beaches formed approximately seven to five thousand years ago, when post glacial sea level rise significantly decelerated (Vacchi et al., 2017), allowing the formations of the barrier system that evolved into the current sandy coastline with its lagoon systems behind (Deiana et al., 2015). Presently, the main siliciclastic sediment inputs come from the Santa Gilla lagoon, which prevalently feeds the western part of the Gulf, whereas the eastern parts are mainly supplied by the erosion of the carbonatic and siliciclastic rocks of the Cape S. Elia promontory and by the authigenic bioclastic sediment produced by the *Posidonia oceanica* meadows (Porta et al., 2020).

Poetto beach is sandy, 8 km long and has a maximum width of about 100 m. Its dune systems appear to be very threatened by human activities. In particular, erosion processes have been triggered by the construction of a pedestrian/cycling route along the shoreline on the foredunes, while embryo dunes reveal cross-shore fragmentation as a consequence of pedestrian access to the beach. A nourishment project (about 300,000 m^3 of sand) was carried out in 2002 on the western side to limit erosion. The coarser and bioclastic sediments used for the nourishment have significantly modified the textural, compositional and morphological features of the backshore, shoreline and shoreface (De Muro, Ibba, et al., 2017; Lai, 2008). The coastal sector of Giorgino is characterized by a complex system of lagoonal mouths, which are periodically dredged, and the sediment transported away from the beach system. A road limits the beach amplitude landwards in this sector. The canal harbour (Figure 5.1) was built close to the city of Cagliari in 1970 and currently extends to 2500 m, with 1600 m of the quay providing berths for transhipment and ship cargo. The seabed in front of the canal harbour pier is repeatedly subjected to dredging and is characterized by muddy sediment and turbidity (De Muro, Porta, et al., 2018).

The main geographical fetch at Poetto beach is between 120° and 145°, while the possible directions for approaching storms range from 117° to 202° (Figure 5.1A; De Muro, Ibba, et al.,

2017); at Giorgino beach, the dominant geographical fetch is between 118.5° and 141.5°, with the directions of approaching storms ranging from 102° to 174° (De Muro, Porta, et al., 2018). The tidal range is low (less than 20 cm), reaching a maximum of about 40 cm (Brambilla et al., 2016).

The prevalent winds recorded in the study area (Figure 5.1C) come from the NW (27% of occurrence), but the winds that give rise to the principal wave events come from southern directions: SE (40% of the occurrence), SW (20%) and SSE (10%; Figure 5.1D; De Muro, Porta, et al., 2018). This is because the beach system is naturally protected by Cape Carbonara to the east and Cape Spartivento to the west (Brambilla et al., 2016; De Muro, Porta, et al., 2018; Passarella, 2019).

In general, wind from SE generates opposite longshore currents that develop on the Poetto beach. The convergence of these currents produces a main rip current flowing offshore for about 400 m and is located about 1 km eastwards of the western limit of the beach (Brambilla et al., 2016; De Muro, Ibba, et al., 2017), Fig. 5.3a. Meanwhile, at Giorgino, a northwards longshore current (Fig. 5.3c) flows with a magnitude in the order of 0.5 m s^{-1} along the entire coastline. A rip current flows along the port pier in the northern-most part of this beach, near the canal harbour.

Wind from SW produces several cells that are active on the shoreface of Poetto (Brambilla et al., 2016; De Muro, Ibba, et al., 2017). These cells produce various longshore currents running from the south west to the south east and several rip currents (Fig. 5.3b). Meanwhile, in the western sector of the Gulf of Cagliari, a weak northeast-oriented longshore current (Fig. 5.3d) develops during SW events in shallow waters feeding a weak rip current that flows along the embankments of lagoonal mouths in the eastern-most sector of Giorgino (De Muro, Porta, et al., 2018).

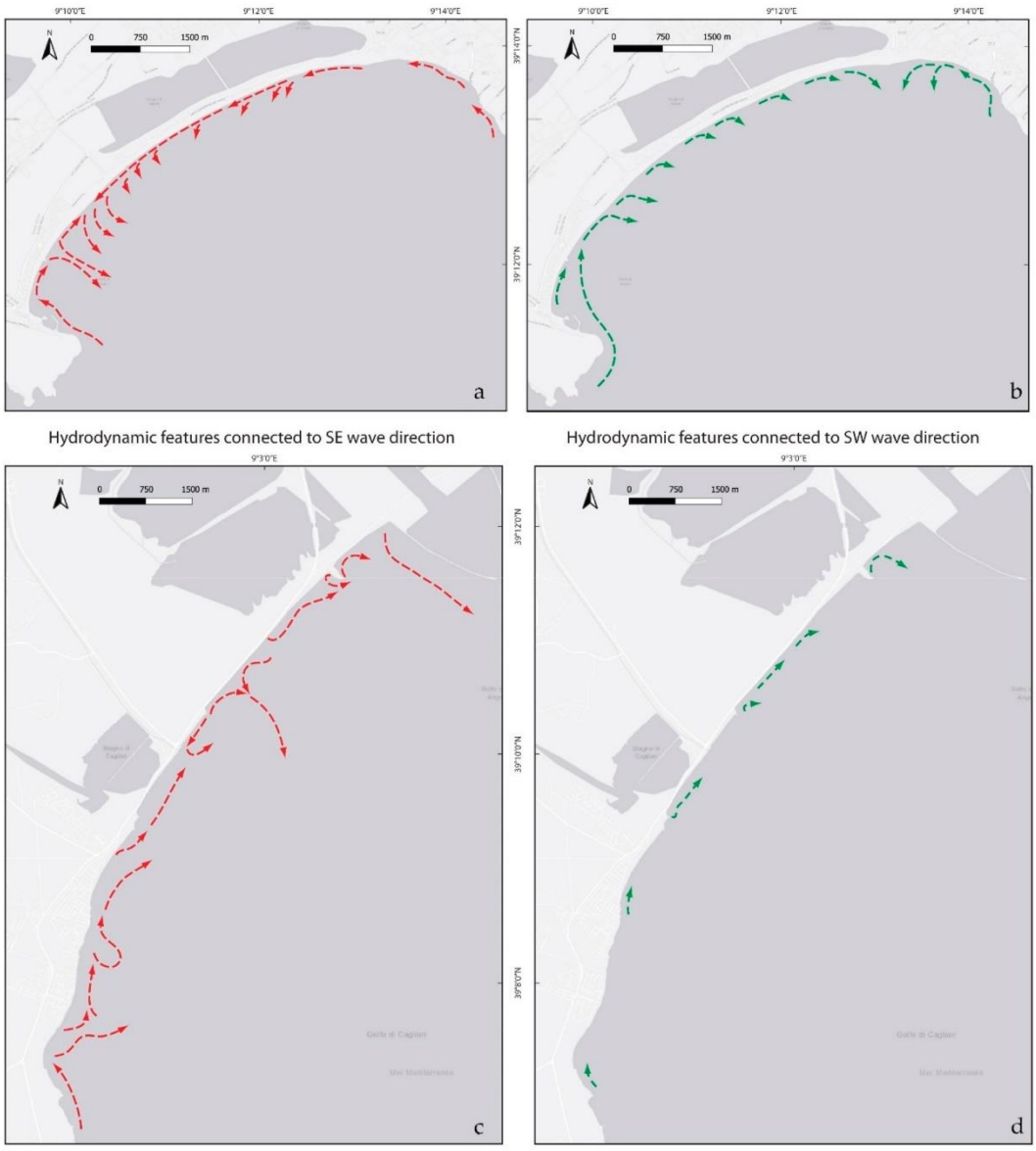

Figure 5.3 - Schematic representation of Delft3D modelling simulation of main induced coastal currents associated with SE and SW winds at the Poetto ((a) and (b)) and Giorgino ((c) and (d)) beaches. Figures modified from DeMuro et al., 2017a and 2018a.

5.3 Anthropic Pressure and Impacts

The Poetto beach develops in front of the metropolitan city of Cagliari. The relatively natural state of its 8 km length of sandy shore, when compared to the neighbouring urban beach of Giorgino, makes it one of the most frequented beaches of the entire island of Sardinia (De Muro et al., 2017). The Poetto beach has been long affected by anthropogenic pressures such as urbanization, coastal structures, intensive recreational and touristic activities. In particular, during the last century, the alongshore building of a yacht marina (Figure 5.1) and of other recreational infrastructure (such as a piers and several kiosks) caused significant modification of longshore and aeolian transports (De Muro et al., 2018; Porta et al., 2020). Furthermore, the roads and extra parking spaces constructed in recent years, in order to accommodate the vast

numbers of tourists visiting the beach each year, caused the complete erosion and fragmentation of the beach foredune habitats (De Muro et al., 2017; Porta et al., 2020; Strazzera et al., 2010; Brambilla et al., 2016). Current practices of seasonal beach cleaning operations, performed with heavy mechanical vehicles, presently cause further negative impacts on the backshore by compacting the sediment and depriving the beach of its natural protection (represented by seagrass berms) against wave energy and wave run-up; furthermore, extensive boating activities have caused damage to the meadows of *P. oceanica* (De Muro et al., 2017; Brambilla et al., 2016) over the shelf areas.

Giorgino is a 11 km long embayed beach found on the western side of the Gulf of Cagliari. It is a complex system characterized by the inland presence of large wetlands and some minor fluvial systems (Figure 5.1). Giorgino is a heavily urbanized beach, and residential developments and the presence of ports and industrial activities have greatly altered the coastal morphology and dynamics. The growth of the residential urban area of Frutti D'Oro, in the south-western part of the bay, is thought to have caused modification of the local fluvial catchments (Rio San Gerolamo and Rio Santa Lucia; Figure 5.1) with a consequential reduction of terrigenous sediment inputs to the beach (De Muro et al., 2018). Moreover, the Giorgino coastline hosts the Port of Cagliari, built in the 1930s, and the Canal Harbor (Porto Canale; Figure 5.1) established in 1970 to offer berths for cargos and ships; port construction and associated activities have greatly modified the shoreline geometry and longshore sediment transports (De Muro et al., 2017a; Porta et al., 2020; (De Muro et al., 2017b).

Other man-made features at this site include a dry dock (Pontile Syndial, ex Rumianca), several groynes constructed in 2014 to counteract beach erosion and a road (SS195) which runs parallel to almost the entire length of the shoreline and which limits the landward development of the beach (Figure 5.1). In addition, the seabed in front of the Giorgino beach was dredged in the 1930s to mine the sediments that were used for the reclamation of the wetland area located behind the promontory of Cape S. Elia, in the south-east of the city of Cagliari (De Simone, 1928). In general, the building of coastal infrastructures, the wharf, dredging and navigation activities (loading, unloading and anchorage), roads and discharges of municipal untreated sewage and industrial wastes are considered to be the main causes of pollution, turbidity, coastal erosion, modification of drift currents and fragmentation of seagrass meadows in the coastal area of Giorgino (De Muro et al., 2018). With regard to seagrass communities, the mixed *P. oceanica*, *Caulerpa prolifera* and *Cymodocea nodosa* meadows indeed appear discontinuous, with numerous erosive intermattes at depths between −4 and −20 m (De Muro et al., 2018).

5.4 Methods

The two different approaches for the historical analysis of the urban coastal area of Cagliari concerned in:

- Geomorphological study and multitemporal analysis of orthophotos, satellite images and topographic maps. Moreover, focuses on topographic and morphobathymetric surveys (routes and sampling point) and side-scan sonar cover. The data reported in this study were collected and analyzed through the 1) “Beach Environment, management And Coastal Hazard” (BEACH), 2) Natural Erosion Prevision Through Use of Numerical Environment (NEPTUNE) and 3) NEPTUNE2 projects (De Muro et al., 2017a and 2018a; Porta et al., 2020; Brambilla et al., 2016; Ruju et al., 2018), carried out since 2013 by the Coastal and Marine Geomorphology Group (CMGG) of the University of Cagliari.

- Statistical measurements of historical shoreline changes through the application of the ArcGIS ™ Digital Shoreline Analysis System (DSAS) extension (Thieler et al., 2009), which has proved to be a reliable tool for quantifying erosion rates / accretion from several studies (Manca et al., 2013; Thieler et al., 2009; Del Río et al., 2013; Virdis et al., 2012). Spatio-temporal displacements of the shoreline position were evaluated and quantified along the two urban beaches of Poetto and Giorgino across a time frame of over 60 years. The assessment of historical shoreline changes is done by examining different statistical parameters such as the end point rate (EPR), the linear regression rate (LRR), the shoreline change envelope (SCE) and the net shoreline movement (NSM). The first two parameters represent the speed of accretion and erosion in meters per year. The EPR is obtained by dividing the distance (m) between two shorelines by the time spanning between the earliest and the latest shoreline (Thieler et al., 2009; Genz et al., 2007), the LRR is determined by fitting a least squares regression line to all shoreline points and, therefore, represents a modelled forecast of the shoreline rates of change. The SCE is a measure of the total change in shoreline movement considering all available shoreline positions and reporting their distances, without reference to their specific dates. NSM reports the distance between the oldest and the youngest shorelines (Thieler et al., 2009; Temitope D. Timothy Oyedotun, 2014).
  In order to ease interpretation and discussion of the results, the two studied beach systems were sampled separately and divided into four sub-sectors each (Figures 5.4 and 5.5). The length of each sub-sector was determined only by looking at the general trends of shoreline change rates following DSAS computations. For the Giorgino beach system, statistical rates were calculated considering the total dataset time-frame (1954−2016); whereas, for the Poetto beach, in order to differentiate between long-term shoreline changes occurring prior to and after the artificial sand nourishment carried out in 2002 in the western sectors of the beach, images were grouped into two time-series datasets: the first set included the aerial photographs acquired between 1954 and 1998 and the second dataset comprised the images acquired post beach nourishment, between 2003 and 2016.

5.5 Results

The analysis of historical maps shows that the urban area of Cagliari in 1885 was constituted of a single nucleus close to the port infrastructures. A wide system of wet environments (lagoon, saltmarshes and saltworks) extended to the west of the city and was separated from the sea by a continued longshore sandy bar. Six lagoonal mouths connected this wet environment with the sea. A small island (Sa Illetta) was located in the lagoon at approximately 1500 m from the coastline northwards. On the south-west side of the Cape S. Elia promontory, south of the urban nucleus, a small gulf was bordered by ancient saltworks. At the east of the city, Poetto beach was constituted of a longshore sandy bar with a wide dune system. Residential areas and marinas were not present.

In 1945, the urban surface stretched to northern, eastern and southern areas, and several urban nucleuses and a network of roads were built in the promontory of Cape S. Elia. The saltworks located in the promontory at the south of the city were reclaimed and filled by man-made materials. The dune systems of the two beaches narrowed (by up to 80%) due to the construction of hard structures (like roads) landwards. Coastal embankments and the development of harbour infrastructures (piers and breakwaters) were the most significant morphological modifications between 1945 and 2016.

The results of the shoreline evolution, with the DSAS technique, along the Gulf of Cagliari between 1954 and 2016, applied in the two different beaches, are summarized in table 5.1 and in figures 5.4 and 5.5.

Table 5-1 - Summary of the results showing the calculated mean, min and max values for all of the statistical parameters.

Poetto Pre-Nourishment (1954–1998)												
	SCE (m)			**NSM (m)**			**EPR (m y^{-1})**			**LRR (m y^{-1})**		
	Mean	**Min**	**Max**	**Mean**	**Min**	**Max**	**Mean**	**Min**	**Max**	**Mean**	**Min**	**Max**
P1	9.98	3.68	20.25	-7.63	-20.25	-1.65	-0.17	-0.46	-0.04	-0.19	-0.45	-0.07
P2	10.56	3.71	16.27	3.21	-6.94	14.94	0.07	-0.16	0.34	0.05	-0.12	0.28
P3	6.71	1.23	11.06	-3.23	-10.98	8.18	-0.07	-0.25	0.19	-0.07	-0.24	0.20
P4	41.77	3.33	77.60	39.52	-7.69	77.60	0.90	-0.17	1.76	0.89	-0.16	1.68
Poetto Post-Nourishment (2003–2016)												
	SCE (m)			**NSM (m)**			**EPR (m y^{-1})**			**LRR (m y^{-1})**		
	Mean	**Min**	**Max**	**Mean**	**Min**	**Max**	**Mean**	**Min**	**Max**	**Mean**	**Min**	**Max**
P1	38.15	11.05	55.39	-38.02	-55.39	-9.33	-2.92	-4.26	-0.72	-2.69	-3.76	-0.89
P2	10.47	1.99	24.62	5.21	-10.04	17.75	0.40	-0.77	1.37	0.35	-0.92	1.28
P3	5.65	1.03	11.63	-3.03	-6.86	5.16	-0.23	-0.53	0.40	-0.31	-0.61	0.29
P4	7.74	2.00	17.56	3.68	-3.40	13.08	0.28	-0.26	1.01	0.18	-0.50	0.95
Giorgino (1954–2016)												
	SCE (m)			**NSM (m)**			**EPR (m y^{-1})**			**LRR (m y^{-1})**		
	Mean	**Min**	**Max**	**Mean**	**Min**	**Max**	**Mean**	**Min**	**Max**	**Mean**	**Min**	**Max**
G1	44.12	10.02	111.27	-31.46	-110.75	20.77	-0.51	-1.79	0.34	-0.47	-1.76	0.44
G2	30.00	9.43	48.05	12.26	-9.31	43.07	0.20	-0.15	0.69	0.20	-0.33	0.80
G3	40.63	13.17	57.56	-20.03	-28.63	-0.21	-0.32	-0.46	0.00	-0.50	-0.61	-0.05
G4	38.96	13.24	72.85	32.66	0.65	65.28	0.53	0.01	1.05	0.47	-0.04	1.14

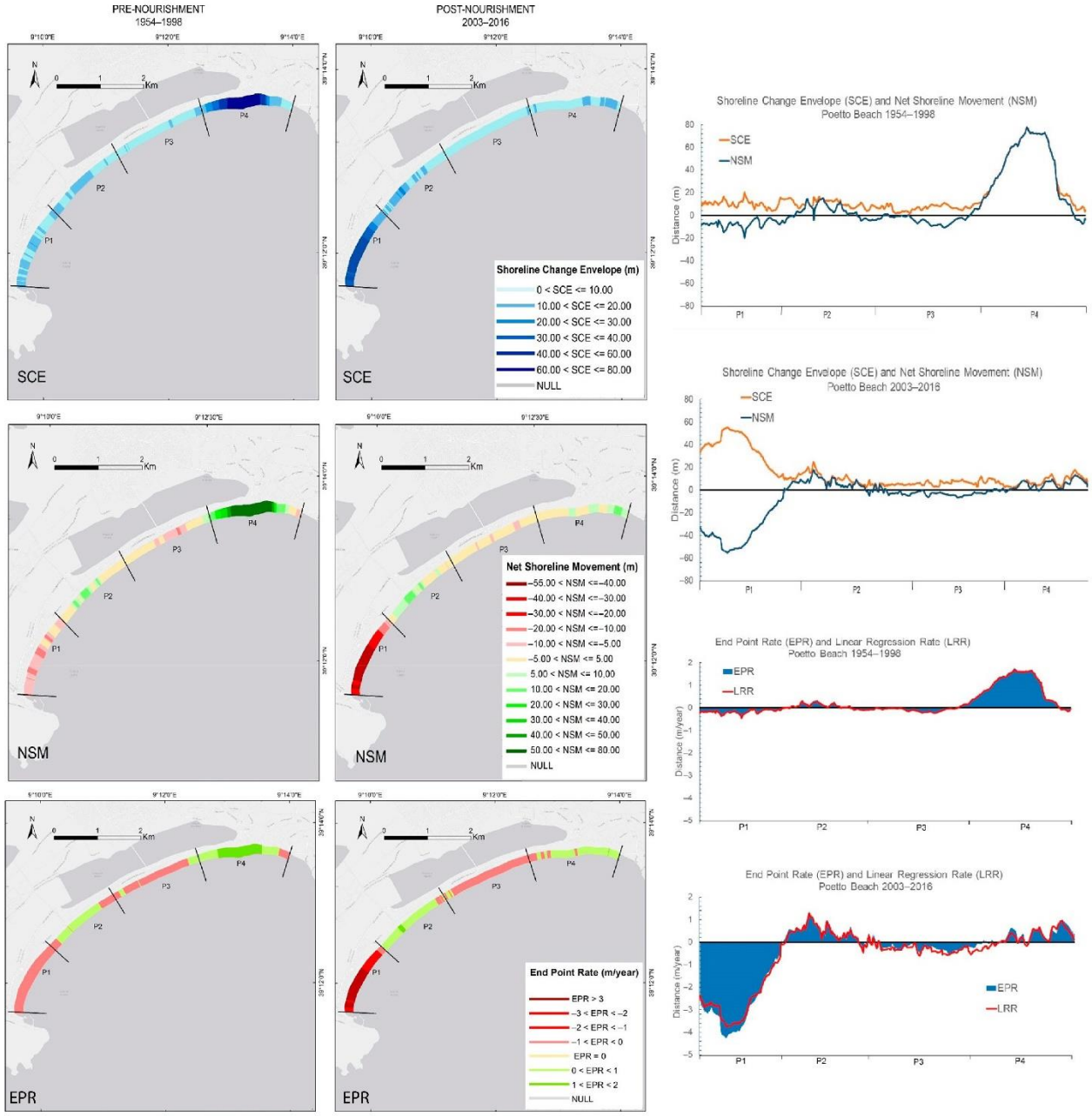

Figure 5.4 - Maps (above) showing the spatial distribution of shoreline change envelope (SCE), net shoreline movement (NSM) and the rates of shoreline movement, expressed as end point rates (EPRs) and linear regression rates (LRRs), along the Poetto beach for pre-nourishment (1954–1998) (left) and post-nourishment (2003–2016) (right) years, superimposed with the limits of the four discriminated sectors (P1–P4); SCE, NSM, EPR and LRR trends (on the right) plotted against distance (west to east), with the x-axis showing the limits of the P1−P4 sectors. Positive values indicate areas of accretion, whilst negative values indicate areas of shoreline retreat.

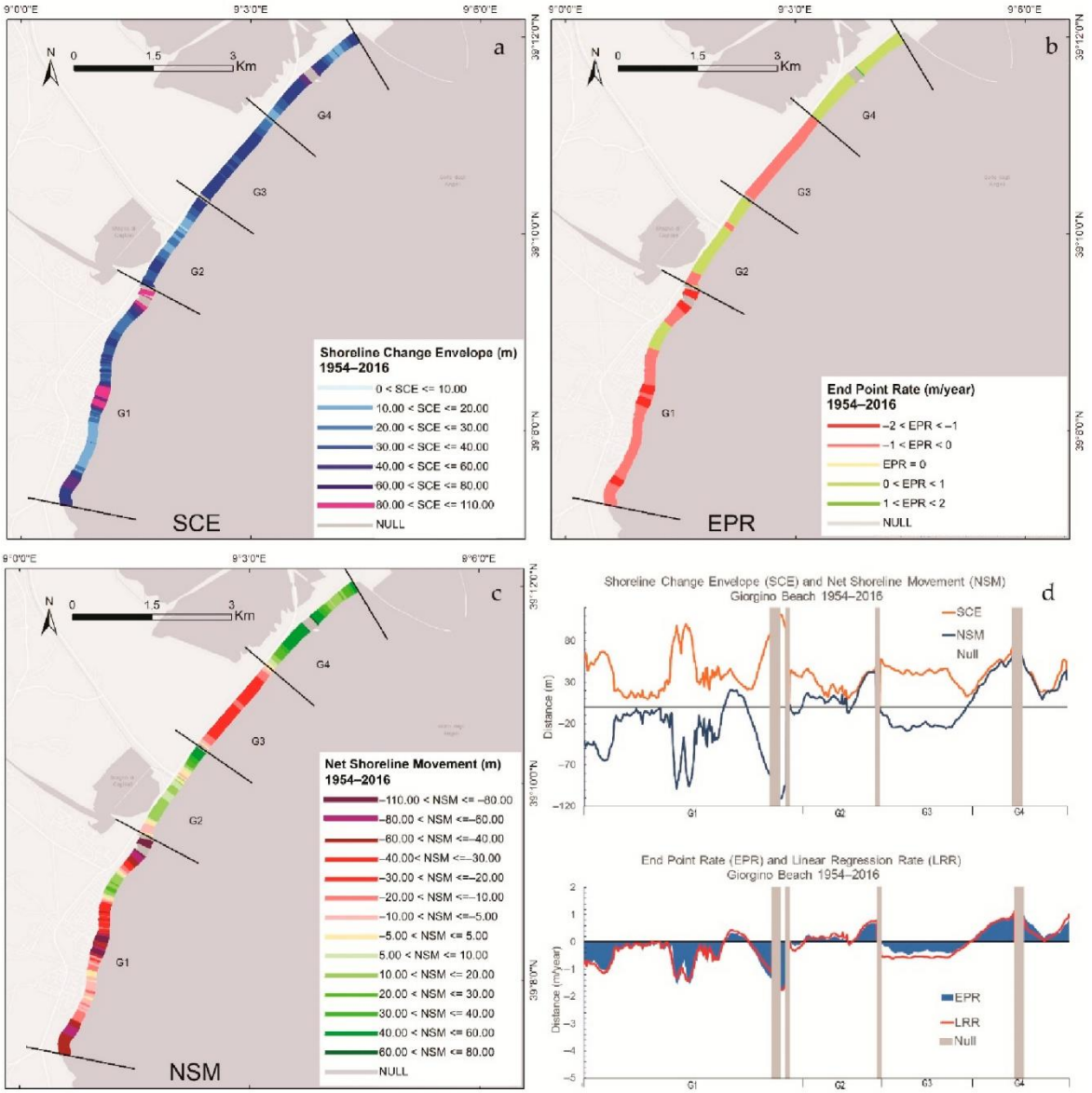

Figure 5.5 - Maps showing the spatial distribution of shoreline change envelope (SCE) (a), end point rate (EPR) (b) and net shoreline movement (NSM) (c) along the Giorgino beach for the years 1954–2016, superimposed with the limits of the four discriminated sectors (G1–G4); SCE, NSM, EPR and LRR trends (d) plotted against distance (west to east), with the x-axis showing the limits of the G1–G4 sectors. Positive values of NSM and EPR indicate areas of accretion, whilst negative values indicate areas of shoreline retreat.

5.6 Discussion

The analysis of the data and the comparison of historical maps and orthophotos has enabled the identification of the most relevant natural and human-induced changes that have occurred in the urban coastal area of Cagliari. These changes were moderate between 1885 and 1945, but thereafter the urban coastal area was altered by several modifications linked to the increase in urbanization in a system where waves and littoral currents are the dominant coastal processes for the transport and deposition of sediment. For example, the construction of the canal harbour and other port infrastructures diminished the coast, changing the water circulation by modifying the natural sediment-accumulation processes and altering the continuity of the *Posidonia*

oceanica meadow. In particular, the urbanization has caused the narrowing and hardening of the Poetto and Giorgino beaches due to the building of roads and temporary and permanent structures in dynamic zones. These activities have interfered with natural processes and indirectly influenced the erosion of the dune system. In fact, human infrastructure appears to be more vulnerable to direct damage due to wave collision and long-term flooding in Poetto beach. The infrastructure could interfere with the maximum run-up, causing erosion of the scarp and scours on the areas where a collision between run-up/up-rush and man-made structures occurs (De Muro, Ibba, et al., 2017; Passarella, De Muro, Ruju, & Coco, 2018). The coarsening of sediment, from natural siliciclastic to a coarser version with a higher carbonate content (Lai, 2008), during the beach nourishments has led to another crucial imbalance in Poetto beach. In addition, beach-cleaning operations, which are regularly carried out mainly in spring and summer, flatten and lower the backshore level, compacting the sediment and making this zone more vulnerable to overwash (De Falco et al., 2008; Simeone, De Falco, Como, Olita, & De Muro, 2008; Simeone, De Muro, & De Falco, 2013). Prior to the development of the city of Cagliari (twentieth century), the Poetto and Giorgino beaches were connected by a continuous aeolian, cross- and along-shore sediment supply (De Muro, Porta, et al., 2018). After 1945, urban development and the reclamation works on the wetlands located south of the city interrupted this sediment input, which is now: mainly siliciclastic from the Santa Gilla lagoon towards the inner shelf of Cagliari Gulf; and mainly carbonate and siliciclastic from the cliff erosion of the Cape S. Elia promontory. However, the defence structures at sea (attached and parallel breakwaters), and slope-stabilization in the cliffs (e.g. reinforced geogrids and pinned nets) located at the eastern and western bases of the cape, limit the carbonate and siliciclastic sediment-supply originating from cliff erosion. Today, an important authigenic bioclastic sediment input comes from the *Posidonia oceanica* meadow (VV.AA., 2013, 2016), which also plays a key role in protecting the beach system from erosion (De Muro, Kalb, et al., 2010; De Muro, Porta, Passarella, & Ibba, 2017; Gómez-Pujol, Orfila, Álvarez-Ellacuría, Terrados, & Tintoré, 2013). In fact, the seagrass meadow attenuates hydrodynamic forces, increasing sediment retention and reducing sediment resuspension (De Muro, Pusceddu, Buosi, & Ibba, 2017; Ruju et al., 2018; Tecchiato, Buosi, Ibba, Ryan, & De Muro, 2016). A recent study (De Muro, Porta, et al., 2018) showed a wide area of degraded and discontinuous *P. oceanica* and dead meadow in front of Giorgino beach (from −4 to −20 m). Reflecting the poor ecological state of the seabed (De Muro, Porta, et al., 2018), low biodiversity values of the benthic foraminiferal assemblages and the high abundance of opportunistic and stress-tolerant foraminiferal species have been documented (Buosi et al., 2013; Schintu et al., 2016). At Poetto, even though the dune system appears to be influenced by major human pressure, the benthic foraminiferal assemblages do not seem to be affected and the ecological status appears to be good (De Muro, Ibba, et al., 2017).

5.7 Conclusions

The geomorphological map of the urban coastal area of Cagliari enables us to highlight the connections between historical urban development, man-made transformations, geomorphological processes and human impact on coastal ecosystems. These findings are relevant, not only in relation to the management and maintenance of the beaches and wetlands, but also with respect to decisions about future measures concerning risk-mitigation, sea-level rises and erosion.

A multidecadal analysis of shoreline changes was performed using the DSAS tool on historical ortho-rectified photo mosaics acquired between the years 1954 and 2016. Such analysis was performed for the first time along the two beach systems of Poetto and Giorgino in order to quantify net shoreline position variability in relation to natural and anthropogenic forcings. Despite some limitations (Thieler et al., 2009), the DSAS allowed us to identify the most vulnerable zones of the study areas. Eight sectors with interchanging net erosive or accretional trends were identified along both beaches. The most vulnerable coastal sector, which in the last six decades experienced the highest erosion rates, appeared to be in the westernmost part of the study area (at Giorgino beach). The higher levels of human interventions occurring in this coastal zone (including stabilization of river mouth, coastal engineering structures, backbeach and dune occupation and consequent strong reduction of terrigenous sediment supply) were considered the main causes for the landward retreat evidenced by our long-term analysis. A comparable landward displacement of the shoreline was observed in the western sector of the Poetto beach, for both pre- and post-nourishment analyses. Erosion rates in this sector appeared to be significantly increased after artificial sand nourishment, suggesting that, during the 14 years following beach nourishment, the system rapidly reached its equilibrium state and most of the replenished material was naturally rearranged along the beach by the local hydrodynamics. In general, several causes of anthropic origins, some of which date back to almost a century ago, were recognized as the causes of the shoreline retreat observed during the last six decades along the Poetto and Giorgino beaches. In particular, low resilience levels were the result of coastal structures which interrupted the longshore and cross-shore continuity of the two beach systems. The whole study area is subject to important flooding phenomena, meaning that anthropic developments can greatly exacerbate long-term ongoing natural dynamics and make the entire sandy coastline of the Gulf of Cagliari more vulnerable to the effects of extreme events. Understanding system dynamics and impacts is particularly important in insular Mediterranean microtidal wave-dominated beaches, where fluvial sedimentary inputs are considerably reduced when compared to large continental systems (e.g., Rhône delta) characterized by the availability of large amounts of siliciclastic sediments. In Mediterranean beaches, insularity induces a more fragile and unstable equilibrium that climate change and increasing human pressure can potentially aggravate, posing serious threats to the survival of the urban beach systems that

cannot accommodate these modifications. In this context, the analysis of past shoreline dynamics carried out in this study constitutes an important step towards better environmental planning. Sustainable management aimed at system restoration becomes extremely difficult when facing historical large-scale land modification and should therefore reinforce those regulations aimed at system maintenance, prioritizing the protection of all those natural buffers in a beach system, such as dune and *P. oceanica* habitats. We believe that, beside adequate management strategies, enhancing the natural recovery ability of coastal systems is possibly the most powerful "passive" tool for coastal managers. Lockdown measures worldwide taught us that nature has an incredible ability to restore itself after disturbance; therefore, we believe that allowing ecosystems to restore naturally and then be given the space to persist should be made one of the fundamental tools in coastal management plans.

Chapter 6
ECOSYSTEM SERVICES AND MANAGEMENT OF REED AND SEAGRASS DEBRIS ON A URBAN MEDITERRANEAN BEACH (POETTO, ITALY)

The main findings of this chapter have been published in:

Ruju, A.; Buosi, C.; Coco, G.; Porta, M.; Trogu, D.; Ibba, A.; De Muro, S. *Ecosystem services and management of reed and seagrass debris on a urban Mediterranean beach (Poetto, Italy).* Estuarine, Coastal and Shelf Science, Vol. 271 (2022), 107862, https://doi.org/10.1016/j.ecss.2022.107862.

6.1 Introduction

Worldwide shorelines are often littered with biomass originating from terrestrial and marine ecosystems (Pan et al., 2021). Regardless of its origin, this material is ultimately deposited on the backshore by waves under storm conditions. Recent work has addressed the role of woody debris in coastal processes such as dune evolution and growth (Eamer and Walker, 2010; Grilliot et al., 2019). These studies have shown that dead trees and large logs (commonly referred to as driftwood) are a significant agent affecting morphodynamics of sandy beaches subject to appreciable aeolian sand transport. In fact, foredune development can benefit from the presence of woody debris that promote accumulation of windblown sand in the backshore. Moreover, Kennedy and Woods (2012) suggest that woody debris act as a buffer to waves during storm events on gravel beaches.

Posidonia oceanica meadow is another source of biomass, along Mediterranean and south-western Australian coastlines (Tecchiato et al., 2016; De Muro et al., 2018), that storms uproot and transport from the shoreface, eventually accumulating it on the backshore (Vacchi et al., 2017). The presence of seagrass necromass (leaves and rhizomes mixed with sand, commonly referred to as banquette or beach-cast litter) mitigates beach erosion induced by winter storms by promoting sediment retention and reducing sediment resuspension (Simeone et al., 2013; Trogu et al., 2020).

The aforementioned work has contributed to the characterization of coastal processes induced by large woody debris and Posidonia oceanica banquettes, drawing attention to their ecosystem services. However, beside the services identified by the scientific community, the presence of this biomass often poses a management issue especially on beaches devoted to tourism. For instance, despite being a common feature on Mediterranean beaches, the Posidonia oceanica banquette is not always perceived positively by tourism service providers and beach-goers (McLachlan et al., 2013). This has led local authorities to prepare guidelines devoted to the

identification of strategies for the management of banquettes. Due to its recognized services offered in terms of coastal protection, in Italy the regulation of Posidonia oceanica falls within the exclusive competence of the state legislator. The regional legislative competence in the field of tourism can be exercised, only insofar as it is not in contrast with the state discipline. In Sardinia, the 2016 regional resolution (40/13 of July 6, 2016) entitled "Operational guidelines for the management of *Posidonia oceanica* deposits on beaches" suggests that the preferred management strategy is to keep the wracks on site. In the event that, for technical reasons that objectively hinder the usability of the beach in the summer season, keeping the Posidonia deposits on site is extremely problematic, the option of moving and subsequent repositioning of the accumulations and the transfer to waste disposal or recovery plants can be pursued following some procedural and operating instructions.

Large woody debris and Posidonia oceanica wracks are not the only source of biomass on Mediterranean beaches. Small and medium-size woody debris, such as reeds proceeding from fluvial systems, are a common feature whose role in beach morphodynamics has received less attention by the scientific community (Battisti et al., 2020). In particular, to the best of the authors' knowledge, a quantitative assessment of the role played by beach berms reinforced by seagrass and reed wracks on the protection of sandy beaches has not been reported. Moreover, probably due to the rarity of large reed deposition events, the management of these deposits is less regulated than the case of Posidonia oceanica. The absence of regulation leaves coastal managers without clear guidelines for the management of reed deposits on beaches.

This study reports the scientific inquiry carried out within the management process of an exceptional accumulation of reeds (*Arundo donax* proceeding from local fluvial systems) and seagrasses on the berm of the Poetto beach (Cagliari, Southern Sardinia). Although reed deposition on Poetto beach is not unusual, an exceptional event occurred on December 2019 with a magnitude that had not been previously observed. The great amount of this biomass accumulated nearby the shoreline raised concerns especially among local tourism service providers, worried about its negative impacts. The municipality of Cagliari disposed the measures to bring the beach back to the previous state and, due to the absence of a legislation on the management of reed deposits, commissioned the CMGG (Coastal and Marine Geomorphology Group) of the University of Cagliari to prepare a scientific inquiry, including the monitoring of the beach berm processes before, during and after the removal of reeds. The main purpose of the inquiry is thus to scientifically support and motivate the management decisions.

A special attention in the scientific inquiry is devoted to runup and flooding on Poetto beach, characterized by low-lying sandy backshore and the implications for coastal protection and management. The shape of Poetto beach profile, with a berm higher than a large portion of the emerged beach, allows to consider the implications of using vertical and horizontal runup values

in the assessment of beach flooding. The runup assessment conducted through a numerical approach benefited from the preparatory field work, including beach surveys and permeability tests. Beach surveys reported large spatial variability of hydraulic conductivity across the beach, related to the distribution of reed and seagrass deposits within the sediment. The role of infiltration/exfiltration processes on a low-lying sandy beach under overwash events is investigated in detail. For this purpose, we identified the major storms that hit the study area during the monitoring period to assess the storm-induced coastal flooding through numerical modelling including groundwater flow processes.

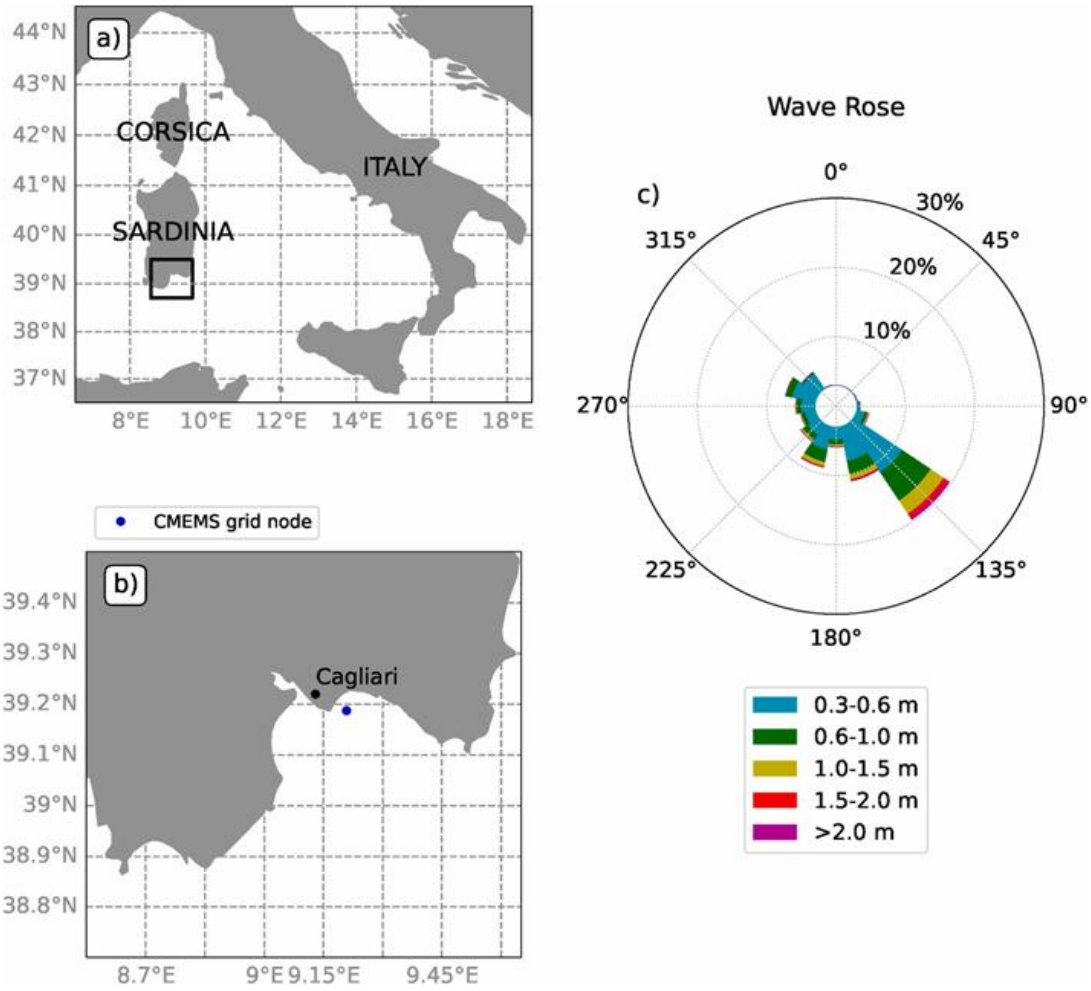

Figure 6.1 - a) and b) Geographical settings with the location of the virtual buoy in front of the Poetto beach indicated by the blue dot in panel b). c) Wave rose at the virtual buoy from the CMEMS database (2006–2018).

6.2 Geographical settings

Poetto beach lies in the innermost part of the Gulf of Cagliari, Southern Sardinia (Italy), inside the metropolitan area of Cagliari (Fig. 6.1). It is a micro-tidal urban sandy beach with a length of 8 km and a maximum width of about 100 m. The beach is backed by a relatively narrow primary dune system (foredunes and embryo dunes) bordered by a residential neighborhood and a 4-lane motorway that connects the two main towns of the metropolitan area: Cagliari and Quartu

Sant'Elena. Moreover, from the administrative point of view, the beach is divided into two sectors of similar size: the municipality of Cagliari manages the western sector whereas Quartu Sant'Elena manages the eastern part. A nourishment project carried out in 2002 in the Cagliari municipality sector has significantly modified the textural, compositional and morphological features of the backshore, shoreline and shoreface (De Muro et al., 2017). Besides, an increasing anthropic pressure, mainly related to the touristic sector, is responsible for an impact on the beach system, significantly affecting morphodynamic processes (Biondo et al., 2020).

Wave conditions along Poetto beach system result from a combination of Mediterranean swells and locally-generated wind waves, with directions mainly ranging from South-East to South-South-West, see the wave rose in Fig. 6.1. The Copernicus Marine Environment Monitoring Service (CMEMS) database covering the period 2006–2018 gives a mean significant wave height Hs of 0.4 m at the virtual buoy in front of the beach. Scirocco storm events drive the most intense swells that hit the beach from South-East and South-South-East directions. Moreover, the South-South-West sector contains considerable wave energy that is mainly related to West-South-West swells that enter the Gulf of Cagliari. Under these conditions, the wave direction in front of Poetto beach is the result of the shelter offered by Capo Spartivento (the Southernmost promontory of Sardinia) and wave refraction in the nearshore. The emerged beach of Poetto is periodically flooded by South-East storms, with a flooding extension that episodically can reach the coastal street and nearby proprieties (De Muro et al., 2017).

6.3 Event analysis

Heavy rain precipitation events occurred between the December 18, 2019 and the December 22, 2019 in the metropolitan area of Cagliari. The meteorological station located on the roof of a building in close proximity to the Poetto beach recorded precipitation peaks above 25 mm h^{-1} between 18:00h and 24:00h of the December 18, 2019 (the average yearly total precipitation is on the order of 500 mm in Cagliari). This weather events triggered a rapid increase of runoff discharged by surface streams to the Gulf of Cagliari. The resulting flows were able to put in motion and transport to the sea a considerable amount of biomass. The upper panels of Fig. 6.2 display the wave propagation in the Gulf of Cagliari at the moment of the two rain peaks indicated as R1 and R2 in the lower plot.

Once it reached the sea, this biomass, made mostly up of uprooted reeds (Arundo donax) from local streams, was transported and spread by marine currents and waves driven by the energetic South-East swell that battered Southern Sardinia coasts during these days. Fig. 6.2a shows that the significant wave height was above 1.5 m in the nearshore of the Gulf of Cagliari. Few days later the event that triggered the reed transport to the sea, a massive South-West storm approached the southern Sardinian coasts. Significant wave heights of above 6 m were expected

on the western coasts of the islands of San Pietro and Sant'Antioco. This massive swell, although attenuated by the shelter offered by Capo Spartivento (the southernmost Sardinian land), entered the Gulf of Cagliari and played a role in the redistribution of reeds along the shore, see Fig. 6.3a. Fig. 6.2c shows the evolution of the rain rate during the third week of December 2019, together with the significant wave height maps during the two rain rate peaks identified as R1 and R2 in the figure. The precipitation was measured by a meteorological station managed by the CMGG, located on the roof of a hospital immediately behind Poetto beach. Wave data proceed from the CMEMS database that uses the spectral wave model WAM to simulate the wave evolution with a spatial resolution of 1/25o of latitude and a time resolution of 1 h.

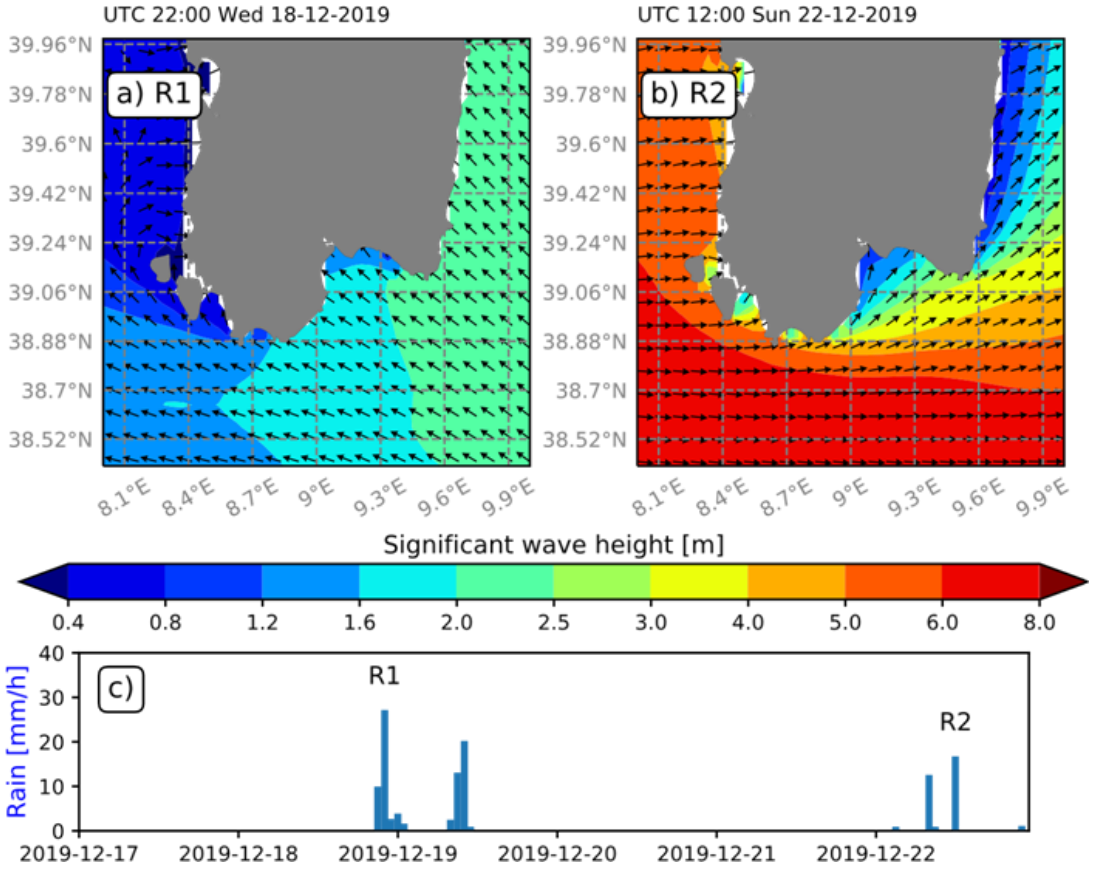

Figure 6.2 - a) and b) Significant wave height during the two events R1 and R2 that drove the reed deposition and redistribution along the Poetto beach (Wave data from the CMEMS database). c) Precipitation rate measured at the Poetto beach.

The great amount of biomass accumulated on the shoreline raised concerns especially among local tourism service providers, worried about its negative impacts in terms of beach accessibility. Due to the absence of legislation and the strategic importance of the beach for the local community, the municipality of Cagliari involved stakeholders, the University and local authorities in the decision making process with the objective of identifying a shared strategy about the management of this exceptional event. Once the options of 1) keeping the deposits on site and 2) their temporal movement have been considered as not viable options, the municipality of Cagliari disposed the measures to remove the reed deposits from the beach and commissioned the CMGG group of the University of Cagliari for the monitoring of the beach berm

processes. Following the suggestion made by the CMGG and in agreement with the guidelines listed by the Sardinian legislation for the Posidonia oceanica management, the municipality disposed that the removal operations of reed berms should have been carried out in a sustainable way, preserving the natural characteristics of the beach. In fact, the reeds were removed manually (see Fig. 6.3b) avoiding the use of heavy machinery that usually causes a considerable loss of sediments, resulting in changes in the beach morphology (e.g., flattening of the beach profile, sediment compacting and obliteration of sedimentary features like berms, beach-face steps, etc).

The management of this local exceptional event was affected by a larger global exceptional event: the corona virus (COVID-19) emergency. To contain the emergency, in March 2020 the Italian government imposed a national lockdown with strong restrictions on economic activities and the closure of beaches to public access. The lockdown lasted until May 2020 and, under this period, scientists had the unprecedented opportunity to observe ecosystem dynamics with almost no human interference. The beach berm reinforced by the presence of reeds stayed in place until its removal that occurred in April and May 2020. The municipality of Cagliari reported 35 tons of removed reed debris from this stretch of coast.

Figure 6.3 - a) Reed accumulation on the berm of Poetto beach. b) Removal operations of reed deposits.

6.4 Methods

6.4.1. Monitoring program

The monitoring of the eco-geomorphological dynamics at Poetto beach included actions before and after the reeds removal: topographic and bathymetric surveys, collection of the rectified images through the videomonitoring system and permeability tests. This section describes only the topographic/bathymetric surveys and the permeability tests.

The topographical surveys were carried out along two transects in the western sector of the beach. Data were collected using DGPS in a GNSS (Global Navigation Satellite System) at frequency of 1 Hz. The transects run over the emerged beach from the dune system to the shallow shoreface at about 1 m depth. The shoreface bathymetry along each transect was recorded using a single-beam echo-sounder coupled with a DGPS receiver interacting with a navigation software (frequency of 5 Hz). The topographic and bathymetric data were combined to obtain a morphological profile of the emerged and submerged beach, from the dune system up to the upper limit of the Posidonia oceanica meadow (depths 10–15 m at Poetto). Fig. 6.4 shows the beach profiles surveyed along the two transects T3 and T7 before the removal of the reeds. In Fig. 6.4c (green circle) it is also possible to identify the upper limit of the Posidonia oceanica meadow that lies where the profile becomes noisy due to the presence of seagrass below 8/10 m depth for transects T7.

Infiltrometric tests conducted with double-ring infiltrometers allowed the characterization of the hydraulic conductivity on the sandy beach and on the beach berm with banquette. The permeability coefficients on sand ranged between 0.00003 m s^{-1} on the backshore and 0.0003 m s^{-1} on the beach berm with buried reeds. Larger permeability coefficients were measured on the beach berm with seagrass litter: they ranged between 0.14 and 0.15 m s^{-1}.

6.4.2. Storm identification

Incoming wave conditions at Poetto beach, for the period comprised between the deposition of reeds in December 2019 and their complete removal in May 2020, were collected from the CMEMS hindcast time series (Ravdas et al., 2018). For this purpose, we chose the grid node of the computational domain located in front of Poetto beach. Fig. 6.1b shows the location of the CMEMS system grid node indicated as virtual buoy, whereas Fig. 6.5 plots the time series of the incident wave parameters at that location: significant wave height (Hs), mean period (Tm) and mean direction (θ). Panel d) of Fig. 6.5 shows the mean sea level (msl) evolution recorded by the tide gauge located inside the Cagliari harbour, 4 km away from the Poetto beach. The analysis of the evolution of the significant wave height highlights several storms, among which it is possible the identification of the two storms that drove the reed deposition and their following redistribution along the Poetto beach in the month of December 2019. The most intense storm

in the observation period occurred from the 20th to the January 23, 2020 (with a peak on the evening of the 21st of January with significant wave heights of 2.9 m).

We used the peak-over-threshold (POT) (Mathiesen et al., 1994) method to identify the 48-h independent storms occurred during the observation period at the virtual buoy location represented by the CMEMS grid node. We identified the storms based on the prominence parameter for the significant wave height Hs: the prominence threshold was chosen equal to 0.6 m. Although the threshold value of 0.6 m may seem low for extreme event analysis, due to the moderate incoming wave energy levels at Poetto (mean Hs is 0.4 m), this method allowed the identification of 12 storms during the five-month period considered. We retained only the storms with a persistence above the threshold longer than 6 h, that met the independence criterion with more than 48 h between the peak of a storm and the peak of the following one. The extreme wave parameters representative of each storm of the sample were selected as the values occurring at the time in which the maximum wave height was observed during the storm duration.

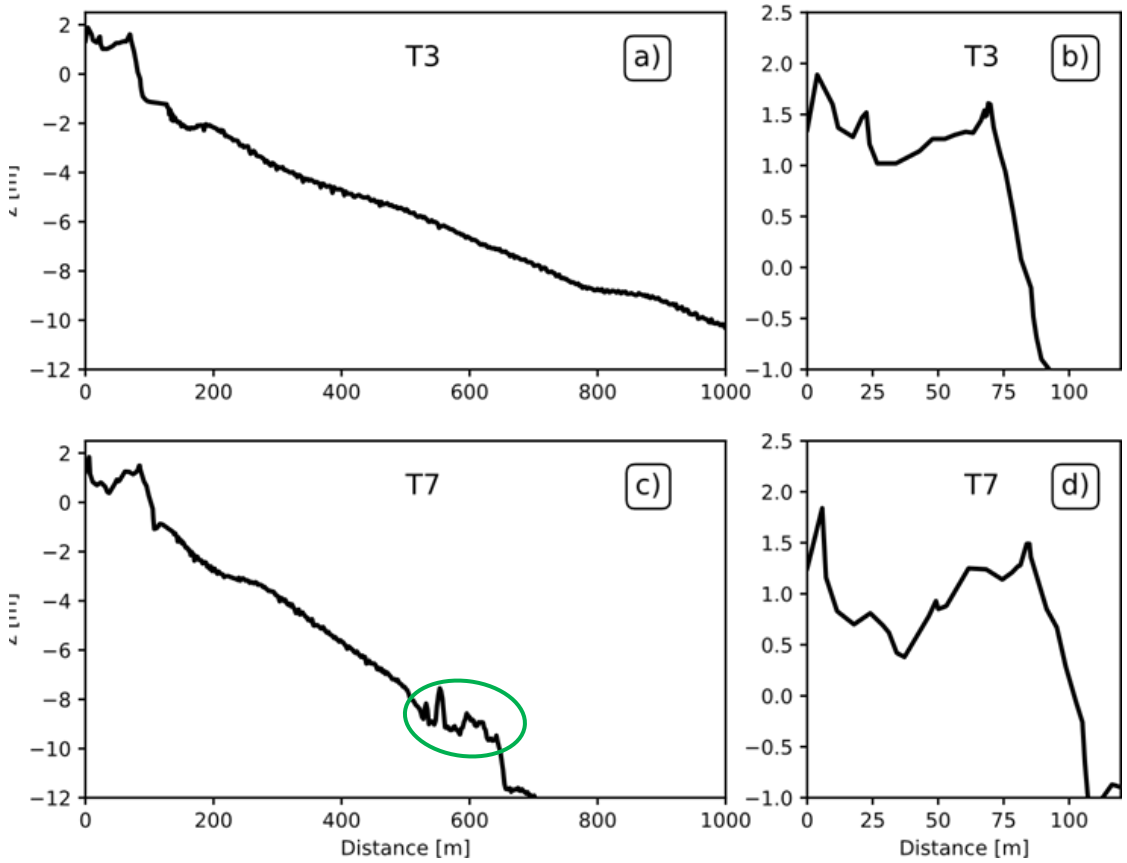

Figure 6.4 - a) and c) Beach profiles along the two transects T3 and T7. b) and d) Details of the foreshore and emerged beach profiles.

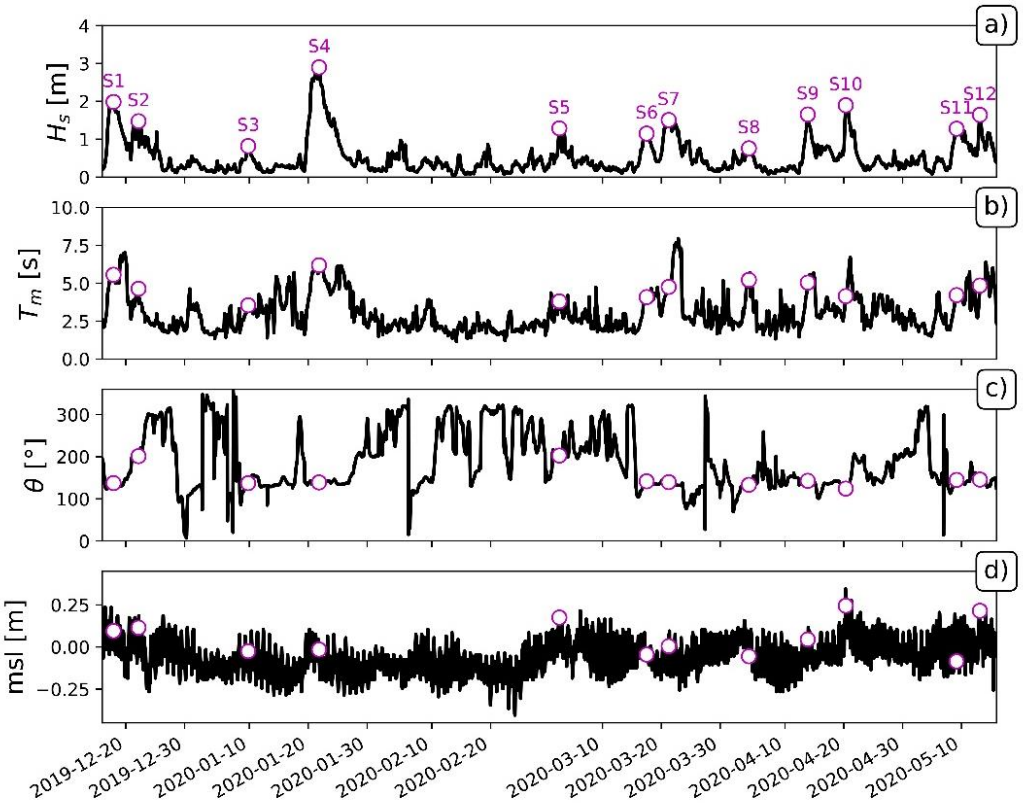

Figure 6.5 - Time series of wave parameters and mean sea level at the Poetto beach during the observation period. a) Significant wave height, b) mean period, c) mean wave direction, d) mean sea level. The circles highlight the main storm events.

Table 6.1 reports the dates of occurrence together with the wave parameters and the mean sea level of the identified 12 storms. The last column of the table lists the effects observed from the video monitoring system.

Table 6-1 - Wave parameters and mean sea level during the storms occurred in the period December 2019-May 2020 at Poetto beach. The last column lists the effects observed from the video monitoring system.

Storm	Date	Hour	H_s [m]	T_p [s]	T_m [s]	Dir [o]	msl [m]	Effects
S1	2019-12-17	22:00	1.98	8.39	5.56	137.30	0.09	overwash
S2	2019-12-22	04:00	1.48	11.17	4.64	201.35	0.11	none
S3	2020-01-09	19:00	0.82	5.73	3.54	137.14	-0.02	none
S4	2020-01-21	20:00	2.90	8.39	6.18	138.90	-0.02	overwash
S5	2020-03-02	16:00	1.29	5.73	3.80	202.74	0.17	none
S6	2020-03-17	12:00	1.15	6.93	4.08	141.53	-0.05	none
S7	2020-03-21	06:00	1.51	7.63	4.76	139.53	0.01	none
S8	2020-04-03	21:00	0.76	8.39	5.22	133.24	-0.05	none
S9	2020-04-13	21:00	1.65	6.93	5.04	142.70	0.04	none
S10	2020-04-20	08:00	1.90	7.63	4.15	124.24	0.24	overwash
S11	2020-05-09	04:00	1.28	6.30	4.22	144.79	-0.09	none
S12	2020-05-13	03:00	1.64	6.93	4.85	145.67	0.21	none

6.4.3. Modelling approaches

- Phase-averaged modelling

To evaluate the role played by the organic berm in coastal protection from flooding, the incident wave conditions collected at the nearshore grid nodes of the CMEMS system were numerically propagated in the nearshore with the SWAN model (Zijlema and van der Westhuysen., 2005). The SWAN model is a spectral wave model based on the wave action equation. It is nowadays widely used to address wave nearshore processes (Bellotti et al., 2021; Stokes et al., 2021). The wave spectra reconstructed at six nodes of the CMEMS system represented the wave conditions imposed at the boundary of the numerical grid used for the wave propagation with SWAN (Fig. 6.6). The six grid nodes lie along the open SWAN boundaries at West, South and Est of the grid. The spectral reconstruction routine was necessary since CMEMS does not provide the full frequency-directional spectra but it makes available the partition parameters (Hs, Tm and θ) for two swells and one wind sea component. The partition parameters from CMEMS were used to reconstruct the full spectra at the boundary nodes. For this purpose, we inferred the full frequency-directional spectrum as a sum of the three partitioned spectra (primary and secondary swell and wind wave component) reconstructed from the partition parameters, assigning a parametric spectral shape (JONSWAP) with a large directional spread to the wind wave component with respect to the swell components. The routine of spectrum reconstruction at each node can be summarized as follows:

• reconstruction of the frequency-directional spectrum with JONSWAP shape (γ=3.3) and directional spread of 19° from the bulk wave parameters of the primary swell partition provided by CMEMS

• reconstruction of the frequency-directional spectrum with JONSWAP shape (γ=3.3) and directional spread of 19° from the bulk wave parameters of the secondary swell partition provided by CMEMS

• reconstruction of the frequency-directional spectrum with JONSWAP shape (γ=3.3) and directional spread of 25° from the bulk wave parameters of the wind-wave partition provided by CMEMS

• the total spectrum is the sum of the three previous spectra

This routine with the spectrum reconstruction from wave spectral partitions represents an improvement with respect to the reconstruction from total bulk wave parameters (adopted, for instance, by Bellotti et al., 2021) since it allows the characterization of multi-modal seas. Figure 6.7 shows the result of the spectral reconstruction routine for storm S12. From the

comparison of panels a) and c) it is possible to appreciate the different shapes of the swell and the wind wave spectra with the latter characterized by a larger directional spread. Panel b) suggests that for storm S12 the secondary swell virtually carry no energy, which is a common situation in a closed basin as it is the Mediterranean Sea. As a result, the total spectrum for storm S12 is simply given by the sum of the primary swell (the secondary swell is close to zero) and the wind wave spectra.

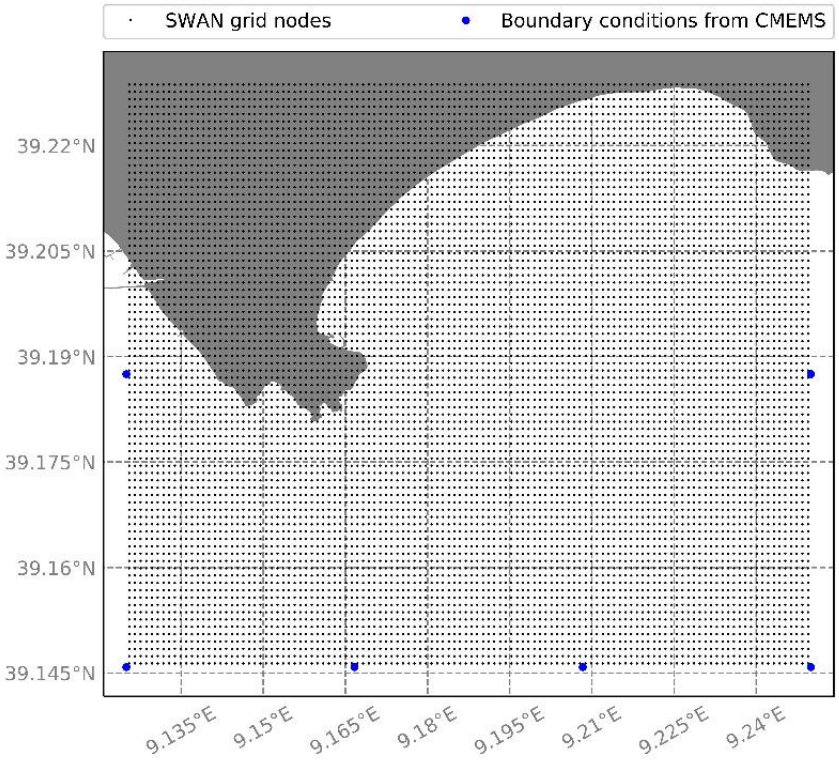

Figure 6.6 - Computational grid domain in SWAN. The blue points are the CMEMS grid nodes in which the boundary conditions for SWAN are reconstructed.

The grid used in the SWAN simulation (Fig. 6.6) has a spatial resolution of 1/16 of nautical mile (about 115 m) and allows the achievement of the wave conditions in the proximity of Poetto beach and the identification of the main wave transformation processes in coastal water.

The reliability of the spectral wave modelling approach is assessed by comparing the SWAN output with wave measurements in coastal water. Since we do not have measurements available in the observation period, we use the data collected by an AWAC (Acoustic Wave And Current) profiler deployed in the nearshore of Poetto at a water depth of 18 m during two field campaigns conducted, respectively, in Spring (2017) and Fall 2020. Further details about the field campaign and the exact AWAC location can be found in Ruju et al. (2019a). The adoption of the procedure described in section 6.4.2 allows the identification of 5 wave events, whose Hs is between 0.9 and 2.8 m. These events are simulated with SWAN following

the routine described in section 7.4.3. Here, we adopt the normalized root-mean-square-error *NRMSE,* define as follows:

$$NRMSE = \sqrt{\frac{\sum(O_i - M_i)^2}{\sum O_i^2}} \quad (1)$$

where O_i and M_i are the observed and modelled variables. The NRMSE of Hs is equal to 0.137. This value of NRMSE is consistent with the error metrics range reported by recent studies dealing with spectral wave modelling in coastal water (Bellotti et al., 2021; Ravdas et al., 2018), thus proving the ability of the adopted approach in modelling nearshore wave dynamics.

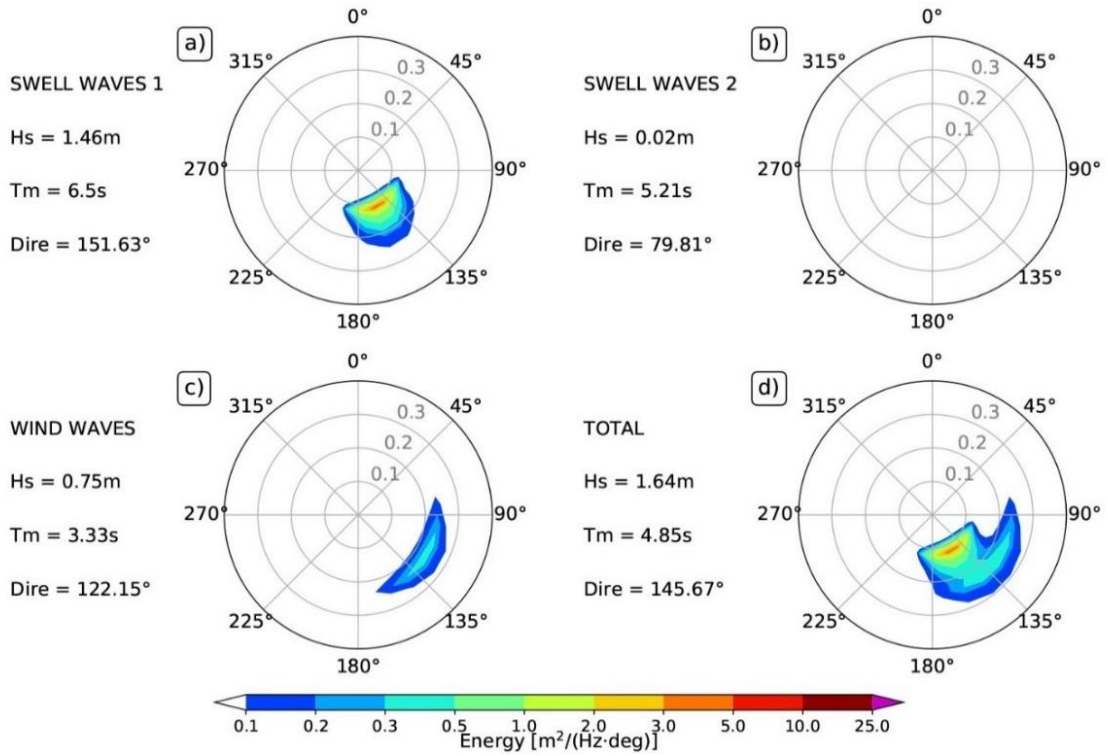

Figure 6.7 - Reconstruction of spectral wave boundary conditions (storm S12) from bulk swell and wind wave parameters. a) Primary swell wave spectrum, b) secondary swell wave spectrum, c) wind wave spectrum, d) total wave spectrum.

- Phase-resolving modelling

The spectra obtained as output of the SWAN simulations were used as a boundary conditions for the wave-resolving model XBeach (Roelvink et al., 2018) covering the shallow water area. The nonhydrostatic module of XBeach used in this study is based on the nonlinear shallow water equations, including a nonhydrostatic term to account for frequency dispersion in intermediate water. Simulations were setup in 1D cross-shore mode along the two transects T3 and T7, see Fig. 6.8. The numerical domain covered the nearshore area from 14 m of

depth up to the toe of the dune system. The seaward boundary with a water depth of 14 m was chosen since it lies in proximity of the outward boundary of surf zone of major storms at Poetto. The choice of the offshore water depth for the 1D XBeach simulations follows from a compromise between two considerations. On one hand it is desirable to have the boundary as close as possible to the shore so that the wave field includes the effects of the refraction processes caught by SWAN. On the other hand, a boundary placed in water too shallow would lead to strong nonlinearities with a large and unrealistic second-order long-wave generation. See also the recent work of Fiedler et al. (2019) addressing the role offshore boundary conditions in surf zone modelling.

The mean water level of each XBeach simulation was set according to the level measured by the tidal gauge. To provide a detailed description of swash zone processes, the horizontal spatial grid resolution increased shoreward from 3.5 m in the generation zone up to 0.5 m in the swash zone, see Fig. 6.9. The offshore boundary generated the time series of incoming waves from the SWAN spectrum and absorbed the outgoing waves resulting from beach reflection. The model accounted for friction through the Chezy coefficient setup to 30 $m^{0.5}/s$, which is consistent with previously reported constant friction coefficients of 0.015 (Raubenheimer et al., 1995). Infiltration/exfiltration processes were simulated by including a constant permeability coefficient of 0.0003 m/s, equal to that measured on the beach berm in presence of reeds. We identify the runup toe as the shoreward point with water depth larger than 0.05 m.

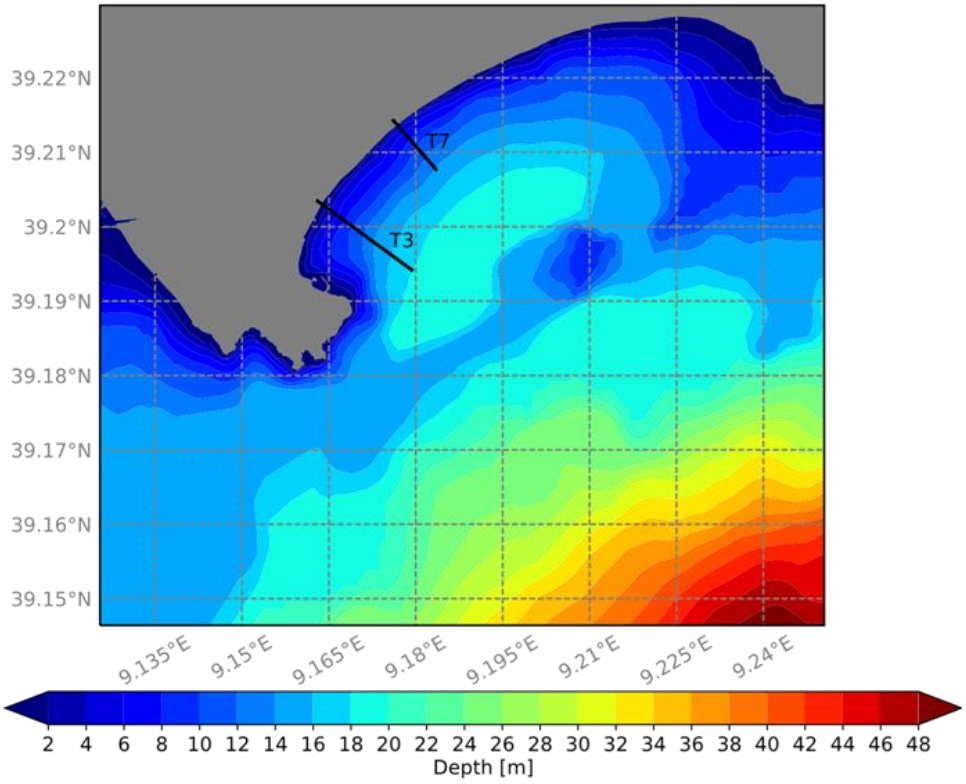

Figure 6.8 - Detail of the bathymetry in the Gulf of Cagliari with the transects T3 and T7.

To assess the role played by the reed-reinforced berm in coastal protection, we calculate the storm-induced runup both with an empirical approach and with XBeach modelling. We focus on the aforementioned 12 storms occurred in the period of observation. The total water level TWL is calculated as:

$$TWL = MSL + R_{2\%} \quad (2)$$

in which MSL is the mean sea level and $R_{2\%}$ is the 2% exceedance level for runup. *MSL* is obtained from the tide gauge installed inside the Cagliari harbour.

In the empirical approach, the runup contribution to the flooding level is determined from the spectral wave parameters (HS and Tp) computed by SWAN along the two transects T3 and T7 at a water depth of 14 m. The runup contribution to the flooding elevation is then obtained through:

$$R_{2\%} = 1.1\left(\langle\eta\rangle + \frac{S}{2}\right), \quad (3)$$

where $\langle\eta\rangle$ is the wave setup and S is the significant swash. Here, $\langle\eta\rangle$ and S are estimated from Hs, Tp and the foreshore slope β according to Stockdon et al., 2006.

$$R_{2\%} = 1.1\left(0.35tan\beta(H_0L_0)^{1/2} + \frac{[H_0L_0(0.563tan\beta^2+0.004)]}{2}\right) for\xi_0 \geq 0.3, \quad (4)$$

and

$$R_{2\%} = 0.043(H_0L_0)^{1/2}\, for\xi_0 < 0.3, \quad (5)$$

where H_0 and L_0 are the deep-water significant wave height and wavelength. ξ_0 is the Iribarren number or surf similarity parameter, computed as:

$$\xi_0 = \frac{tan\beta}{(H_0L_0)^{1/2}}. \quad (6)$$

In the numerical approach based on XBeach, $R_{2\%}$ is obtained directly from the computed runup time series.

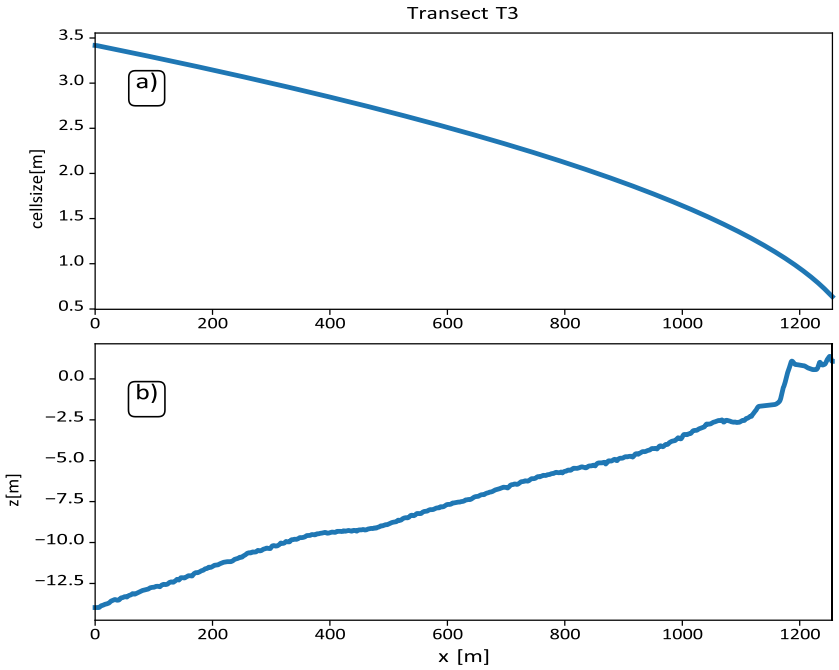

Figure 6.9 - a) Grid size variation across the XBeach computational domain for transect T3. b) Beach profile along T3.

6.5 Results

The TWL values from the empirical and numerical approaches are compared in Fig. 6.10. TWL calculated with the empirical method and TWL from XBeach are in good agreement. Since both approaches include the same MSL (from the tidal gauge), they can only differ as a result of the runup parameter $R_{2\%}$. This agreement highlights the general reliability of these different methods for runup and flooding calculations. Considering the XBeach output as reference value, the NRMSE of the TWL is equal to 0.235 and 0.179 for transects T3 and T7, respectively. Moreover, Fig. 6.10 is in good agreement with visual observations obtained from the video camera system. In fact, the images captured from the video camera revealed significant berm overwash during the S1 and S4; whereas storms S10 and S12 led to isolated overwash events. These four storms are identified as those driving the highest TWL values at the two transects at Poetto beach.

Fig. 6.11 shows the horizontal total water distance TWD from XBeach simulations. Both the TWL and the TWD include the $R_{2\%}$ parameter computed as the 2% exceedance level from the XBeach runup time series. TWL takes into account the vertical runup, whereas the horizontal runup contributes to TWD. The TWD parameter gives an insight of the flooding magnitude that is more difficult to achieve from the vertical TWL. This is mainly due to the fact that large part of the emerged beach lies below the berm elevation. In fact, sea conditions leading to overwash such as S1 and S4 give a TWL only few cm above the berm height, whereas the TWD is few meters beyond the berm crest location, indicated by the dashed line in Fig. 6.11. Fig. 6.11 is consistent with Fig. 6.10 allowing the identification of the four storms driving berm overwash. In addition,

Fig. 6.11 reveals the difference in flooding magnitude between the most severe storm S4 and the less strong storms S10 and S12.

Fig. 6.12 displays the time series of swash dynamics during storm S1, providing details of overwash dynamics on a low-lying backshore. Panel c) shows that vertical runup does not significantly overcome the berm elevation, although major uprushes are able to drive overwash. Instead, the horizontal runup time series (Fig. 6.12d) allows the identification of uprush events leading to overwash in which the berm crest location is exceeded. The upper panel highlights how effectively the infiltration processes drain the volume of water that overwashes the berm. In the simulation of the storm S1, the water accumulated by an overwash event over the emerged beach is completely drained before the arrival of the next overwash.

To investigate the importance of infiltration processes, we conducted another set of XBeach simulations using the hydraulic conductivity measured on the backshore on the sandy substrate, without the presence of buried reeds. Fig. 6.13 compares the computed flooding induced by the identified storms on the profile with a permeability coefficient of 0.00003 m/s with that computed on the profile with a permeability coefficient of 0.0003 m/s. In other words, the XBeach boundary conditions were the same in the two configurations that differed only in the hydraulic conductivity. To prevent the possible variability linked to wave groupiness (Rutten et al., 2021), not only the spectral shape but also the time series of the boundary conditions were conserved. In general terms, under the same environmental forcing, a lower hydraulic conductivity seems to increase the flooding extension under overwash conditions. The strongest TWD increases are found in run S4 on transect T3 (13 m) and in run S1 on transect T7 (7 m). On the other hand, under moderate wave conditions without overwash, infiltration processes have no significant effect of runup and TWD values.

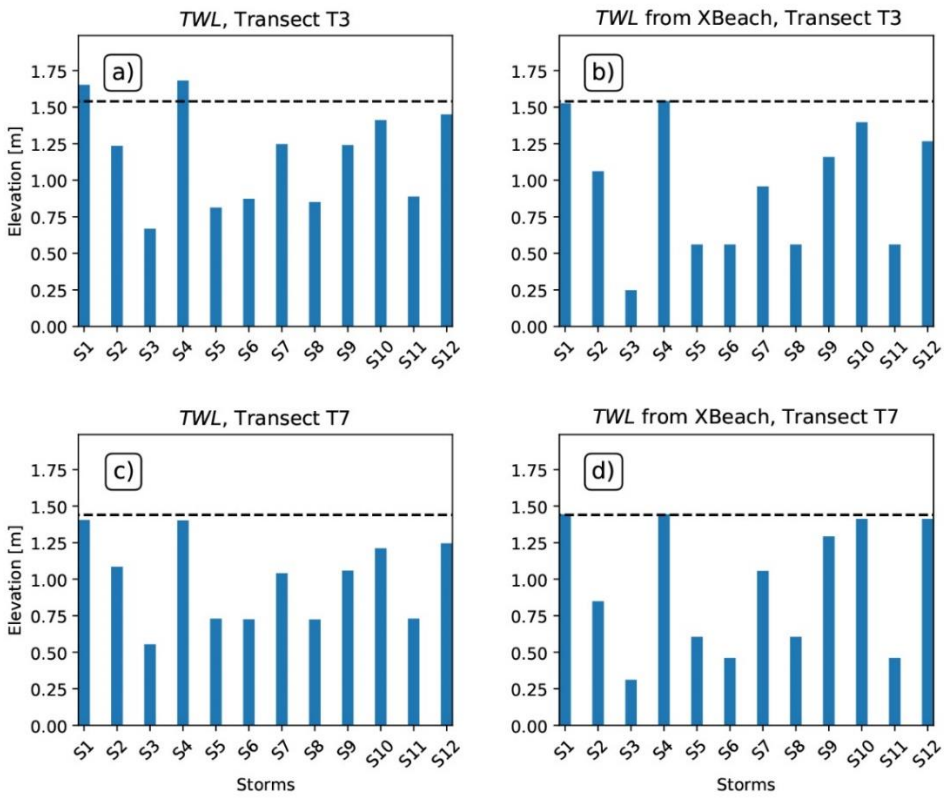

Figure 6.10 - Total water level TWL using parametric formulas for runup (a and c) and from XBeach simulations (b and d). The dashed line is the beach berm height above mean sea level.

The assessment of beach flooding through a numerical approach shows that four storms (S1, S4, S10 and S12) drove berm overwash during the observation period. Storms S1 and S4 led to significant overwash and flooding, whereas storms S10 and S12 produced only isolated overwash events with limited beach flooding. These results confirm the analysis of the images obtained from the videomonitoring system (the videomonitoring system did not detect overwash under storm S12 probably because this event happened at night and the moderate overwash left no visible marks on the beach). Under energetic conditions, once the berm is overwashed, the relative depression in the beach geometry favours the beach flooding towards the dune system. Numerical simulations conducted with different hydraulic conductivity coefficients allow the assessment of the role played by beach permeability on runup and flooding. According to previous studies (Masselink and Li, 2001)

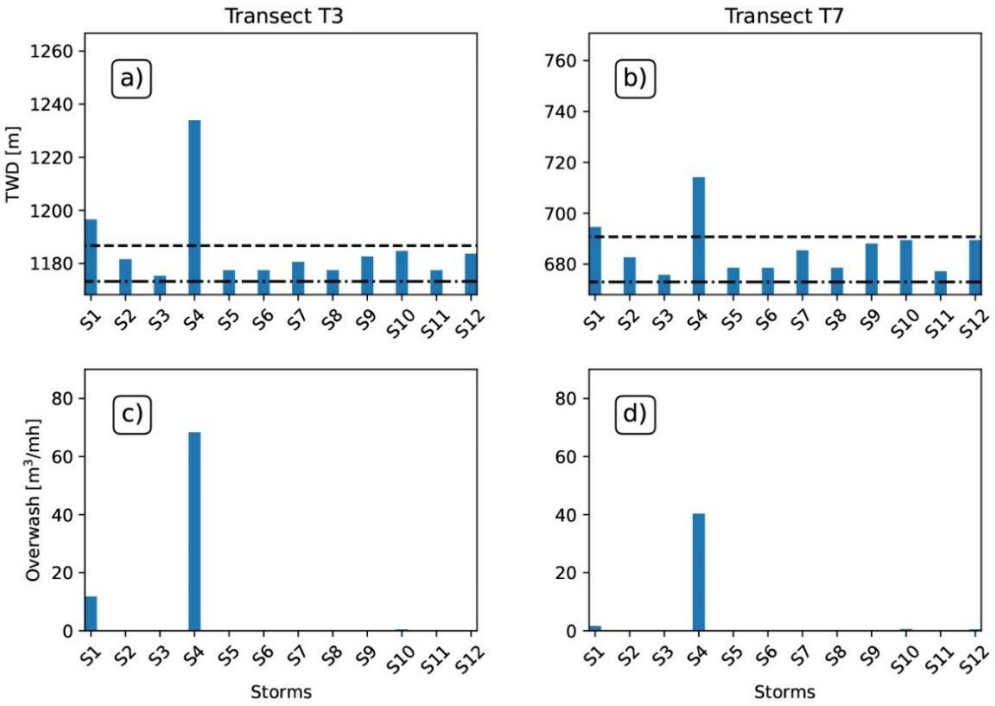

Figure 6.11 - a) and b) Horizontal total water distance from XBeach simulations. The dashed line and the dot-dashed line are the cross-shore location of the beach berm crest and the mean water level, respectively. c) and d) Overwash rate.

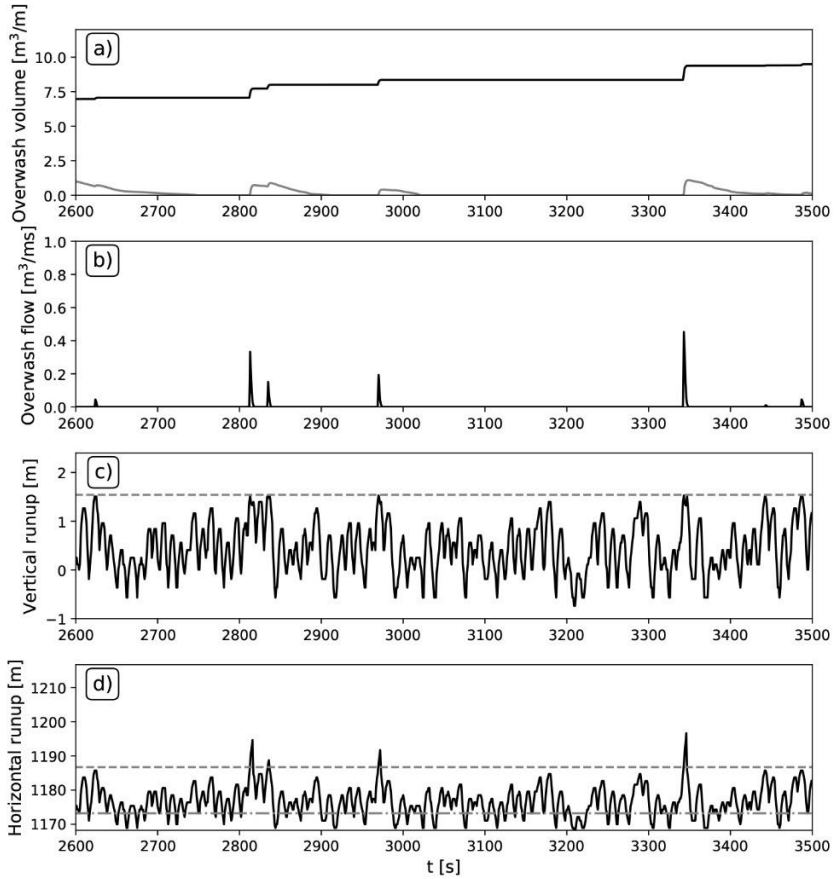

Figure 6.12 - Time series of swash dynamics. a) The black line is the cumulative overwash volume; the grey line is the water volume accumulated over the emerged beach. b) Instantaneous overwash flow. c) Vertical runup. The dashed line is the berm crest elevation. d) Horizontal runup. The dashed line is the berm crest location, whereas the dot-dashed line is the intersection between the mean water level and the beach profile.

suggesting that on sandy beaches weak infiltration processes are not able to modify swash dynamics, no appreciable differences in runup are found for moderate wave conditions in which the swash zone does not exceed the berm crest. Nevertheless, the results suggest that a low permeability coefficient tends to increase flooding under severe forcing leading to overwash. This process can be observed in Fig. 6.14 showing the comparison of two snapshots taken at the same moment in which a wave is overwashing the berm from the XBeach simulations of storm S1. The difference in permeability does not yield appreciable changes in the runup location (indicated by the red dot) in proximity of the berm. At the same time, the panel c) of the figure highlights how the low permeability precludes a complete evacuation of the water from the emerged beach. The water that overwashes the berm tends to accumulate on the emerged beach, eventually increasing the flooding area.

The simulations carried out so far have considered a homogeneous friction factor (Chezy equal to 30 $m^{0.5}/s$) over the entire beach profile. However, it is plausible that seagrass and reed deposits can enhance friction dissipation by increasing roughness at the bed. To quantify possible implications for coastal flooding, we have run a new set of simulations in which the friction was increased in the region of the profile covered with wracks over the T3 profile (we did not consider T7 since it is not in the area monitored from the video camera system). On the day in which the topographic survey was conducted, the videocamera system showed seagrass and reed wracks deposits that extended over 5 m landward from the berm of the profile of transect T3. The Chezy friction coefficient was set to 10 $m^{0.5}/s$ over this area, a value chosen according to Chow (1959) (vegetal lining). The permeability and other parameters were kept constant as in the previous simulations. Whereas the TWD induced by the most energetic storm S4 is not affected by the change in friction, a slightly reduction of 1 m is observed only for run S1 (not shown). This may be related to the flooding extension whose landward limit falls in proximity of the wracks in run S1. As expected, the locally-increased friction does not yield any TWD change under moderate storm conditions in which no overwash occurs.

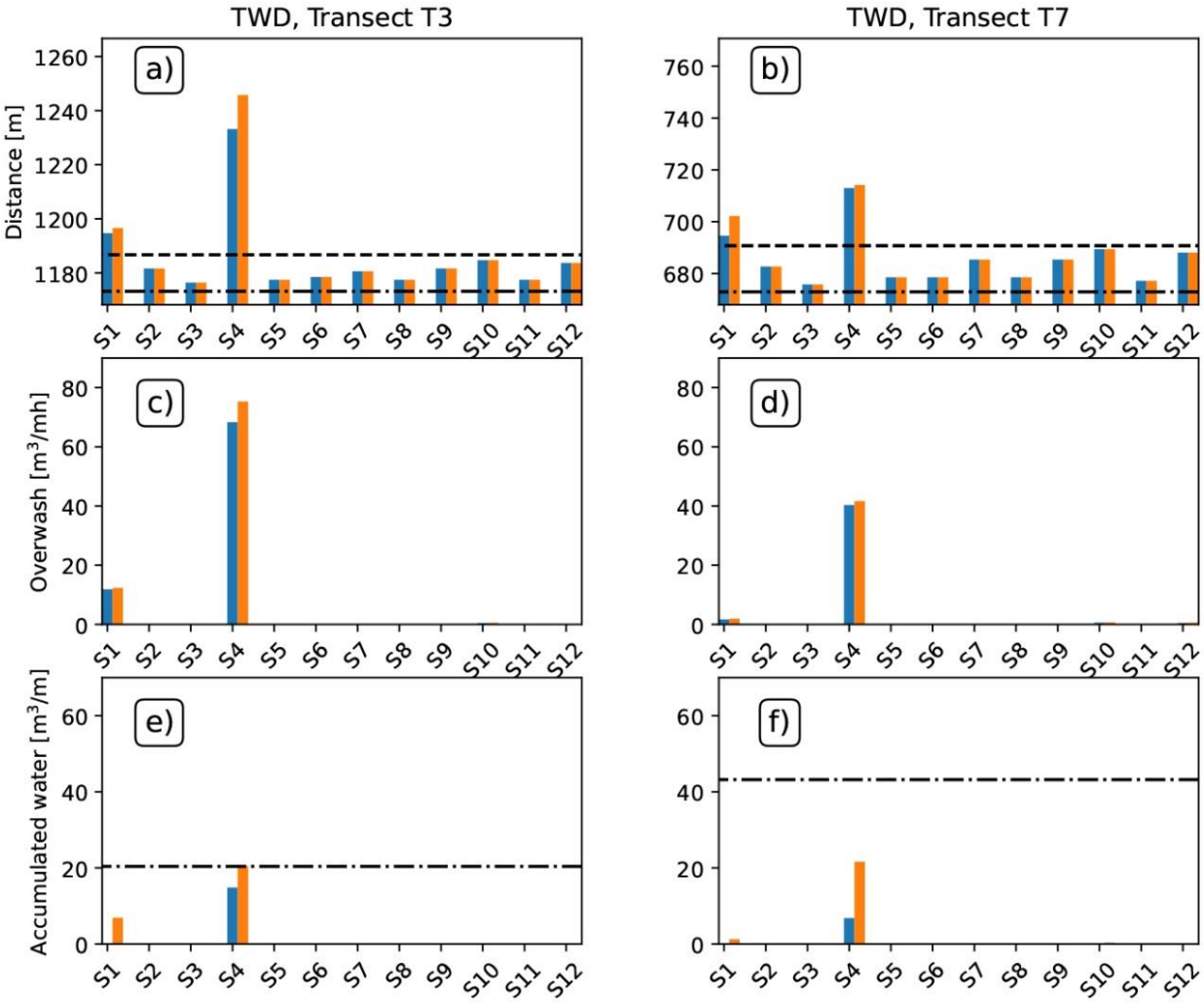

Figure 6.13 - Comparison of the results from XBeach simulations using the permeability coefficient of 0.0003 m/s (blue) and using the permeability coefficient of 0.00003 m/s (orange). a) and b) Horizontal total water distance TWD. The dashed line is the berm crest location, whereas the dot-dashed line is the intersection between the mean water level and the beach profile. c) and d) Cumulative overwash volume. e) and f) Accumulated water volume over the emerged beach at the end of the simulation. The dot-dashed line is the maximum water volume that can be stored between the berm and the dune system.

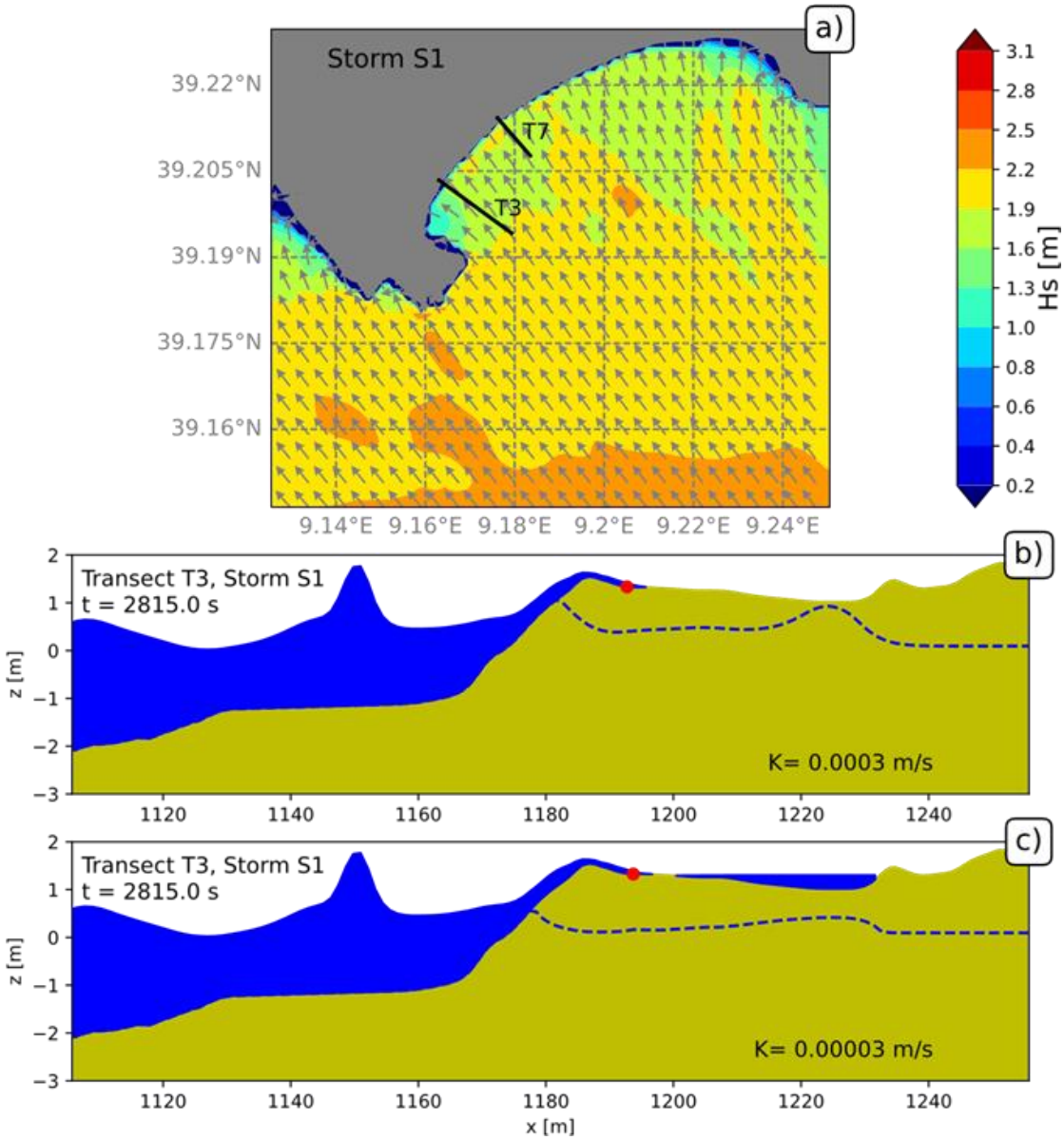

Figure 6.14 - a) Significant wave height field computed by SWAN for storm S1. b) and c) Snapshot of the XBeach simulations for Storm S1 along the transect T3 with a permeability coefficient (K) equal to 0.0003 m/s and 0.00003 m/s, respectively. The red dot shows the moving shoreline (runup) location. The blue dashed line indicates the groundwater table elevation.

6.6 Discussion

The approach followed in this work allows the assessment of runup and flooding on a low-lying backshore following an exceptional event of reed (*Arundo donax*) deposition. Particular attention is devoted to the overwash dynamics over the berm and to the infiltration processes occurring on the emerged beach. This section discusses the implications of the results together with the limitations and assumptions related to the adopted methodology.

We estimate the runup and flooding at Poetto beach through a model chain with increasing spatial resolution. The model chain, with the nesting of a phase-resolving model into a phase-averaged model, provides an accurate characterization of the main nearshore and shallow water processes driving wave runup dynamics, limiting the number of assumptions involved. However,

few assumptions are still present in the XBeach simulation setup. For instance, the cross-shore configuration precludes the characterization of longshore dynamics. The validity of the cross-shore approach in surf zone modelling has been extensively addressed by Fiedler et al., 2018, 2019. In particular Fiedler et al. (2018) tested the 1D assumption and concluded that it is a reasonable assumption for the prediction the bulk properties of runup observed on natural beaches for a wide range of incident wave conditions. In fact, as long as the offshore boundary of the 1D model lies outside the surf zone but sufficiently close to the shoreline (in this study it lies at a point with 14 m depth), refraction processes of shoaling waves lead to a near normal wave incidence at this boundary.

A good agreement is found between the vertical runup values calculated with the empirical formulation by Stockdon et al. (2006) and those computed with XBeach, see Fig. 6.10. Among different runup formulations that have been proposed during the last decades (Atkinson et al., 2017; Passarella et al., 2018a), we have chosen to apply the Stockdon et al. (2006) formulation due to its wide diffusion within the coastal engineering community (Tomas et al., 2016; Cohn and Ruggiero, 2016). Although empirical formulations still lack to address the effects induced by complex nearshore morphology (Cox et al., 2013; Guedes et al., 2012) and by incoming wave features (Guza and Feddersen, 2012; Ruju et al., 2019b), they have proven to provide a first order assessment of wave runup under a wide range of wave and environmental conditions (Passarella et al., 2018b). This justifies their use for a first order assessment of runup in those situations in which the use a phase-resolving model is not recommended, for instance for operational systems whose routines are run daily and computational efficiency is of paramount importance (Stokes et al., 2021).

Previous studies have reported highly dynamic banquettes that evolve, form and recede according to the wave forcing variability (Simeone and De Falco, 2012; Simeone et al., 2013; Gomez-Pujol et al., 2013; Trogu et al., 2020). Although the evolution of beach-cast *Posidonia oceanica* litter has been widely reported, fewer studies have addressed dynamics of small woody debris and reed deposits. Gomez-Pujol et al. (´ Gomez-Pujol et al., 2013´) and Trogu et al. (2020) showed that the permanence of banquettes on wave-exposed beaches is transitory and these features hardly withstand energetic storms. This variability raises doubts about the effective coastal protection offered by seagrass wracks under storm conditions. Nevertheless, observations of the berm dynamics during the winter and spring 2019–2020 at Poetto suggest that major storms are able to shift shoreward the organic berm location but not to dismantle it (see Fig. 6.15 showing the presence of reed wracks both before and at the end of storm S4). In other words, the presence of intertwined reeds and seagrasses within the beach berm seems to increase its flexibility and preserve it against destructive wave action. More detailed analyses on the variability of the extension of reed and seagrass wracks according to wave and environmental forcing will be presented in a future paper.

Since the larger permeability coefficients have been found in areas with sand mixed with buried reeds, this result suggests that intertwined reed and seagrass wracks can mitigate the effects of overwash and flooding by increasing the beach permeability, promoting infiltration and thus water evacuation from the emerged beach. In this study, the effects of a locally-increased bottom friction by reed ad seagrass deposits seems to have a limited and secondary impact on coastal flooding. The discussed assumptions involved in this study, such as the use of a single permeability coefficient over the entire beach profile, suggest that these findings should be confirmed by more refined and more exhaustive swash modelling in future works.

In terms of coastal protection from flooding, these results suggest that keeping the reed deposits in place appears as a sound solution. The reed deposits can be regarded as an ecosystem-based solution and their services be should be taken into account in a sustainable coastal planning strategy. At the same time, it is evident that these barriers of dead plants on Mediterranean beaches considerably limit the suitability for bathing. Therefore, in these cases, their removal must be considered, creating the problem of reconciling environmental protection and tourist use. In this context, making available to local authorities an assessment of how the reed and seagrass deposition affects coastal processes can be beneficial towards a sustainable coastal management. In principle, the same approach adopted by the legislation for the Posidonia oceanica management can be extended to reed wracks: keeping the biomass in place, compatibly with the touristic vocation of a specified beach. In fact, the intertwined reed and seagrass wracks have the effect of increasing the permeability of the beach, thus favouring the drainage of water from the emerged beach, eventually reducing flooding. Nevertheless, in this particular case, the touristic vocation of Poetto beach precluded the possibility of keeping the huge amount of reed deposits in place, as they constituted a significant obstacle in terms of beach fruition and shoreline accessibility.

6.7 Conclusions

This work devotes a special attention to runup processes induced by storms at a low-lying backbeach in the presence of reed and seagrass deposits. The methodology included a model chain with increasing spatial resolution and details. Data showed that, due to the beach profile with the berm higher than the emerged beach, the horizontal runup provided a quantification of the flooding extension that is more difficult to achieve from the vertical runup. Using the hydraulic conductivity parameter measured in a beach area with sand and buried reeds, infiltration processes allowed the beach to drain the overwashed water and its return to the sea. The role of beach permeability on runup was assessed by running a new set of wave simulations using a low hydraulic conductivity parameter, equal to that measured in a beach area with sand only. Under overwash conditions, runup and flooding extensions were increased by a low permeability coefficient. These results highlight the role of the ecosystem services provided by

intertwined reed and seagrass wracks on beaches, suggesting that they must be taken into account in a sustainable coastal planning strategy.

Figure 6.15 - View of the Poetto beach from the video camera system. a) picture taken before S4 storm (19/01/2020); b) picture taken at the tail of S4 storm (24/01/2020).

Chapter 7
ON THE ROLE OF BEACH-CAST LITTER FOR THE CONSERVATION OF A URBAN MICROTIDAL MEDITERRANEAN BEACH THROUGH VIDEOMONITORING SYSTEM DATA ANALYSIS

7.1 Introduction

Mediterranean beaches can be characterized by the presence of meadows composed by *Posidonia oceanica* (L.) Delile, an endemic Mediterranean seagrass species (monocotyledonous angiosperms) (Duarte, 1991; Duarte, 2004). Depending on the hydro-dynamics of the beach, *Posidonia oceanica* can live in a bathymetric range from the surface to 30–40 m depth in clear waters (Pergent et al., 1995), and releases its leafs in autumn. *Posidonia oceanica* rests, often also composed by roots and rhizomes, are transported by waves and currents to the foreshore and backshore, building a sedimentary structure, known as banquette (Boudouresque and Meisnesz, 1982) or seagrass berm (Short, 1999; Simeone et. al, 2013b). These structures, depending on wave motion, can be found throughout the year on natural, embayed beaches. In urbanized beaches they can be found only from autumn to late spring because of the anthropic practise of beach cleaning with heavy vehicles removing the banquette (Simeone et. al, 2013a).

The *P. oceanica* meadows hosts the most productive marine ecosystem in the Mediterranean (Calizza et al., 2013; Duarte et al., 1999) acting as nursery and habitat for a lot of fish species, invertebrates, foraminifers, etc. Their leaves are able to fix CO_2 as organic matter by subtracting it from the sea water. Another fundamental role played by *P. oceanica* meadows, largely documented in literature, is that they dissipate the energy of the wave motion during storm events (Sánchez-González et al., 2010; Elginoz et. al, 2011; Infantes et al., 2012; Koftis et al., 2012; De Muro et al., 2014; etc.). For all these reasons it is protected (both alive and dead) by “Habitat Directive” (92/43 / EEC) and is classified as a priority habitat (1120).

Many studies dealing with seagrass berm and videomonitoring system have been carried out (Gómez-Pujol et. al, 2013; Simeone et. al, 2013b; Passarella, 2019; Ruju et. al, 2019; Paquier et. al, 2020; Trogu et. al, 2020; etc.). The goals of these works mainly focused on the composition of seagrass berms, their role in wave energy dissipation and the shoreline change positions induced by the deposition of beach-cast litters. The debate on the role of banquettes in dissipating wave energy is still open. Gómez-Pujol et al. (2013) argue that banquettes have little or no effect on wave dissipation as they are dismantled before the storms arrive. Other authors (e.g., Passarella, 2019) highlight how the presence of banquettes affects the swash processes, making the beach profile more reflective.

The aim of the present study is to improve the knowledge of the dynamics of the seagrass berm along the beach shoreline. We investigated the processes of deposition and destruction of the

banquette along three transects in an urban, microtidal and wave dominated Mediterranean beach by analysing of a four years database of daily images. Using geo-rectified images, we measured the width of the banquette on the three transects for each day and then relate their presence and extent with wave and wind parameters.

7.2 Geographical settings, wave climate and hydrodynamics

Poetto is an urban, microtidal and wave dominated beach, located in the Gulf of Cagliari, southern Sardinia, Italy, western Mediterranean (Figure 7.1). This sandy beach has a length of 8 km and a maximum width of about 100 m and is confined at southwest by the Cape S. Elia (its eastern portion as known as "Sella del Diavolo") promontory, in the municipality of Cagliari and at east by Margine Rosso in the Quartu S. Elena communal area. A residential neighbourhood and a 4-lane motorway interrupt the natural beach profile, mainly the dune system. No river flows across the beach and there is not a direct terrigenous-sedimentary supply, except the poor contribution made by the erosion of the carbonatic and siliciclastic rocks of the Cape S. Elia promontory, a mainly calcareous formation of Miocene age (Porta et. al, 2020) (Figure 7.1B). Poetto beach formed approximately seven to five thousand years ago, when post glacial sea level rise significantly decelerated allowing the formations of the barrier system that evolved into the current sandy coastline with Molentargius Pond system behind (Vacchi et. al, 2017; Porta et. al, 2020; Biondo et. al, 2020). The mostly sedimentary supply comes from the authigenic bioclastic sediment produced by the *Posidonia oceanica* meadows (Porta et. al, 2020; Biondo et. al, 2020) (Figure 7.1B).

In this study we investigate the southwest sector of the beach, along three transects (T1, T2, T3), located in areas with different anthropic impacts. T1 is ≈35m long and is located inside a beach property built over the dune system. T2 is ≈38m long and is located almost outside the beach property, where the buildings are further away from the shoreline, even if the presence of a network delimits the area. T3 is ≈92m long and is located in a stretch of the beach with slightly less anthropogenic impacts (compared do T1 and T2), as it starts immediately behind the dunes and reaches the shoreline (Figure 7.1C). Throughout this area of the beach, in 2002, a nourishment that modified the textural, compositional and morphological features of the backshore, shoreline and shoreface, have been carried out. This is also the area where the *Posidonia oceanica* meadow is furthest from the shoreline (about 1,4 km – De Muro et al., 2017) and where, as the historical photos show, the accumulation of seagrass berm is a cyclic, natural phenomenon.

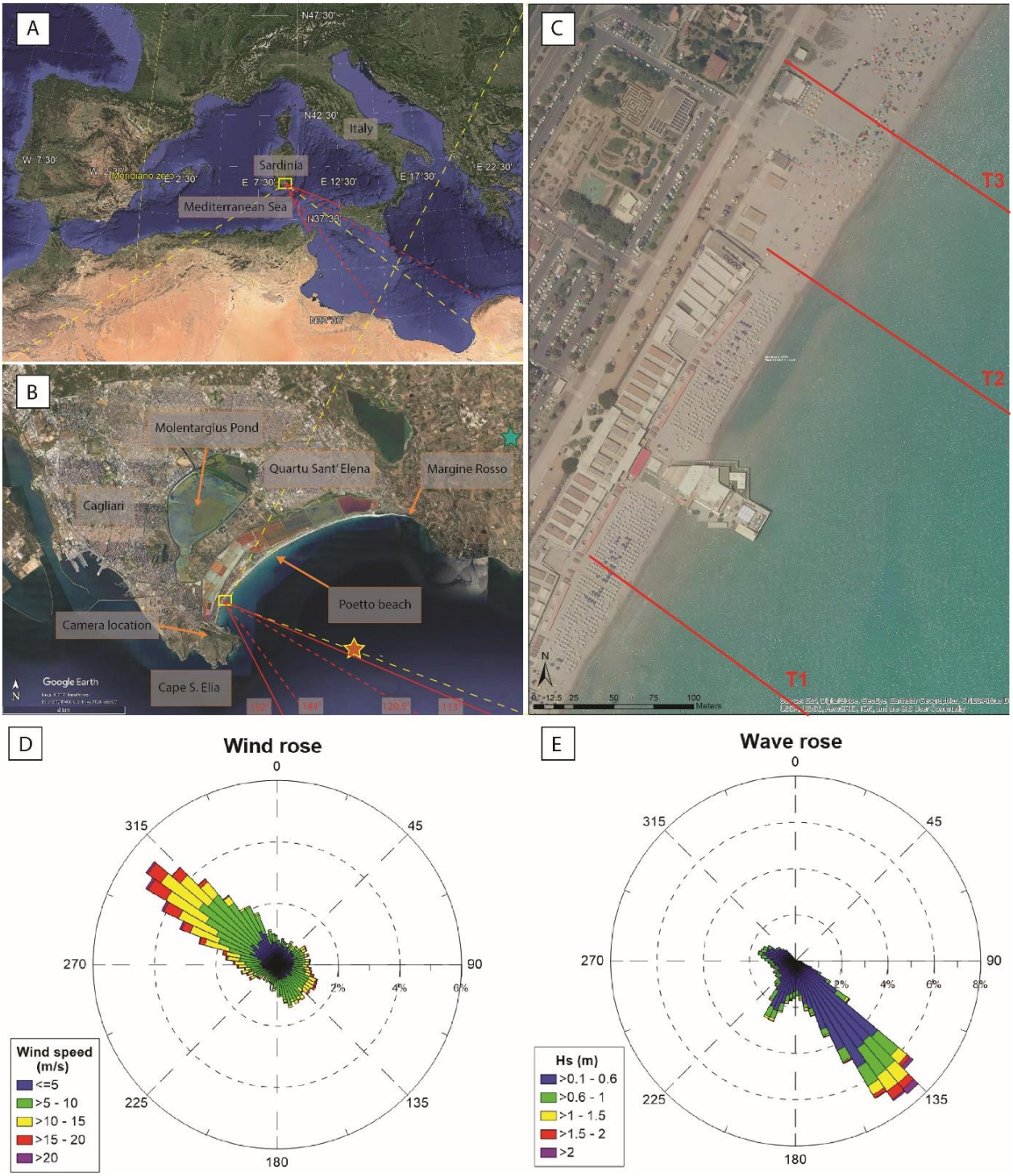

Figure 7.1 – Geographical setting of the study area (western Mediterranean Sea) with: (A) wave exposure angles (referred to the N = 0°) and fetch for the study area within Poetto beach; (B) Location of videomonitoring system and limits of Poetto beach; (C) Detail of study area and the three transects; (D) Wind speed and direction from the ERA5 reanalysis dataset (green star in panel B); (E) Significant wave height and direction at the Copernicus Marine Environment Monitoring Service hindcast and forecast (orange star in panel B).

The possible directions of storms at Poetto beach are comprised between 117° and 202°, while the dominant geographical fetch ranges from 120° to 145°. For the study area these values change from 113° to 152° for approaching storms and 120,5° to 144° for the geographical fetch and their length is between 1283 and 908 km respectively, with a maximum extension of 1360

km (Figure 7.1A and 7.1B). However, the limited extent of cyclonic perturbations in the Mediterranean suggests considering, in any case, maximum effective fetches at 500 km (Piscopia et.al, 2004). A 2016-2019 hindcast and 2020 forecast wave data delivered by the Copernicus Marine Environment Monitoring Service (CMEMS) have been used to characterize wave climate of the area (Figure 7.1E). We extracted the wave parameters (significant wave height Hs, peak period Tp, mean period Tm and mean direction) at the grid node of coordinates 39°11’17” N, 9° 12’ 39” E (orange star in Figure 7.1B) and considered them as representative conditions of the incoming sea states. Poetto beach can be classified as a microtidal beach because the average tidal range is less than 20 cm, but this can reach a maximum of about 40 cm at spring tides (Brambilla et al., 2016).

7.3. Methods

This study investigates the natural mechanism of deposition and removal of banquette by the analysis of a four years videomonitoring system database, composed by a digital, 12 megapixel ultra HD, network camera (Dahua Technology, model DH-IPC-HF81200E), which ensure a high-resolution dataset. The camera was installed on the Sella del Diavolo Promontory (39°11'24.05" North, 9°9'29.65" East) at a high of 125 m above SWL (Figures 7.1B and 7.2), using an existing steel structure of a previous videomonitoring system and powered by photovoltaic panels (Brambilla, 2015; Brambilla et al., 2016, Passarella, 2019).

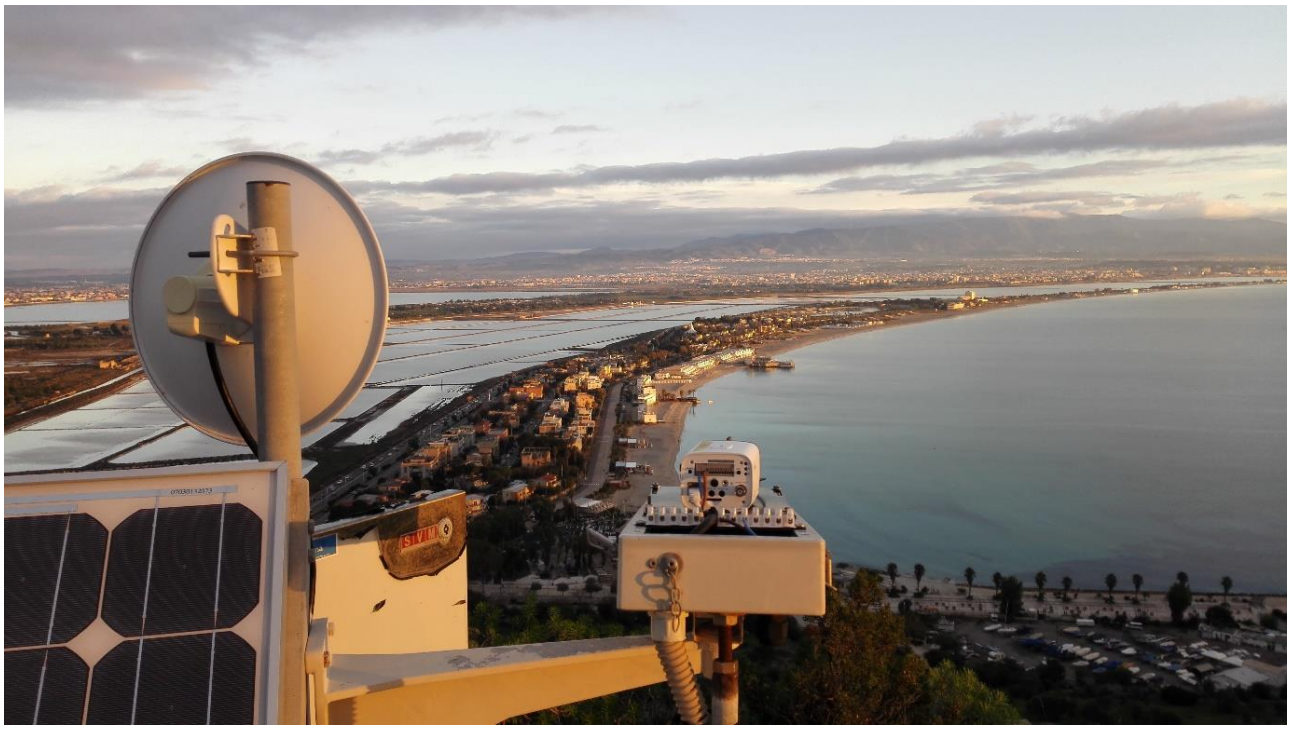

Figure 7.2 – Videomonitoring system on the Sella del Diavolo Promontory. On the left is visible the radio antenna and the photovoltaic panel. The camera (on the right) is without its protective suit because an ordinary, periodic maintenance.

The system nowadays is set to record data four times per days, every 3 hours (from 8:00 to 17:00), for 30 minutes long intervals at a frequency of acquisition of 4Hz. The data acquired are sent to a local server via a radio link. Due to the high spatial and temporal resolution, the high amount of data collected needs a large space to be stored before analysis (about ≈ 400 GB per month). In order to correct the images from the distortions induced by the camera lens, the internal camera parameters were computed (e.g. focal length, principal point position, radial and tangential distortion coefficients) and the camera was calibrated (Passarella, 2019).

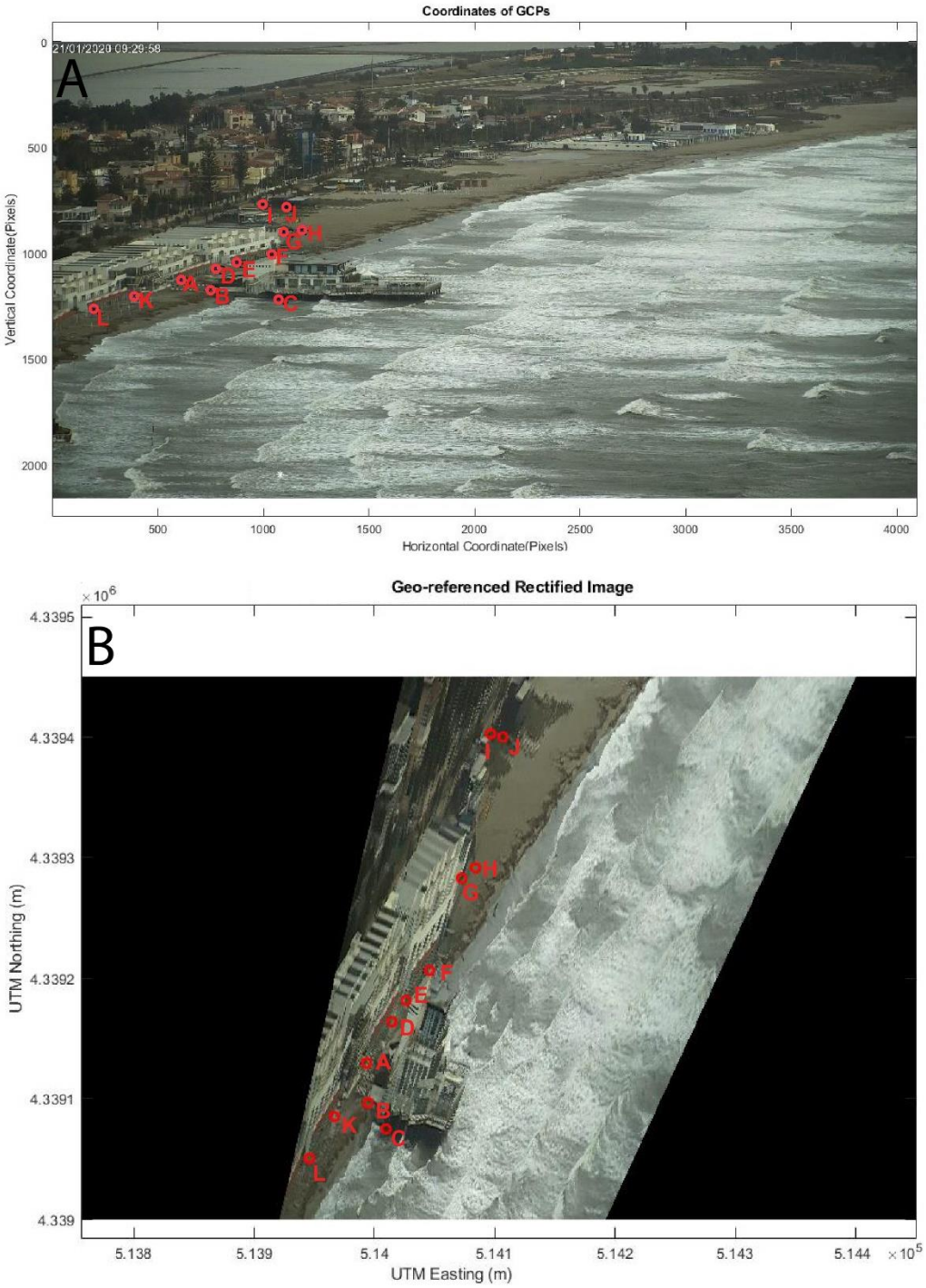

Figure 7.3 - Fixed Ground Control Points at study area.

For this study, we took a single snapshot for each day, from 28/09/2016 to 28/09/2020, and the acquired images, once corrected by lens distortion, are rectified and georeferenced by the means of 12 ground control points (GCPs) obtained through the analysis of orthophotos of "Sardegna Geoportale", an open-source geodatabase made by "Regione Autonoma della Sardegna". In this way we obtained the coordinates (Datum WGS84, Projection UTM 32N) of fixed points in time, such as edges of buildings, visible from the oblique images of the camera. For each GCP the image coordinates in pixel (2D) are associated with real-world ground coordinates (3D). The correlation between GCPs image and ground coordinates was found manually by the operator (Figure 7.3).

We chose this method because, in the four years, during periodic maintenances, the camera has moved, although by very little, at least 30 times. Since the camera is set with a high zoom, every slightest movement changes the framing of the image. Every time the camera moved it was necessary to perform a new rectification and georeferencing of the images and for each time the camera has moved, no RTK-DGPS surveys were available to obtain GCPs from the topographic surveys. For this reason, we preferred to use only the orthophotos for the normalization of the data. Although the camera has moved over time, the focal length (and therefore the distortion given by the lenses) has never changed; consequently, it was not necessary to perform new calibrations of the lenses. Once elaborated the images we mapped, manually by the operator, the limits of banquette, when it is present, along three transects located in areas with different anthropic impacts and subsequently we were able to measure the cross-shore extension of the banquette for all four years of acquisitions. (Figure 7.1C). A time series with these extensions has been done for each transect, showing when the banquette is built and how wide it is. During the four years of acquisitions the video monitoring system did not always work, leaving a total of 446 days without recordings, especially in the period between October 2017 and September 2018 (Figure 7.4).

We also obtained the hourly waves parameters (Hs, Tp, Tm and wave direction) by the Copernicus Marine Environment Monitoring Service, from a hindcast (from 28/09/2016 to 31/12/2019) and a forecast (from 01/01/2020 to 28/09/2020), located at a bathymetry of -18 m (Figure 7.1B). Starting from the wave parameters, we used linear wave theory to obtain the wavelength and the celerity group and therefore the wave energy flux through the formula (Liang et al., 2017):

$$Energy\ flux = \frac{\rho g^2 H_s^2}{16}\ C_G$$

where ρ is water density, g is the gravity acceleration and C_G is the celerity group.

Wind speed and direction came from the ERA5 reanalysis dataset (Figure 7.1B, 7.1D), and these parameters are provided every 3 hours.

We used the peak-over-threshold method to identify the 48-h independent storms occurred during the observation period at the virtual buoy location represented by the CMEMS grid node. We identified the storms based on the prominence parameter for the significant wave height Hs: the prominence threshold was chosen equal to 0.8 m. Although the threshold value of 0.8 m may seem low for extreme event analysis, due to the moderate incoming wave energy levels at Poetto (mean Hs is 0.4 m), this method allowed the identification of 87 storms, of which 58 recorded by the camera, during the period considered. We retained only the storms with a persistence above the threshold longer than 6 h, that met the independence criterion with more than 48 h between the peak of a storm and the peak of the following one.

7.4 Results

The results of our study are summarized in Figure 7.4. The time-series of the banquette extension at the three transects (T1, T2, T3) are related to wave parameters Hs and Tp along the four years of acquisitions. For a better comprehension of this image we choose to split it into three different images, leaving out the periods without seagrass berm depositions and the periods of the camera inactivity (Figure 7.5, 7.6 and 7.7).

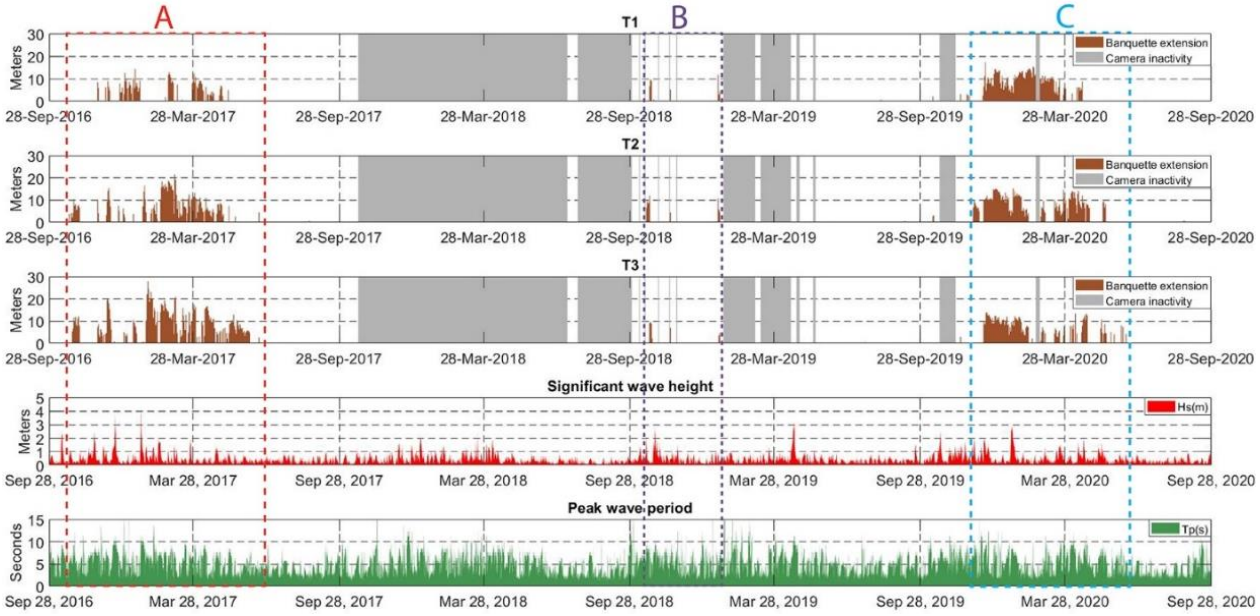

Figure 7.4 – Time-series of banquette extensions along the four years of acquisitions with related the significant wave height (Hs) and peak wave period (Tp). A, B and C are the portion that have been split respectively in Figure 7.5, 7.6 and 7.7

The most energetic storm registred during the 4 years has happened in the first interval (Figure 7.5, 7.4A), exatly between 21 and 22/01/2017, Hs 4,02 m. During this period, comparing the extensions of the banquettes between the three transects, it can be seen that in T1 the depositions occur at slightly different times and extensions compared to T2 and T3.

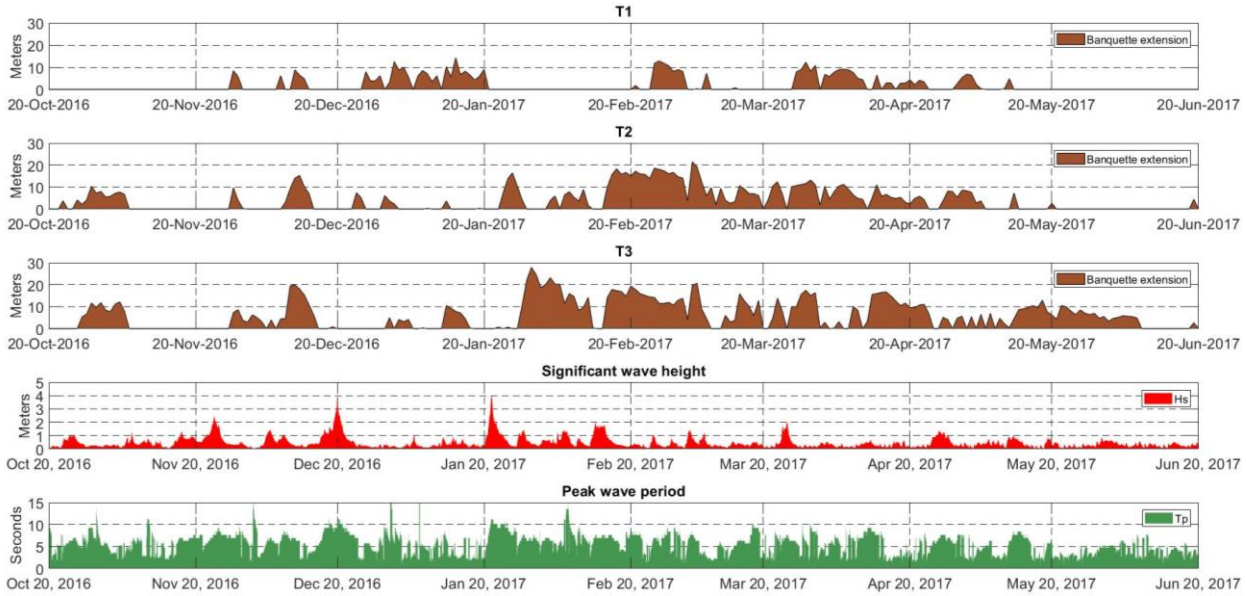

Figure 7.5 – Time-series for the period from 20 October 2016 to 20 June 2017.

The second interval (Figure 7.6, 7.4B) is the shortest of the periods examined, from 18 October 2018 to 22 January 2019 (from 24 January 2019 the camera went off until 4 March 2019). During this period there were no fierce storms, except that of 18 October 2018 and that between 28 and 29 October 2018, with Hs of 2.13 and 2.85 m respectively. The first one led to the deposition of a banquette about 10 meters long in all three transepts, albeit with a few days of difference in the deposition. The second one led to overwash the beach berm and flooding of the backbeach. Despite this, at the end of the storm, there was no deposition of banquette.

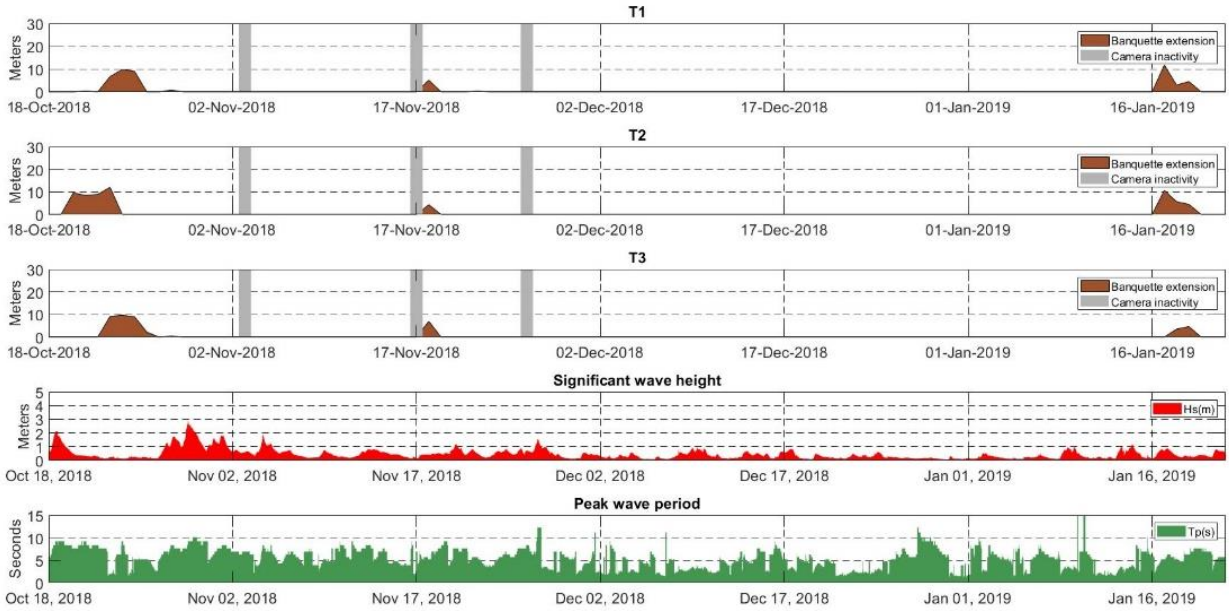

Figure 7.6 – Time-series for the period from 18 October 2018 to 22 January 2019.

The last interval (Figure 7.7, 7.4C) is particular because, in addition to the *P. ocenica* rests, there has been a huge deposition on the beach berm of *Arundo donax* reeds between 18 and 19 december 2019, which intertwined with the banquette, forming a sedimentary structure that somehow it seems to be more resistant to erosion induced by wave motion. This sedimentary structure in facts resists to fierce storms during this interval, like that beteween 20 and 21 January 2020, with Hs 2.9 m. This storm simply moved the reeds from the beach berm along the emerged beach. Only human intervention, through the municipalities of Cagliari and Quartu Sant'Elena, allowed the manual

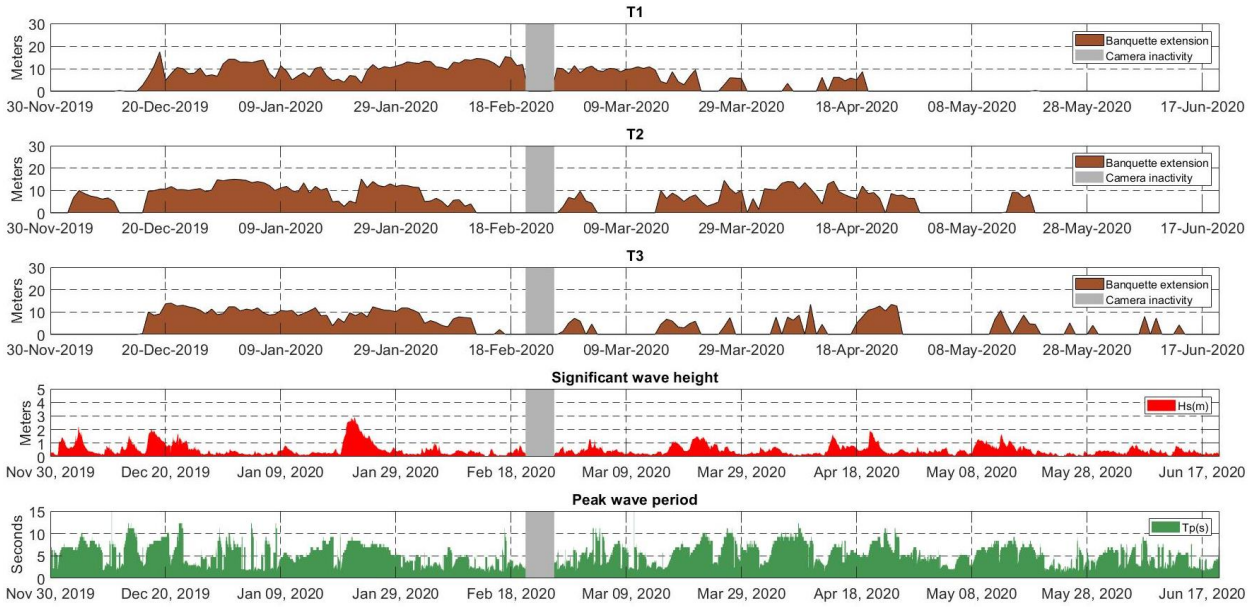

Figure 7.7 – Time-series for the period from 15 December 2019 to 20 June 2020. The seagrass berm in this period is largely mixed with Arundo donax reeds that seem to make the structure more resistant to erosion.

removal of the reeds from the beach (which had been partially covered by sand), which took place between April and May 2020.

To try to understand the mechanisms that lead to the deposition and destruction of banquettes we initially looked for a correlation (through the *cross-correlation* formula) between the conditions of the wave motion (using the wave parameters of the time interval between one daily snapshot and the next) and the banquettes width. The cross correlation analysis was carried out also for the daily variations of the banquette (obtained through the MatLab *diff* formula) but the results show a poor correlation in both cases. We repeated the same procedure for the three single time intervals described in figure 7.4, but without ever seeing a characteristic wave parameters pattern for the deposition or retreat of the banquette.

The days on which a change of 4m or more (advance or retreat) of the banquette occurred were examined, and we obtained the average values of the wave parameters for both deposition and destruction along the three transects. The same procedure was carried out for another virtual transect (T_max in Table 7.1) which is the maximum variation registered along the three transects. Also this analysis shows a poor correlation between wave parameters and dynamics of the banquettes, in other words there is not a great difference in the wave parameters between deposition and retreat events (Table 7.1).

By the peak-over-threshold method, we identified 87 storm events, of which 58 were recorded. Of these events, only in 9 cases (Hs mean at the peak of the storm =1,33m) there was a well-structured banquette before the arrival of the storm, in other 12 cases the banquette was very short, or present in little portion of the beach. In 8 of the 9 cases when the banquette was well-structured, at the end of the storm then it redeposits itself.

Table 7-1 – Mean wave parameters for the depositional and retreat banquette events along the studied transects.

Variation ± 4 m	Hs depos.	Hs retreat	Tp depos.	Tp retreat	Tm depos.	Tm retreat	n° events depos.	n° events retreat	EnFlux depos.	Enflux retreat
T1	0,750	0,774	7,553	7,115	4,069	4,166	27	32	27052	42437
T2	0,784	0,723	7,737	7,179	4,536	4,026	44	43	34021	19910
T3	0,730	0,735	7,945	7,238	4,284	3,963	57	55	30217	22801
T_max	0,830	0,796	7,811	6,789	4,306	3,901	57	55	38868	34619

We have therefore examined the wind parameters to look for some relationship with the retreat of the banquette and, indeed, we have noticed a mean wind speed of about 42,2 km h^{-1} during the retreat events, while the mean wind speed during the four years is about 24,6 km h^{-1}. Although there does not seem to be a clearly predominant direction, the winds of the fourth quadrant (which

in the study area correspond to offshore winds) blow with a slightly higher frequency and intensity than the other ones (Figure 7.8).

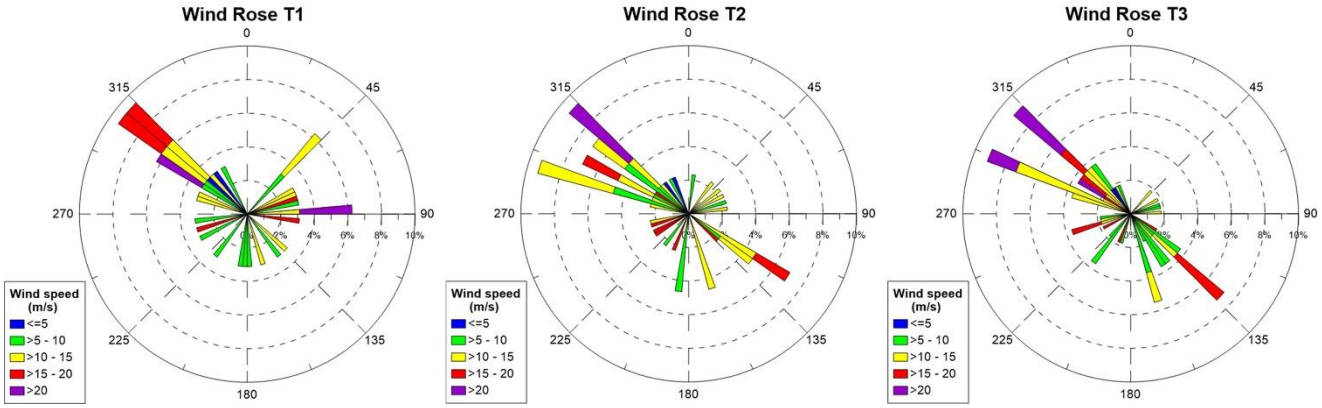

Figure 7.8 - wind roses concerning retreat events for the studied transects. The mean wind speeds are, respectively: 11,2 m/s for T1; 11,9 m/s for T2 and 12,1 m/s for T3 during the banquette retreat events.

7.5 Discussion

As can be seen from figures 7.4, 7.5, 7.6 and 7.7 the depositions of the banquettes generally occur in low wave energy conditions, often at the end of the storms. This does not mean that at the end of each storm there has been deposition of banquette. It is thought that the natural conditions leading to the deposition of the banquettes are closely linked to the availability of organic material in the upper shoreface, in addition to the low energy of the wave motion. In fact, during the four years it has been seen how, with same wave conditions, it is possible to have and not have banquettes deposition. For this reason, it can be said that the deposition of the banquettes occurs in conjunction with low wave energy and the presence of *P. oceanica* rests on the submerged beach (as seagrass litter), in agreement with Simeone and De Falco, 2012; Gómez-Pujol et al., 2013; Vacchi et al., 2017. Obviously, there are larger depositions at the end of intense storms, which are able to set in motion both the leaves just uprooted from the *P. oceanica* meadow, and other rests of *P. oceanica* already present in the litter, in the submerged beach (Figure 7.9). The presence of this litter also allows the deposition of the banquette not only in autumn (when *P. oceanica* naturally releases its leaves), but also throughout the year, including summer.

Figure 7.9 – an example of foreshore with large presence of litter.

The results presented show that the wave motion seems to play a secondary role in the banquette retreat and/or destruction. This outcome is in agreement with Gómez-Pujol et al. (2013) who assert *that "seagrass cast accumulations are continuously built up and destroyed and rarely persist before the arrival of new sea storms"*. The analysis of four years videomonitoring system data in fact shows how banquettes, when present, rarely persist until the arrival of the storm peaks.

It has also been noted that wind processes also influence the retreat and/or destruction of the banquette (Figure 7.8). In fact, this phenomenon can carry away the *P. oceanica* rests inshore (in the case of offshore winds) or disperse them along the emerged beach (in the case of inshore winds). Another process generated by the offshore winds, that does not make the banquette visible from the images from the camera, is that of carrying sand over them, covering them (Figure 7.10).

Figure 7.10 – an example of banquette covered by sand at Poetto beach. Photo by Daniele Trogu.

This phenomenon is highlighted in the event that occurred between 4 and 5 February 2021: in fact, between these two dates there was an average retreat of the banquette of about 7m with very low wave energy but with strong offshore winds (mean speed = 61.2 km h^{-1}), which seem to have partly covered with sand and partly removed the banquette. It can also be seen how the beach property building slows down the offshore winds and for this reason the banquette in the T1 area remains more stable than that in the T2 and T3 area (Figure 7.11).

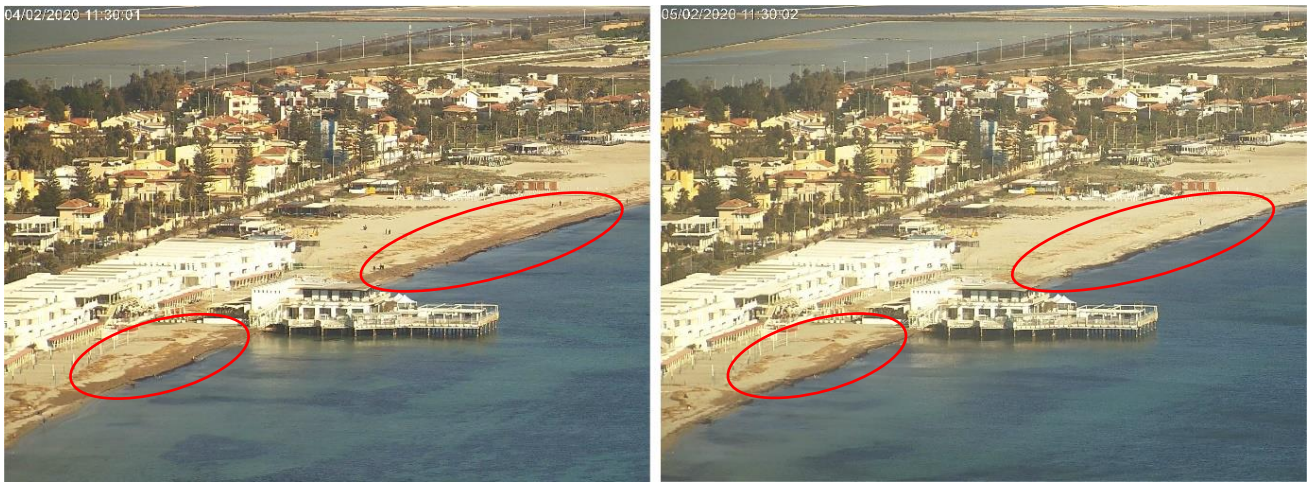

Figure 7.11 – Banquette partly removed and partly covered with sand between 4 and 5 February 2021.

During the summer season, in addition to the natural processes analysed so far, the variability of the banquette can be affected by the daily cleaned operations with heavy vehicles to facilitate the presence of tourists. This often does not allow to observing directly the banquettes in Poetto beach during the summer, but in other Mediterranean natural beaches the banquettes are well visible during the whole year (Trogu et al., 2020).

7.6 Conclusions

This work analyses four years of video monitoring data at the Poetto beach (Gulf of Cagliari, southern Sardinia, Italy, western Mediterranean). The main purpose was to analyse the depositions and the width variation of the banquette along three transects, by crossing the measurements made on the rectified images with the wind and wave data from CMEMS and ERA5 reanalysis dataset. It has been noted that the low energy conditions of the wave motion (generally at the end of storms of varying intensity), associated with the availability of organic material on the foreshore and shoreface, lead to the deposition of the banquettes which can remain on the shoreline for several days. The process that leads to the retreat or total destruction of the banquette is not to be found exclusively in the wave motion, as the analysed data tell us that the reductions in width occur mainly in conjunction with medium-strong winds that can carry away the organic material both offshore and inshore or cover the banquette with sand. This last process increases the permeability of the beach, reducing the runup and flooding extension, as seen in chapter 6.

Chapter 8
CONCLUSIONS

This work contributed to improving the knowledge of the morphodynamic processes related to biomasses in Mediterranean coastal areas, both in natural and urbanized zones, through a multidisciplinary methodology such as topographic and bathymetric surveys, drone surveys, analysis of coastal videomonitoring system databases, aerial orthorectified photographs, and specific instrumental measurements like water infiltrometric tests.

We examined two different coastal belts of southern Sardinia: Piscinnì beach (in chapter 4), which presents a highly natural system; and the urban coastal belt of Cagliari (in chapter 5, 6 and 7), which has instead undergone numerous anthropogenic impacts over the years, both structural (such as the construction of ports, roads and buildings above the dunes, etc.) and due to bad practices (such as the periodic cleaning of beaches with heavy vehicles).

In chapter 4, by comparing the position of the shorelines, mapped in the days before and after the storm events, the high resilience of a beach system characterized by minimal anthropic impacts has been highlighted. From the image processing acquired with the video monitoring system, large and voluminous deposits of seagrass beach-cast litters, mainly *Posidonia oceanica*, accumulated in the shoreline causing beach accretion (up to 30 m) two days after the storm event. In several cases, it was observed that the seagrass berm can be covered by sand transported by winds blowing from the backbeach and the dune zones. This process contributes to stabilize the seagrass deposits and can lead to a progradation of the shore.

Quite the opposite, in chapter 5, the historical analysis of the shoreline and the urban area of Cagliari has shown how the anthropic impacts have generated a more or less marked erosion of the coastal zone in the entire Gulf of Cagliari. Some of these impacts (such as roads and buildings built on the original dune system) are difficult to mitigate. Another kind of impact however, such as the bad practise of beach cleaning with heavy vehicles, flatten and lower the backshore level, compacting the sediment, decreasing the beach permeability and making this zone more vulnerable to overwash and flooding. This kind of human impact, if mitigated could bring great benefits to the restoration of the natural resilience of the beach system.

The fundamental role played by the deposition of biomasses on the emerged beach is highlighted in chapter 6. The original contribution of this work shown how a portion of beach with biomasses has an infiltration rate greater than an order of magnitude compared to an area without biomasses (on the banquette the permeability is even greater). Although this difference in permeability does not have much effect on the runup and flooding during moderate wave conditions with no overwash, under overwash conditions, runup and flooding extension were increased by a low permeability coefficient. These results highlight the role of the ecosystem

services provided by *Arundo donax* reeds and *Posidonia oceanica* wracks, suggesting that they must be taken into account in a sustainable coastal planning strategy.

Finally, in chapter 7, a last innovative contribution of this research is linked to the dynamics of the deposition and dismantling of the banquettes. It has been seen how the waves have a greater influence on the deposition processes, generally at the end of storms, in medium-low Hs and Tp conditions, especially when there were biomasses in the surf zone before the storm. The dismantling processes, on the other hand, do not show correlations with the wave parameters and seem more linked to the winds that can either redistribute the biomasses along the beach, or cover them with sand, promoting the accretion of the beach, increasing its permeability and resilience.

We believe that the original contributions of this PhD research can be a useful tool for the mitigation of coastal hazards and the protection and management of Mediterranean beaches. In particular, it was highlighted that the bad practice of removing the organic rests (banquette, reeds, etc.) with heavy vehicles leads to a decrease in the draining capacity of the beaches. This material, which in any case is covered or carried away naturally by the winds, is indispensable for the stability and the resilience of Mediterranean beaches.

Coastal areas nowadays are exposed to several hazard due the climate global change and the sea level rise. This scenario can modify the wave parameters, like significant wave height (Hs), mean wave period (Tm) and mean wave direction (degree), globally and locally, causing coastal erosion, flooding and damage to infrastructure built near the coast. In agreement with the United Nations 2030 Agenda, we think that it is fundamental to establish proper coastal management, aiming for sustainable development and try to find actions that can mitigate the anthropogenic impacts on the beaches.

Bibliography

- Allan, J.C.; Komar, P.D.; Priest, G.R. Shoreline Variability on the High-Energy Oregon Coast and its Usefulness in Erosion-Hazard Assessments. J. Coast. Res. 2003, 38, 83–105.
- Amarouche, K.; Akpınar, A. Increasing Trend on Storm Wave Intensity in the Western Mediterranean. Climate 2021, 9, 11. https://doi.org/10.3390/cli9010011
- Atkinson, A.L.; Power, H.E.; Moura, T.; Hammond, T.; Callaghan, D.P.; Baldock, T.E. Assessment of runup predictions by empirical models on non-truncated beaches on the south-east Australian coast. Coastal Engineering 2017, 119, 15 – 31. doi:https://doi.org/10.1016/j.coastaleng.2016.10.001.
- Bartole, R.; De Muro, S. Acoustic facies and seabed features of the mixed carbonate-siliciclastic deposits of the last eustatic cycle in the La Maddalena Archipelago (North Sardinia, Italy). Ital. J. Geosci. 2012, 131, 102–122.
- Bathrellos, G. D. (2007). An overview in urban geology and urban geomorphology. Proceedings of the 11th International Congress, Athens, May, 2007. Bulletin of the Geological Society of Greece, 40, 1354–1364.
- Battisti, C.; Fanelli, G.; Filpa, A.; Cerfolli, F. Giant Reed (Arundo donax) wrack as sink for plastic beach litter: First evidence and implication. Marine Pollution Bulletin 2020, 155, 111179. doi:https://doi.org/10.1016/j.marpolbul.2020.111179.
- Batzella, T., Pusceddu, N., Kalb, C., Ferraro, F., Ibba, A., & De Muro, S. (2011). (2011) – Bars and troughs dynamic and evolution trend of La Cinta beach (San Teodoro OT) – NE Sardinia – Rend. Online Soc. Geol. It., Vol. 17 (2011), pp. 17-23 (DOI 10.3301/ROL.2011.13)
- Bellotti, G.; Franco, L.; Cecioni, C. Regional Downscaling of Copernicus ERA5Wave Data for Coastal Engineering Activities and Operational Coastal Services. Water 2021, 13. doi:10.3390/w13060859.
- Biondo, M.; Buosi, C.; Trogu, D.; Mansfield, H.; Vacchi, M.; Ibba, A.; Porta, M.; Ruju, A.; De Muro, S. Natural vs. Anthropic Influence on the Multidecadal Shoreline Changes of Mediterranean Urban Beaches: Lessons from the Gulf of Cagliari (Sardinia). Water 2020, 12.
- Blott, S. J., & Pye, K. (2001). GRADISTAT: A grain size distribution and statistics package for the analysis of unconsolidated sediments. Earth Surface Processes and Landforms, 26(11), 1237–1248. doi:10.1002/esp.261
- Blumberg, A. F., & Bruno, M. S. (2018). The urban ocean. The interaction of cities with water. Cambridge, UK: Cambridge University Press.
- Boak, E.; Turner, I. Shoreline Definition and Detection: A Review. J. Coast. Res. 2005, 21, 688–703.
- Bonaduce, A.; Pinardi, N.; Oddo, P.; Spada, G.; Larnicol, G. Sea-level variability in the Mediterranean Sea from altimetry and tide gauges. Clim. Dyn. 2016, 47, 2851–2866.
- Boudouresque, C.; Bernard, G.; Pergent, G.; Shili, A.; Verlaque, M. Regression of Mediterranean seagrasses caused by natural processes and anthropogenic disturbances and stress: A critical review. Bot. Mar. 2009, 52.
- Brambilla, W. Caratterizzazione Morfodinamica Della Spiaggia del Poetto; University of Cagliari: Cagliari, Italy, 2015.
- Brambilla, W., van Rooijen, A., Simeone, S., Ibba, A., & De Muro, S. (2016). Field observations, coastal video monitoring and numerical modeling at Poetto Beach, Italy. Journal of Coastal Research, Special Issue, 75(2), 825– 829. doi:10.2112/SI75-166.1

- Brandolini, P., Cappadonia, C., Luberti, G. M., Donadio, C., Stamatopoulos, L., Di Maggio, C., … Del Monte, M. (2019). Geomorphology of the Anthropocene in Mediterranean urban areas. Progress in Physical Geography: Earth and Environment. doi:10.1177/ 0309133319881108
- Brandolini, P., Faccini, F., Paliaga, G., & Piana, P. (2017). Urban geomorphology in coastal environment: Manmade morphological changes in a seaside tourist resort (Rapallo, Eastern Liguria, Italy). Quaestiones Geographicae, 36(3), 97–110.
- Brandolini, P., Faccini, F., Paliaga, G., & Piana, P. (2018). Man-made landforms survey and mapping of an urban historical center in a coastal Mediterranean environment. Geografia Fisica e Dinamica Quaternaria, 41, 23–34. doi:10.4461/ GFDQ.2018.41.2
- Briand, F. Transformations and evolution of the Mediterranean coastline. Ciesm Sci. Ser. 3Bull. Inst. Oceanogr. 1997, 18, 1–243.
- Buosi, C., Cherchi, A., Ibba, A., Marras, B., Marrucci, A., & Schintu, M. (2013). Benthic foraminiferal assemblages and sedimentological characterisation of the coastal system of the Cagliari area (southern Sardinia, Italy). Bollettino Della Società Paleontologica Italiana, 52, 1–9. doi:10.4435/BSPI.2013.04
- Buosi, C., Del Rio, M., Orrù, P., Pittau, P., Scanu, G. G., & Solinas, E. (2017). Sea level changes and past vegetation in the Punic period (5th–4th century BC): Archaeological, geomorphological and palaeobotanical indicators (south Sardinia – west Mediterranean Sea). Quaternary International, 439, 141–157. doi:10.1016/j.quaint.2016.07.005
- Buosi, C., Ibba, A., Passarella, M., Porta, M., Ruju, A., Trogu, D., & De Muro, S. (2019). Geomorphology, beach classification and seasonal morphodynamic transition of a Mediterranean gravel beach (Sardinia, Gulf of Cagliari). Journal of Maps, 15(2), 165–176. doi:10.1080/17445647. 2019.1567402
- Buosi, C., Tecchiato, S., Pusceddu, N., Frongia, P., Ibba, A., & De Muro, S. (2017). Geomorphology and sedimentology of Porto Pino, SW Sardinia, western Mediterranean. Journal of Maps, 13(2), 470–485. doi:10.1080/17445647. 2017.1328318
- Buosi, C.; Cherchi, A.; Ibba, A.; Marras, B.; Marrucci, A.; Schintu, M. Preliminary data on benthic foraminiferal assemblages and sedimentological characterisation from some polluted and unpolluted coastal areas of Sardinia (Italy). Boll. Soc. Paleontol. Ital. 2013, 52, 35–44.
- Buosi, C.; Ibba, A.; Passarella, M.; Porta, M.; Ruju, A.; Trogu, D.; De Muro, S. Geomorphology, beach classification and seasonal morphodynamic transition of a Mediterranean gravel beach (Sardinia, Gulf of Cagliari). J. Maps 2019, 15, 165–176.
- Campagne, C.S.; Salles, J.-M.; Boissery, P.; Deter, J. The seagrass *Posidonia oceanica*: Ecosystem services identification and economic evaluation of goods and benefits. Mar. Pollut. Bull. 2015, 97, 391–400.
- Carobene, L. and Brambati, A. (1975) Metodo per l'analisi morfologica quantitativa delle spiagge. Bollettino Società Geo- logica Italiana, 94, 479-493.
- Carmignani, L., Oggiano, G., Funedda, A., Conti, P., & Pasci, S. (2016). The geological map of Sardinia (Italy) at 1:250,000 scale. Journal of Maps, 12, 826–835. doi:10. 1080/17445647.2015.1084544
- Carreño, A.; Lloret, J. Environmental impacts of increasing leisure boating activity in Mediterranean coastal waters. Ocean and Coastal Management 2021, 209, 105693. doi:https://doi.org/10.1016/j.ocecoaman.2021.105693.

- Casula, G., Cherchi, A., Montadert, L., Murru, M., & Sarria, E. (2001). The Cenozoic graben system of Sardinia (Italy): Geodynamic evolution from new seismic and field data. Marine and Petroleum Geology, 18, 863–888.
- Chelli, A., Bellotti, P., Bini, M.,… Valente, A. (2018). Morphodynamics of coastal areas represented in the new geomorphologic map of Italy: Draw the landforms of the past to outline the future. Alpine and Mediterranean Quaternary, Vol. 31 (Quaternary: Past, Present, Future - AIQUA Conference, Florence, 13-14/06/2018), 17 - 21
- Cherchi Pomesano, A.; Pecorini, G. Ricerche geologiche e biostratigrafiche sul Campidano meridionale (Sardegna). Mem. Della Soc. Geol. Ital. 1969, 8, 421–451.
- Cherchi, A.; Da Pelo, S.; Ibba, A.; Mana, D.; Buosi, C.; Floris, N. Benthic foraminifera response and geochemical characterization of the coastal environment surrounding the polluted industrial area of Portovesme (South-Western Sardinia, Italy). Mar. Pollut. Bull. 2009, 59, 281–296.
- Cherchi,A.; Montadert,L. Oligo-Miocene rift of Sardinia and the early history of the Western Mediterranean Basin. Nature 1982, 298, 736–739.
- Ciavola, P.; Coco, G. Coastal Storms: Processes and Impacts; Ciavola, P., Coco, G., Eds.; Wiley-Blackwell: Hoboken, NJ, USA, 2017; p. 288.
- Coates, D. R. (1976). Urban geomorphology. Binghamton, NY: The Geological Society of America, Special Paper 174.
- Cohn, N.; Ruggiero, P. The influence of seasonal to interannual nearshore profile variability on extremewater levels: Modelingwave runup on dissipative beaches. Coastal Engineering 2016, 115, 79 – 92. Swash-zone Processes, doi:https://doi.org/10.1016/j.coastaleng.2016.01.006.
- Cooke, R. U. (1976). Urban geomorphology. Geographical Journal, 142(1), 59–65.
- Cowell, P. and Thom, B. (1994). Morphodynamics of coastal evolution. Cambridge University Press, Cambridge, United Kingdom and New York, NY, USA.
- Cox, N.; Dunkin, L.M.; Irish, J.L. An empirical model for infragravity swash on barred beaches. Coastal Engineering 2013, 81, 44–50. doi:https://doi.org/10.1016/j.coastaleng.2013.06.008.
- Crossland, C. J., Kremer, H. H., Lindeboom, H. J., Crossland, J. I. M., & Le Tissier, M. D. A. (2005). Coastal fluxes in the Anthropocene—the land-ocean interactions in the Coastal Zone Project of the International Geosphere-Biosphere Programme. Global change—the International Geosphere-Biosphere Program Series. Springer: Berlin/Heidelberg, Germany, 2005; pp. 1–37.
- Crossland, C.J.; Baird, D.; Ducrotoy, J.-P.; Lindeboom, H.; Buddemeier, R.W.; Dennison, W.C.; Maxwell, B.A.; Smith, S.V.; Swaney, D.P. The Coastal Zone—A Domain of Global Interactions. Global change—the International Geosphere-Biosphere Program Series. Berlin: Springer.
- Cuevas Jimenez, A.; Euán, J.; Villatoro, M.; Silva, R. Classification of Beach Erosion Vulnerability on the Yucatan Coast. Coast. Manag. 2016, 333–349.
- Cummins, V., Burkett, V., Day, J., Forbes, D., Glavovic, B., Glaser, M., & Pelling, M. (2014). LOICZ Signpost: Consultation Document Signalling New Horizons for Future Earth—Coasts. LOICZ. Retrieved from https://s3-eu-west-2.amazonaws.com/futureearthcoasts/wp-content/uploads/2018/05/30154928/LOICZ-Signpost-Web.pdf
- De Falco, G., Simeone, S., Solinas, G., Batzella, T., Cancemi, G., Cancemi, M., & De Muro, S. (2008b). Shoreline retreat and *Posidonia oceanica* banquette removal in the beach of Paragan (southern Corse). Rendiconti Online della Società Geologica Italiana, 3(1), 296–297.
- De Falco, G.; Budillon, F.; Conforti, A.; De Muro, S.; Di Martino, G.; Innangi, S.; Perilli, A.; Tonielli, R.; Simeone, S. Sandy beaches characterization and management of coastal erosion on western Sardinia island (Mediterranean Sea). J. Coast. Res. 2014, 70, 395–400.

- De Falco, G.; Molinaroli, E.; Baroli, M.; Bellacicco, S. Grain size and compositional trends of sediments from *Posidonia oceanica* meadows to beach shore, Sardinia, western Mediterranean. Estuar. Coast. Shelf Sci. 2003, 58, 299–309.
- De Falco, G.; Molinaroli, E.; Conforti, A.; Simeone, S.; Tonielli, R. Biogenic sediments from coastal ecosystems to beach–dune systems: Implications for the adaptation of mixed and carbonate beaches to future sea level rise. Biogeosciences 2017, 14, 3191–3205.
- De Falco, G.; Simeone, S.; Baroli, M. Management of Beach-Cast *Posidonia oceanica* Seagrass on the Island of Sardinia (Italy, Western Mediterranean). J. Coast. Res. 2008, 24, 69–75.
- De Leo, F.; Besio, G.; Mentaschi, L. Trends and variability of ocean waves under RCP8.5 emission scenario in the Mediterranean Sea. Ocean Dyn. 2020.
- De Muro, S., Batzella, T., De Falco, G., & Porta, M. (2010). Sedimentological map of Bonifacio Strait inner shelf. Rendiconti Online della Società Geologica Italiana, 11(2), 752–753.
- De Muro, S., Batzella, T., Kalb, C., & Pusceddu, N. (2008). Sedimentary processes, hydrodynamics and modeling of the beaches of Santa Margherita, Solanas, Cala di Trana and La Sciumara (Sardinia – Italy). Rendiconti Online della Società Geologica Italiana, 3(1), 308–309.
- De Muro, S., Ibba, A., & Kalb, C. (2016). Morpho-sedimentology of a Mediterranean microtidal embayed wave dominated beach system and related inner shelf with *Posidonia oceanica* meadows: The SE Sardinian coast. Journal of Maps, 12(3), 558–572. doi:10.1080/17445647. 2015.1051599
- De Muro, S., Ibba, A., Simeone, S., Buosi, C., & Brambilla, W. (2017a). An integrated sea-land approach for mapping geomorphological and sedimentological features in an urban microtidal wave-dominated beach: A case study from S Sardinia, western Mediterranean. Journal of Maps, 13(2), 822–835. doi:10.1080/17445647.2017.1389309
- De Muro, S., Kalb, C., Ibba, A., Ferraro, F., & Ferrara, C. (2010). Sedimentary processes, morphodynamics and sedimentological map of “Porto Campana” SCI beaches (Domus De Maria - SW Sardinia). Rendiconti Online della Società Geologica Italiana, 11(2), 754–755.
- De Muro, S., Porta, M., Passarella, M., & Ibba, A. (2017b). Geomorphology of four wave-dominated microtidal Mediterranean beach systems with *Posidonia oceanica* meadow: A case study of the northern Sardinia coast. Journal of Maps, 13(2), 74–85. doi:10.1080/17445647. 2016.1259593
- De Muro, S., Pusceddu, N., & Kalb, C. (2010). Sedimentological map of the seafloor between Porto Pozzo Bay and Capo Ferro - NE Sardinia. Rend. Online Soc. Geol. Ital. 2010, 11, 756–757.
- De Muro, S., Pusceddu, N., Buosi, C., & Ibba, A. (2017c). Morphodinamics of a Mediterranean microtidal wavedominated beach: Forms, processes and insights for coastal management. Journal of Maps, 13(2), 26–36. doi:10.1080/17445647.2016.1250681
- De Muro, S., Tecchiato, S., Porta, M., Buosi, C., & Ibba, A. (2018c). Geomorphology of marine and glacio-lacustrine terraces and raised shorelines in the northern sector of Península Brunswick, Patagonia, Straits of Magellan, Chile. Journal of Maps, 14(2), 135–143. doi:10.1080/ 17445647.2018.1441759
- De Muro, S.; De Falco, G. Handbook of Best Practices for the Study, Monitoring and Management of Sardinian Beaches; University Press—Scienze Costiere e Marine: Cagliari, Italy, 2015.
- De Muro, S.; Ibba, A.; Biondo, M.; Buosi, C.; Porta, M.; Ruju, A.; Trogu, D. Scientific Technical Support Activities Aimed at the Ecogeomorphological Supervision of the Preparatory, Executive and Post-Operam Interventions on the Poetto Beach (Cagliari, Southern Sardinia)

during the Removal of Arundo donax Remains Deposited on the Backshore; Università degli Studi di Cagliari: Cagliari, Italy, 2020.
- De Muro, S.; Kalb, C.; Ibba, A.; Ferraro, F.; Ferrara, C. Sedimentary processes, morphodynamics and sedimentological map of “Porto Campana”. Rend. Online Soc. Geol. Ital. 2010, 11, 756–757.
- De Muro, S.; Porta, M.; Pusceddu, N.; Frongia, P.; Passarella, M.; Ruju, A.; Buosi, C.; Ibba, A. 2018a. Geomorphological processes of a Mediterranean urbanized beach (Sardinia, Gulf of Cagliari). J. Maps 2018a, 14, 114–122. doi:10.1080/17445647.2018.1438931
- De Muro, S.; Pusceddu, N.; Kalb, C. Sedimentological Map of the Seafloor between Porto Pozzo Bay and Capo Ferro-Ne Sardinia. Rend. Online Soc. Geol. Ital. 2010, 11, 758–759.
- De Muro, S.; Tecchiato, S.; Buosi, C.; Porta, M.; Bachis, M.; Ibba, A. 2018b. Geomorphology, Sedimentology, Benthic Habitat as Tools For Supporting Coastal Management: Comparison Between Australian And Mediterranean Beach Systems. Journal of Coastal Research 2018, 85, 1526 – 1530. doi:10.2112/SI85-306.1.
- De Simone, D. La bonifica della spiaggia di Bonaria presso Cagliari. In Annali dei Lavori Pubblici; Ministero dei Lavori Pubblici: Roma, Italy, 1928; Volume 6, pp. 961–996.
- Deiana, G.; Melis, R.T.; Orrù, P.E.; Panizza, V. Field Trip Guidebook: Coastal and Granitic landforms of southeastern Sardinia. Cagliari-Villasimius. In 5th AIGeo National Conference, 6th Young Geomorphologists’ Day; Melis, R.T., Ed.; University of Cagliari: Cagliari, Italy, 2015.
- Del Monte, M., D’Orefice, M., Luberti, G. M., Marini, R., Pica, A., & Vergari, F. (2016). Geomorphological classification of urban landscapes: The case study of Rome (Italy). Journal of Maps, 12, 178–189. doi:10.1080/ 17445647.2016.1187977
- Del Río, L.; Gracia, F.; Benavente, J. Shoreline change patterns in sandy coasts. A case study in SW Spain. Geomorphology 2013, 196, 252–266.
- Diao, C. (1996). An approach to theory and methods of urban geomorphology. Chinese Geographical Science, 6 (1), 88–95.
- Díaz-Cuevas, P.; Prieto-Campos, A.; Ojeda-Zújar, J. Developing a beach erosion sensitivity indicator using relational spatial databases and Analytic Hierarchy Process. Ocean Coast. Manag. 2020, 189, 105146.
- Dolan, R.; Fenster, M.; Holme, S. Temporal Analysis of Shoreline Recession and Accretion. J. Coast. Res. 1991, 7, 723–744.
- Duarte, C.M.; Kennedy, H.; Marbà, N.; Hendriks, I. Assessing the capacity of seagrass meadows for carbon burial: Current limitations and future strategies. Ocean Coast. Manag. 2013, 83, 32–38.
- Eamer, J.B.; Walker, I.J. Quantifying sand storage capacity of large woody debris on beaches using LiDAR. Geomorphology 2010, 118, 33–47. doi:https://doi.org/10.1016/j.geomorph.2009.12.006.
- Faccini, F., Piccazzo, M., Robbiano, A., & Roccati, A. (2008). Applied geomorphological Map of the Portofino Municipal Territory (Italy). Journal of Maps, 4(1), 451– 462.
- Fairweather, P.G.; Henry, R.J. To clean or not to clean? Ecologically sensitive management of wrack deposits on sandy beaches. Ecol. Manag. Restor. 2003, 4, 227–229.
- Fanini, L.; Marchetti, G.M.; Scapini, F.; Defeo, O. Effects of beach nourishment and groynes building on population and community descriptors of mobile arthropodofauna. Ecol. Indic. 2009, 9, 167–178.
- Ferrara, C.; Palmerini, V. Indagine sedimentologica sulla dinamica della linea di costa in facies sabbiosa nel settore centrale del Golfo di Cagliari. Boll. Della Soc. Sarda di Sci. Nat. 1974, XIV, 55–76.

- Fiedler, J.W.; Smit, P.B.; Brodie, K.L.; McNinch, J.; Guza, R. Numerical modeling of wave runup on steep and mildly sloping natural beaches. Coastal Engineering 2018, 131, 106–113. doi:https://doi.org/10.1016/j.coastaleng.2017.09.004.
- Fiedler, J.W.; Smit, P.B.; Brodie, K.L.; McNinch, J.; Guza, R. The offshore boundary condition in surf zone modeling. Coastal Engineering 2019, 143, 12–20. doi:https://doi.org/10.1016/j.coastaleng.2018.10.014.
- Flor-Blanco, G.; Flor, G.; Pando, L. Evolution of the Salinas-El Espartal and Xagó beach/dune systems in north-western Spain over recent decades: Evidence for responses to natural processes and anthropogenic interventions. Geo-Mar. Lett. 2013, 33, 143–157.
- Folk, R. L. (1974). The petrology of sedimentary rocks. Austin, Tex: Hemphill Publishing Co.
- Folk, R. L., & Ward, W. (1957). Brazos River bar [Texas]; a study in the significance of grain size parameters. Journal of Sedimentary Petrology, 27(1), 3–26.
- Franco-Ochoa, C.; Zambrano-Medina, Y.; Plata-Rocha, W.; Monjardín-Armenta, S.; Rodríguez-Cueto, Y.; Escudero, M.; Mendoza, E. Long-Term Analysis of Wave Climate and Shoreline Change along the Gulf of California. Applied Sciences 2020, 10. doi:10.3390/app10238719.
- Gacia, E.; Duarte, C.M. Sediment Retention by a Mediterranean *Posidonia oceanica* Meadow: The Balance between Deposition and Resuspension. Estuar. Coast. Shelf Sci. 2001, 52, 505–514.
- Gallop, S.L.; Kennedy, D.M.; Loureiro, C.; Naylor, L.A.; Muñoz-Pérez, J.J.; Jackson, D.W.T.; Fellowes, T.E. Geologically controlled sandy beaches: Their geomorphology, morphodynamics and classification. Sci. Total Environ. 2020, 731, 139123.
- Genz, A.; Fletcher, C.; Dunn, R.; Frazer, N.; Rooney, J.; Fletcher, A.; Dunn, C.; Frazer, R. The Predictive Accuracy of Shoreline Change Rate Methods and Alongshore Beach Variation on Maui, Hawaii. J. Coast. Res. 2007, 231, 87–105.
- Gómez-Pujol, L., Orfila, A., Álvarez-Ellacuría, A., Terrados, J., & Tintoré, J. (2013). *Posidonia oceanica* beach-caster litter in Mediterranean beaches: A coastal videomonitoring study. Journal of Coastal Research, 165, 1768–1773.
- González-Villanueva, R.; Costas, S.; Pérez-Arlucea, M.; Jerez, S.; Trigo, R.M. Impact of atmospheric circulation patterns on coastal dune dynamics, NW Spain. Geomorphology 2013, 185, 96–109.
- Gourlay, M.R. Beach and Dune Erosion Tests. Delft Hydraulics Laboratory Report No. M935/M936
- Gourlay, M.R. Beach Processes in the Vicinity of Offshore Breakwaters. In Proceedings of the Fifth Australian Conference on Coastal and Ocean Engineering, Perth, Australia, 25–27 November 1981; pp. 132–137.
- Gracia, A.; Rangel-Buitrago, N.; Oakley, J.A.; Williams, A. Use of ecosystems in coastal erosion management. Ocean and Coastal Management 2018, 156, 277–289. SI: MSforCEP, doi:https://doi.org/10.1016/j.ocecoaman.2017.07.009.
- Grilliot, M.J.; Walker, I.J.; Bauer, B.O. The Role of Large Woody Debris in Beach-Dune Interaction. Journal of Geophysical Research: Earth Surface 2019, 124, 2854–2876. doi: https://doi.org/10.1029/2019JF005120.
- Guedes, R.M.; Bryan, K.R.; Coco, G. Observations of alongshore variability of swash motions on an intermediate beach. Continental Shelf Research 2012, 48, 61–74. doi:https://doi.org/10.1016/j.csr.2012.08.022.
- Guza, R.T.; Feddersen, F. Effect of wave frequency and directional spread on shoreline runup. *Geophysical Research Letters* 2012, 39. doi:10.1029/2012GL051959.

- Haerens, P.; Bolle, A.; Trouw, K.; Houthuys, R. Definition of storm thresholds for significant morphological change of the sandy beaches along the Belgian coastline. Geomorphology 2012, 143–144, 104–117.
- Hunt, I.A. Design of Seawalls and Breakwaters. J. Waterw. Harb. Div. 1959, 85, 123–152.
- Idier, D.; Paris, F.; Cozannet, G.L.; Boulahya, F.; Dumas, F. Sea-level rise impacts on the tides of the European Shelf. Cont. Shelf Res. 2017, 137, 56–71.
- Jaramillo, C.; Jara, M.S.; González, M.; Medina, R. A shoreline evolution model considering the temporal variability of the beach profile sediment volume (sediment gain/loss). Coast. Eng. 2020, 156, 103612.
- Jiménez, J.; Sánchez-Arcilla, A.; Bou, J.; Ortiz, M.A. Analysing short-term shoreline changes along the Ebro delta (Spain) using aerial photographs. J. Coast. Res. 1997, 13, 1256–1266.
- Kaarel Orviku, Jaak Jaagus, Are Kont, Urve Ratas, & Reimo Rivis. (2003). Increasing Activity of Coastal Processes Associated with Climate Change in Estonia. Journal of Coastal Research, 19(2), 364–375. http://www.jstor.org/stable/4299178
- Kennedy, D.M.; Woods, J.L. The influence of coarse woody debris on gravel beach geomorphology. Geomorphology 2012, 159-160, 106–115. doi:https://doi.org/10.1016/j.geomorph.2012.03.009.
- Knutson, T., McBride, J., Chan, J. et al. Tropical cyclones and climate change. Nature Geosci 3, 157–163 (2010). https://doi.org/10.1038/ngeo779
- Lai, A. (2008). Studio Geomorfologico e tendenze evolutive del litorale di Cagliari- Quartu Sant'Elena (Doctoral dissertation in Ingegneria del Territorio, Facoltà di Ingegneria, XIX Ciclo). University of Cagliari, Italy. Retrieved from https://iris.unica.it/handle/11584/265961#.Xeego9V7lPY
- Lecca, L., De Muro, S., Cossellu, M., & Pau, M. (2005). Modern terrigenous-carbonate sediments of the continental shelf of the Gulf of Cagliari. Alpine and Mediterranean Quaternary, 18(2), 201–221.
- Legeais, J.F.; von Schuckmann, K.; Melet, A.; Storto, A.; Meyssignac, B. Sea Level, in Copernicus Marine Service Ocean State Report. J. Oper. Oceanogr. 2018, 11, S1–S142.
- Lewis, D. W., & McConchie, D. (1994). Practical sedimentology. New York, NY: Chapman & Hall.
- Lionello, P., Abrantes, F., Gacic, M. et al. The climate of the Mediterranean region: research progress and climate change impacts. Reg Environ Change 14, 1679–1684 (2014). https://doi.org/10.1007/s10113-014-0666-0
- Lionello, P.; Scarascia, L. The relation between climate change in the Mediterranean region and global warming. Reg. Environ. Chang. 2018, 18, 1481–1493.
- Loureiro, C.; Ferreira, Ó.; Cooper, J.A.G. Geologically constrained morphological variability and boundary effects on embayed beaches. Mar. Geol. 2012, 329–331, 1–15.
- Manca, E.; Pascucci, V.; De Luca, M.; Cossu, A.; Andreucci, S. Shoreline evolution related to coastal development of a managed beach in Alghero, Sardinia, Italy. Ocean Coast. Manag. 2013, 85, 65–76.
- Masselink, G.; Li, L. The role of swash infiltration in determining the beachface gradient: a numerical study. Marine Geology 2001, 176, 139–156. doi:https://doi.org/10.1016/S0025-3227(01)00161-X.
- Masselink, G., Hughes, M., and Knight, J. (2011). Introduction to Coastal Processes and Geomorphology, Second Edition. London: Routledge
- Masselink, G.; Scott, T.; Poate, T.; Russell, P.; Davidson, M.; Conley, D. The extreme 2013/2014 winter storms: hydrodynamic forcing and coastal response along the southwest

coast of England. Earth Surface Processes and Landforms 2016, 41, 378–391, [https://onlinelibrary.wiley.com/doi/pdf/10.1002/esp.3836]. doi:10.1002/esp.3836.

- Mastronuzzi, G., Aringoli, D., Aucelli, P. P. C., Baldassarre, M. A., Bellotti, P., Bini, M., … Valente, A. (2017). Geomorphological map of the Italian coast: From a descriptive to a morphodynamic approach. Geografia Fisica e Dinamica Quaternaria, 40, 161–196. doi:10. 4461/GFDQ2017.40.11
- Mathiesen, M., Goda, Y., Hawkes, P. J., Mansard, E., Martín, M. J., Peltier, E., Thompson, E. F., & Van Vledder, G., (1994) Recommended practice for extreme wave analysis, Journal of Hydraulic Research, 32:6, 803-814, DOI: 10.1080/00221689409498691
- McLachlan, A.; Defeo, O.; Jaramillo, E.; Short, A.D. Sandy beach conservation and recreation: Guidelines for optimising management strategies for multi-purpose use. Ocean and Coastal Management 2013, 71, 256–268. doi:https://doi.org/10.1016/j.ocecoaman.2012.10.005.
- Mentaschi, L.; Vousdoukas, M.I.; Pekel, J.-F.; Voukouvalas, E.; Feyen, L. Global long-term observations of coastal erosion and accretion. Sci. Rep. 2018, 8.
- Ministero dell'Ambiente e della Tutela del Territorio – Servizio difesa del mare (2002) – "Mappatura delle praterie di Posidonia oceanica lungo le coste della Sardegna e delle piccole isole circostanti". Cooperativa Nautilus di Vibo Valentia – Ministero dell'Ambiente e della Tutela del Territorio – Servizio difesa del mare 1999-2002;
- Moore, L.; Ruggiero, P.; List, J.H. Comparing mean high water and high water line shorelines: Should proxy-datum offsets be incorporated into shoreline change analysis? J. Coast. Res. 2006, 22, 894–905.
- Nassar, K.; Mahmod, W.; Fath, H.; Masria, A.; Nadaoka, K.; Negm, A. Shoreline change detection using DSAS technique: Case of North Sinai coast, Egypt. Mar. Georesources Geotechnol. 2018, 37, 81–95.
- Ngom, H.; Ndour, A.; Niang, I. Impacts of Protective Structures on Sandy Beaches: Example of the Saly Balnear Station, Petite Côte, Senegal. J. Coast. Res. 2018, 81, 114–121.
- Nicholls, R.J.; Cazenave, A. Sea-level rise and its impact on coastal zones. Science 2010, 328, 1517–1520.
- Nordlund, L.M.; Jackson, E.L.; Nakaoka, M.; Samper-Villarreal, J.; Beca-Carretero, P.; Creed, J.C. Seagrass ecosystem services—What's next? Mar. Pollut. Bull. 2018, 134, 145–151.
- Orrù, P.E.; Antonioli, F.; Lambeck, K.; Verrubbi, V. Holocene sea level change of the Cagliari. Quat. Nova 2004, 8, 193–212.
- Pagán, J.; López, I.; Tenza-Abril, A.; Luis, A.; Villacampa, Y. Urban growth and beach nourishment: Experiences on the coast of Alicante, Spain. In WIT Transactions on the Built Environment Urban Growth 2018; Syngellakis, S., Melgarejo, J., Eds.; WIT Press: Alicante, Spain, 2018; Volume 179, pp. 93–102.
- Pagán, J.; Luis, A.; Tenza-Abril, A.; Pallarés, P. The influence of anthropic actions on the evolution of an urban beach: Case study of Marineta Cassiana beach, Spain. Sci. Total Environ. 2016, 559, 242–255.
- Pan J., Pratolongo P.D., Cuadrado D.G. (2018) Geological, Physical and Chemical Foundations. In: Beninger P. (eds) Mudflat Ecology. Aquatic Ecology Series, vol 7. Springer, Cham. https://doi.org/10.1007/978-3-319-99194-8_2
- Pan, Y.; Flindt, M.; Schneider-Kamp, P.; Holmer, M. Beach wrack mapping using unmanned aerial vehicles for coastal environmental management. *Ocean and Coastal Management* 2021, 213, 105843. doi:https://doi.org/10.1016/j.ocecoaman.2021.105843.

- Passarella, M. On the Prediction of Swash Excursion and the Role of Seagrass Beach-Cast Litter: Modelling and Observations; University of Cagliari: Cagliari, Italy, 2019.
- Passarella, M., De Muro, S., Ruju, A., & Coco, G. (2018a). An assessment of swash excursion predictors using field observations. Journal of Coastal Research, 85, 1036– 1040. doi:10.2112/SI85-208.1
- Passarella, M.; Goldstein, E.B.; De Muro, S.; Coco, G. (2018b). The use of genetic programming to develop a predictor of swash excursion on sandy beaches. Natural Hazards and Earth System Sciences 2018, 18, 599–611. doi:10.5194/nhess-18-599-2018.
- Passarella, M.; Ruju, A.; De Muro, S.; Coco, G. Horizontal Runup and Seagrass Beach Cast-litters: Modelling and Observations. J. Coast. Res. 2020, 95, 143–147.
- Pilkey, O.H.; Cooper, J.A.G. Society and Sea Level Rise. Science 2004, 303, 1781–1782.
- Pilkey, O.H.; Dixon, K.L. The Corps and the Shore, 4th ed.; Island Press: Washington, DC, USA, 1996.
- Pollard, J.; Spencer, T.; Brooks, S. The interactive relationship between coastal erosion and flood risk. Prog. Phys. Geogr. Earth Environ. 2018, 43, 574–585.
- Porta, M.; Buosi, C.; Trogu, D.; Ibba, A.; De Muro, S. An integrated sea-land approach for analyzing forms, processes, deposits and the evolution of the urban coastal belt of Cagliari. J. Maps 2020.
- Poulos, S.; Chronis, G.; Collins, M.B.; Lykousis, V. Thermaikos Gulf Coastal System, NW Aegean Sea: An overview of water/sediment fluxes in relation to air–land–ocean interactions and human activities. Journal of Marine Systems, 25 (1), 47-76. (doi:10.1016/S0924-7963(00)00008-7).
- Porta, M.; Buosi, C.; Trogu, D.; Ibba, A.; & De Muro, S. (2020). An integrated sea-land approach for analyzing forms, processes, deposits and the evolution of the urban coastal belt of Cagliari. Journal of Maps, https://doi.org/10.1080/17445647.2020.1719441 [Taylor & Francis Online]
- Pranzini, E.; Anfuso, G.; Muñoz-Perez, J.J. A probabilistic approach to borrow sediment selection in beach nourishment projects. Coast. Eng. 2018, 139, 32–35.
- Procaccini G., Piazzi L. (2001) – Genetic Polymorphism and Transplantion Success in the Mediterranean Seagrass *Posidonia oceanica*. Restoration Ecology, 9 (3): 332-338.
- Procaccini, G., Orsini, L., Ruggiero, M.V. and Scardi, M. (2001), Spatial patterns of genetic diversity in *Posidonia oceanica*, an endemic Mediterranean seagrass. Molecular Ecology, 10: 1413-1421. https://doi.org/10.1046/j.1365-294X.2001.01290.x
- Prodger, S.; Russell, P.; Davidson, M.; Miles, J.; Scott, T. Understanding and predicting the temporal variability of sediment grain size characteristics on high-energy beaches. Mar. Geol. 2016, 376, 109–117.
- Pusceddu, N., Batzella, T., Kalb, C., Ferraro, F., Ibba, A., & De Muro, S. (2011). Short-term evolution of the Budoni beach on NE Sardinia (Italy). Rendiconti Online Della Società Geologica Italiana, 17, 155–159. doi:2,10.3301/ ROL.2011.45
- Qi, H.; Cai, F.; Lei, G.; Cao, H.; Shi, F. The response of three main beach types to tropical storms in South China. Mar. Geol. 2010, 275, 244–254.
- Qiao, G.; Mi, H.; Wang, W.; Tong, X.; Li, Z.; Li, T.; Liu, S.; Hong, Y. 55-year (1960–2015) spatiotemporal shoreline change analysis using historical DISP and Landsat time series data in Shanghai. Int. J. Appl. Earth Obs. Geoinf. 2018, 68, 238–251.

- Raubenheimer, B.; Guza, R.T.; Elgar, S.; Kobayashi, N. Swash on a gently sloping beach. Journal of Geophysical Research: Oceans 1995, 100, 8751–8760. doi:https://doi.org/10.1029/95JC00232.
- Ravdas, M.; Zacharioudaki, A.; Korres, G. Implementation and validation of a new operational wave forecasting system of the Mediterranean Monitoring and Forecasting Centre in the framework of the Copernicus Marine Environment Monitoring Service. Natural Hazards and Earth System Sciences 2018, 18, 2675–2695. doi:10.5194/nhess-18-2675-2018.
- Reynard, E., Pica, A., & Coratza, P. (2017). Urban geomorphological heritage. An overview. Quaestiones Geographicae, 36(3), 7–20.
- Rodríguez-Santalla, I.; Roca, M.; Martínez-Clavel, B.; Pablo, M.; Moreno-Blasco, L.; Blázquez, A. Coastal changes between the harbours of Castellón and Sagunto (Spain) from the midtwentieth century to present. Regional Studies in Marine Science 2021, 46, 101905. doi:https://doi.org/10.1016/j.rsma.2021.101905.
- Roelvink, D.; McCall, R.; Mehvar, S.; Nederhoff, K.; Dastgheib, A. Improving predictions of swash dynamics in XBeach: The role of groupiness and incident-band runup. Coastal Engineering 2018, 134, 103–123. RISC-KIT: Resilience-increasing Strategies for Coasts – Toolkit, doi:https://doi.org/10.1016/j.coastaleng.2017.07.004.
- Ruju, A., Ibba, A., Porta, M., Buosi, C., Passarella, M., & De Muro, S. (2018). The role of hydrodynamic forcing, sediment transport processes and bottom substratum in the shoreward development of *Posidonia oceanica* meadow. Estuarine, Coastal and Shelf Science, 212, 63–72. doi:10. 1016/j.ecss.2018.06.025
- Ruju, A., Passarella, M., Trogu, D., Buosi, C., Ibba, A., & De Muro, S. (2019a). An operational wave system within the monitoring program of a mediterranean beach. Journal of Marine Science and Engineering, 7, 32. doi:10.3390/ jmse7020032
- Ruju, A.; Lara, J.L.; Losada, I.J. (2019b). Numerical Assessment of Infragravity Swash Response to Offshore Wave Frequency Spread Variability. Journal of Geophysical Research: Oceans, 124, 6643–6657. doi:https://doi.org/10.1029/2019JC015063
- Rutten, J.; Torres-Freyermuth, A.; Puleo, J. Uncertainty in runup predictions on natural beaches using XBeach nonhydrostatic. Coastal Engineering 2021, 166, 103869. doi:https://doi.org/10.1016/j.coastaleng.2021.103869.
- Salvi, G.; Buosi, C.; Arbulla, D.; Cherchi, A.; De Giudici, G.; Ibba, A.; De Muro, S. Ostracoda and foraminifera response to a contaminated environment: The case of the Ex-Military Arsenal of the La Maddalena Harbour (Sardinia, Italy). Micropaleontology 2015, 61, 115–133.
- Schintu, M., Marrucci, A., Marras, B., Galgani, F., Buosi, C., Ibba, A., & Cherchi, A. (2016). Heavy metal accumulation in surface sediments at the port of Cagliari (Sardinia, western Mediterranean): environmental assessment using sequential extractions and benthic foraminifera. Marine Pollution Bulletin, 111, 45–56. doi:10.1016/j.marpolbul. 2016.07.029
- Segre, A.G. Linee di riva sommerse e morfologia della piattaforma continentale italiana relativaalia trasgressione marina versiliana. Quaternaria 1969, 2, 141–154.
- Shepard F.P. (1968) Coastal classification. In: Geomorphology. Encyclopedia of Earth Science. Springer, Berlin, Heidelberg. https://doi.org/10.1007/3-540-31060-6_53
- Short, A. D. (1999). Handbook of beach and shoreface morphodynamics. John Wiley and Sons, New York, NY, USA.
- Simarro G., Bryan K. R., Guedes R M. C., Sancho A., Guillen J., Coco G. (2015) On the use of variance images for runup and shoreline detection, Coastal Engineering, Volume 99, 2015, Pages 136-147, ISSN 0378-3839.

- Simeone, S., De Falco, G., Como, S., Olita, A., & De Muro, S. (2008). Deposition dynamics of banquettes of *Posidonia oceanica* in beaches. Rendiconti Online Della Società Geologica Italiana, 3(2), 726–727.
- Simeone, S.; De Falco, G. Morphology and composition of beach-cast Posidonia oceanica litter on beaches with different exposures. Geomorphology 2012, 151-152, 224–233. doi:https://doi.org/10.1016/j.geomorph.2012.02.005.
- Simeone, S., De Muro, S., & De Falco, G. (2013). Seagrass berm deposition on a Mediterranean embayed beach. Estuarine, Coastal and Shelf Science, 135, 171–181. doi:10.1016/j.ecss.2013.10.007
- Simeone, S.; Palombo, L.; Molinaroli, E.; Brambilla,W.; Conforti, A.; De Falco, G. Shoreline Response to Wave Forcing and Sea Level Rise along a Geomorphological Complex Coastline (Western Sardinia, Mediterranean Sea). Applied Sciences 2021, 11. doi:10.3390/app11094009.
- Small, Christopher and Nicholls, Robert J. (2003) A global analysis of human settlement in coastal zones. *Journal of Coastal Research*, 19 (3), 584-599.
- Stafford, D.B.; Langfelder, J. Air photo survey for coastal erosion. Photogrametric Eng. 1971, 6, 556–575.
- Stokes, K.; Poate, T.; Masselink, G.; King, E.; Saulter, A.; Ely, N. Forecasting coastal overtopping at engineered and naturally defended coastlines. Coastal Engineering 2021, 164, 103827. doi:https://doi.org/10.1016/j.coastaleng.2020.103827.
- Stockdon, H.F.; Holman, R.A.; Howd, P.A.; Sallenger, A.H. Empirical parameterization of setup, swash, and runup. Coastal Engineering 2006, 53, 573 – 588. doi:https://doi.org/10.1016/j.coastaleng.2005.12.005.
- Strazzera, E.; Cherchi, E.; Ferrini, S. Assessment of regeneration projects in urban areas of environmental interest: A stated choice approach to estimate use and quasi-option values. Environ. Plan A 2010, 42, 452–468.
- Syvitski, J.; Vörösmarty, C.; Kettner, A.; Green, P. Impact of humans on the flux of terrestrial sediment to the global coastal ocean. Science 2005, 308, 376–380.
- Tecchiato, S., Buosi, C., Ibba, A., Ryan, D. A., & De Muro, S. (2016). A comparison of geomorphic settings, sediment facies and benthic habitats of two carbonate systems of western Mediterranean Sea and south western Australia: Implications for coastal management. Journal of Coastal Research, 75, 562–566. doi:10.2112/SI75-113.1
- Tecchiato, S.; Buosi, C.; Ibba, A.; Del Deo, C.; Parnum, I.; O'Leary, M.; De Muro, S. Geomorphological and sedimentological surrogates for the understanding of seagrass distribution within a temperate nearshore setting (Esperance Western Australia). Geo-Mar. Lett. 2019, 39, 249–264.
- Tecchiato, S.; Collins, L.; Parnum, I.; Stevens, A. The influence of geomorphology and sedimentary processes on benthic habitat distribution and littoral sediment dynamics: Geraldton, Western Australia. Mar. Geol. 2015, 359, 148–162.
- Telesca, Luca; Belluscio, Andrea; Criscoli, Alessandro; Ardizzone, Giandomenico; Apostolaki, Eugenia T.; Fraschetti, Simonetta; Gristina, Michele; Knittweis, Leyla; Martin, Corinne S.; Pergent, Gérard; Alagna, Adriana (28 July 2015). "Seagrass meadows (*Posidonia oceanica*) distribution and trajectories of change". *Scientific Reports*. 5 (1): 12505. doi:10.1038/srep12505. ISSN 2045-2322. PMC 4516961. PMID 26216526.

- Thieler, E.R.; Himmelstoss, E.A.; Zichichi, J.L.; Ergul, A. The Digital Shoreline Analysis System (DSAS) Version 4.0—An ArcGIS Extension for Calculating Shoreline Change; 2008–1278; U.S. Geological Survey: Reston, VA, USA, 2009.
- Thornbush, M. (2015). Geography, urban geomorphology and sustainability. Area, 47(4), 350–353. doi:10.1111/ area.12218
- Tomas, A.; Mendez, F.; Medina, R.; Jaime, F.; Higuera, P.; Lara, J.; Ortiz, M.; Alvarez de Eulate, M. A methodology to estimate wave-induced coastal flooding hazard maps in Spain. Journal of Flood Risk Management, 9, 289–305. doi:10.1111/jfr3.12198.
- Trogu, D.; Buosi, C.; Ruju, A.; Porta, M.; Ibba, A.; De Muro, S. What Happens to a Mediterranean Microtidal Wave-dominated Beach during Significant Storm Events? The Morphological Response of a Natural Sardinian Beach (Western Mediterranean). J. Coast. Res. 2020, 95, 695–700.
- Uda, T.; Serizawa, M.; Miyahara, S. Prediction of Typical Beach Changes Owing to Human Activities. 2018. Available online: https://www.intechopen.com/books/morphodynamic-model-for-predicting-beachchanges-based-on-bagnold-s-concept-and-its-applications/prediction-of-typical-beach-changes-owingto-human-activities (accessed on 19 December 2020).
- Ulzega, A. Geomorphology and stratigraphy of late Quaternary. Rendiconti del Seminario Della Facoltà di Scienze Dell'università di Cagliari 1995, LXV, 11–14.
- UN General Assembly. Transforming Our World: The 2030 Agenda for Sustainable Development; Division for Sustainable Development Goals: New York, NY, USA, 2015.
- Vacchi, M.; De Falco, G.; Simeone, S.; Montefalcone, M.; Morri, C.; Ferrari, M.; Bianchi, C.N. Biogeomorphology of the Mediterranean *Posidonia oceanica* seagrass meadows. Earth Surf. Process. Landf. 2017, 42, 42–54.
- Valloni, R.; Barsanti, M. Artificial Beach Nourishment Projects in Italy. Rapp. Comm. Int. Mer Médit 2007, 38, 706.
- Virdis, S.G.P.; Oggiano, G.; Disperati, L. A Geomatics Approach to Multitemporal Shoreline Analysis in Western Mediterranean: The Case of Platamona-Maritza Beach (Northwest Sardinia, Italy). Journal of Coastal Research (2012) 28 (3): 624–640 https://doi.org/10.2112/JCOASTRES-D-11-00078.1
- Volker, E. The Effect of Sedimentary Texture on Beach Fill Longevity. J. Coast. Res. 1996, 12, 447–461.
- VV.AA. (1994). Carta Geomorfologica d'Italia – 1,50.000 scale. Quaderni del Servizio Geologico Nazionale, Serie III n.4. Roma: Istituto Poligrafico Zecca dello Stato.
- VV.AA. (2009). Carta Geologica d'Italia - 1:50,000 scale. Quaderni del Servizio Geologico d'Italia, Serie III n.12 fasc.1. Roma: Istituto Superiore per la Protezione e la Ricerca Ambientale ISPRA.
- VV.AA. (2013). Carta Geologica d'Italia alla scala 1:50.000. Foglio 528 Oristano. Roma: Istituto Superiore per la Protezione e la Ricerca Ambientale ISPRA, Servizio Geologico d'Italia. Retrieved from http://www. isprambiente.gov.it/Media/carg/528_ORISTANO/Foglio.
- VV.AA. (2016). Carta Geologica d'Italia alla scala 1:50.000. Foglio 566 Pula. Roma, Istituto Superiore per la Protezione e la Ricerca Ambientale ISPRA, Servizio Geologico d'Italia. Retrieved from http://www. isprambiente.gov.it/Media/carg/566_PULA/Foglio.html
- Wentworth, C. K. (1922). A scale of grade and class terms for clastic sediments. Journal of Geology, 30, 377–392
- Wright, L. and Short, A. D. (1984). Morphodynamic variability of surf zones and beaches: a synthesis. *Marine geology*, 56(1-4):93–118.

- Young, I.R.; Ribal, A. Multiplatform evaluation of global trends in wind speed and wave height. Science 2019, 364, 548.
- Zambrano-Monserrate, M.A.; Ruano, M.A.; Sanchez-Alcalde, L. Indirect effects of COVID-19 on the environment. Sci. Total Environ. 2020, 728, 138813.
- Zijlema, M.; van derWesthuysen, A.J. On convergence behaviour and numerical accuracy in stationary SWAN simulations of nearshore wind wave spectra. *Coastal Engineering* 2005, 52, 237–256. doi:https://doi.org/10.1016/j.coastaleng.2004.12.006.